CHARACTERIZATION OF A MUTANT CHINESE HAMSTER FIBROBLAST LINE RESISTANT TO THE MITOGENIC EFFECTS OF INSULIN.

Aleksandrs Spurmanis

A Thesis

in

The Department

of

Biology

Presented in Partial Fulfilment of the Requirements

for the Degree of Master of Science at

Concordia University

Montreal, Quebec, Canada.

April 1996

ISBN 0-612-18444-7

Canada

ABSTRACT

CHARACTERIZATION OF A MUTANT CHINESE HAMSTER FIBROBLAST LINE RESISTANT TO THE MITOGENIC EFFECTS OF INSULIN.

Aleksandrs Spurmanis

Previously in our lab, a mutant Chinese hamster fibroblast line, designated A1-j, was clonally selected based on its resistance to a toxic insulin-diphtheria A-chain conjugate (Leckett and Germinario, 1992[1]). Subsequent examination revealed that while the parental V-79 strain showed 2-fold insulin-stimulated growth ($P < 0.01$), the mutant exhibited no significant growth above basal levels ($P > 0.10$). Since the mutant's growth was similarly affected in response to insulin-like growth factor-I, but not to 5% fetal bovine serum or unrelated growth factors (i.e., α-thrombin or epidermal growth factor), the mitogenic block appears to be confined to a pathway shared by insulin and IGF-I. Analysis of thymidine incorporation data, as well as *c-fos* and *c-jun* mRNA expression, placed the causative mutation early in the cell cycle (i.e., the $G_1 \rightarrow S$ boundary). Measurement of [^{3}H]-2DG uptake along with [^{14}C]-glucose incorporation into glycogen revealed that insulin stimulation of metabolic pathways, namely glucose transport and glycogen synthesis, is intact in the mutant. Although A1-j cells appear to possess approximately half of the insulin receptor complement of the parental cell line (800 *vs* 1500 receptors per cell as estimated by Scatchard analysis), ligand binding, internalization, autophosphorylation, and tyrosine kinase activity appear to be unaffected. Finally, the A1-j cell line appears to mediate insulin proteolysis which is significantly more resistant to chloroquine inhibition than the wild-type V-79 strain. 100μM chloroquine was able to rescue 26.4 ± 1.4% of a prebound cohort of insulin from degradation in V-79 cells versus only 18.4 ± 1.5% of prebound insulin being rescued in the A1-j cell line under identical conditions ($P < 0.05$). These data are consistent with a mutation in A1-j resulting in an alteration in the normal endosomal routing of insulin and/or its receptor.

ACKNOWLEDGEMENTS:

I would like to express my gratitude to my supervisor Dr. Ralph Germinario for hanging tough through a number of difficult years to provide me with the guidance and encouragement I needed to get through my own trials and tribulations.

I would also like to thank Sue Colby-Germinario, Sue Pratt, Dr. Hung T. Hyun, Johnson Mak, Yue Huang, Steven Lee, Dr. Lenore Beitel, Harvey Miller, Dr. Lorraine Chalifour, Judith Lacoste, Areti Malapetsa, Dr. Lawrence Panasci, Dr. Larry Kleiman, Dr. Michael Pollock, Dr. Michael Parniak, who generously provided me with technical assistance and/or advice.

A special thanks goes to Adrian Noë, Johnathan Bramson, and Angella McQuillan, not only for sharing with me their wealth of knowledge in molecular biology and allowing me to use their equipment, but also for providing badly needed moral support.

An extra-special thanks goes to Eva Nagy and Vik Chopra who took the time to teach me most of what I know about northern blotting. Another "e.s.t." goes to Jing Wang for the super assistance she gave me in the laboratory.

I am grateful to FCAR whose funding helped to finance this endevour.

Finally, I would like to thank my wife Dominique for standing by me and for believing in me even when I had begun to quit on myself.

"Seen from the outside and materially, the best we can say at the moment is that life properly speaking *begins with the cell.* For a century science has concentrated its attention on this chemically and structurally complex unit, and the longer it continues to do so the more evident it becomes that in it lies the secret of which we have as yet no more than an inkling - the secret of the connection between the two worlds of physics and biology. The cell is *the natural granule of life* in the same way as the atom is the natural granule of simple, elemental matter. If we are to take the measure of the transit to life and determine its precise nature, we must try to understand the cell."

- Pierre Teilhard de Chardin,
The Phenomenon of Man,
Harper & Row Publ.,
N.Y. 1959, p 79.

TABLE OF CONTENTS:

LIST OF FIGURES: . . . . . p ix

LIST OF TABLES: . . . . . p xi

ABBREVIATIONS: . . . . . p xiii

INTRODUCTION: . . . . . p 1

1 ***Insulin*** . . . . . p 1

2 ***The insulin receptor*** . . . . . p 2

2.1 *Insulin Receptor Structure* . . . . . p 2
2.2 *The extracellular domains* . . . . . p 3
2.3 *The transmembrane region* . . . . . p 3
2.4 *The insulin receptor tyrosine kinase (IRK)* . . . . . p 4
2.5 *Serine and threonine phosphorylation* . . . . . p 6

3 ***The tyrosine phosphorylation cascade*** . . . . . p 7

3.1 *Insulin receptor substrate- 1(IRS-1)* . . . . . p 8
3.2 *SHC* . . . . . p 9
3.3 *The Phosphatidyl inositol-3 kinase (PI3K) pathway* . . . . . p 11
3.4 *The Ras - MAP kinase pathways* . . . . . p 13
3.5 *Activation of early growth response genes* . . . . . p 15

4 ***Insulin internalization and processing*** . . . . . p 18

4.1 *Endocytosis* . . . . . p 18
4.2 *Intracellular routing of insulin* . . . . . p 20
4.3 *The role of endosomes in insulin signalling* . . . . . p 21

5 ***Control of insulin receptor expression*** . . . . . p 23

6 ***The A1-j mutant*** . . . . . p 25

6.1 *Isolation and initial characterization* . . . . . p 25
6.2 *Experimental objectives* . . . . . p 27

MATERIALS: . . . . . p 28

METHODS: . . . . . p 29

1 ***Tissue culture*** . . . . . p 29

2 ***Lowry protein determination*** . . . . . p 29

3 ***Hexose transport*** . . . . . p 29

4 ***Glycogen synthesis*** . . . . . p 30

5 ***Growth curves and 3-day growth assays*** . . . . . p 30

6 ***Thymidine incorporation studies*** . . . . . p 31

7 ***Insulin binding studies*** . . . . . p 31

8 ***Assay for secreted insulin binding proteins/proteases*** . . . . . p 32

9 ***Insulin degradation studies*** . . . . . p 32

10 ***Peroxovanadium rescue studies*** . . . . . p 33

11 ***Tyrosine phosphorylation of endogenous substrates*** . . . . . p 34

11.1 *Cell culture and protein extraction* . . . . . p 34
11.2 *Western blotting* . . . . . p 35

12 ***Early growth gene expression*** . . . . . p 36

12.1 *Plasmids* . . . . . p 36
12.2 *Cell culture and RNA extraction/purification* . . . . . p 37
12.3 *Northern blotting* . . . . . p 38

RESULTS: . . . . . p 39

1 ***Characterization of the metabolic signalling pathway*** . . . . . p 40

1.1 *Hexose transport* . . . . . p 40
1.2 *Glycogen synthesis* . . . . . p 40

2 ***Characterization of the mitogenic signalling pathway*** . . . . . p 41

2.1 *Growth curves* . . . . . p 41

2.2 3-day growth assays . . . . . p 41

3 Insulin signalling cascade . . . . . p 42

3.1 Thymidine incorporation studies . . . . . p 42
3.2 Insulin binding studies . . . . . p 43
3.3 Release of autocrine insulin binding proteins/ proteases . . p 44
3.4 Insulin degradation . . . . . p 46
3.5 Peroxovanadium rescue studies . . . . . p 48
3.6 Tyrosine phosphorylation of endogenous substrates . . . . . p 49

4 Early growth gene expression . . . . . p 51

4.1 Expression of c-fos . . . . . p 51
4.2 Expression of c-jun . . . . . p 52

DISCUSSION: . . . . . p 53

The mitogenic block is specific to insulin and IGF-I . . . . . p 53

Metabolic signalling in A1-j . . . . . p 54

The G1→S transition is uncoupled from hormonal stimulation in A1-j . . p 56

The known functions of the insulin receptor appear to be intact in A1-j . p 58

Evidence for a post-receptor mutation . . . . . p 60

The involvement of insulin- and insulin receptor-processing . . . . . p 62

Summary . . . . . p 67

Future directions . . . . . p 68

FIGURES: . . . . . p 70

TABLES: . . . . . p 101

REFERENCES: . . . . . p 112

LIST OF FIGURES:

Fig I: The insulin molecule . . . . . p 71

Fig II: The insulin receptor . . . . . p 72

Fig III: Model for insulin receptor activation by dimerization of the transmembrane domain. . . . . p 74

Fig IV: Insulin receptor substrate 1 (IRS-1) . . . . . p 75

Fig V: Map of the functional domains of SHC. . . . . p 76

Fig VI: PI3 kinase . . . . . p 77

Fig VII: The Ras-MAPK cascade. . . . . p 79

Fig VIII: Receptor-mediated endocytosis. . . . . p 80

Fig IX: The role of endosomes in insulin-regulated GLUT4 translocation. p 82

Fig X Internalization of ^{125}I-insulin into V-79 and A1-j cells. . . . . p 98

Fig XI Model for the A1-j mutation. . . . . p 99

Fig 1.2: The effect of insulin concentration on glycogen synthesis in V-79 and A1-j cells. . . . . p 84

Fig 2.1: Growth curve: V-79 *vs* A1-j cells as monitored by daily cell counting. . . . . p 85

Fig 2.2: Insulin-stimulated growth in V-79 and A1-j cells as monitored by 3-day cell counting. . . . . p 86

Fig 3.1A: Time course for thymidine incorporation into TCA-precipitable material. . . . . p 87

Fig 3.1B: Insulin-stimulated thymidine incorporation in V-79 and A1-j cells at 10 and 20 hours post stimulus. . . . . p 88

Fig 3.3A: Insulin and TSH synergism in stimulating thymidine incorporation in FRTL-5 cells. . . . . p 89

Fig 3.3B: The effect of adding cell-conditioned media on thymidine incorporation in FRTL-5 cells maximally stimulated with 6.7 nM insulin and 1.0 nM TSH. . . . . p 90

Fig 3.4A: The measurement of total insulin efflux from the cell monolayer to the conditioning buffer. . . . . p 91

Fig 3.4B: Insulin degradation as monitored by TCA-soluble ^{125}I counts in the conditioning buffer. . . . . p 92

Fig 3.4C: Insulin degradation as monitored by TCA-soluble ^{125}I counts in the cell monolayer. . . . . p 93

Fig 3.5A: The effect of bpV(phen) on 10-hour thymidine incorporation in V-79 and A1-j cells. . . . . p 94

Fig 3.6: Insulin receptor autophosphorylation and endogenous kinase activity in V-79 and A1-j cells *in vivo*. . . . . p 95

Fig 4.1 Serum-stimulated expression of *c-fos* mRNA *vs* time. . . . . p 96

Fig 4.2 Serum-stimulated expression of *c-jun* mRNA *vs* time. . . . . p 97

LIST OF TABLES:

TABLE I

The effect of insulin in combination with other mitogens on V-79 and A1-j cell growth . . . . . p 102

TABLE 1.1

The effect of insulin concentration on hexose transport in V-79 and A1-j cells. p 103

TABLE 1.2A

The time dependence of insulin-stimulated glycogen synthesis in V-79 and A1-j cells . . . . . p 104

TABLE 1.2B

The effect of insulin concentration on glycogen synthesis in V-79 and A1-j cells. p 105

TABLE 2.2

Insulin-stimulated growth in V-79 and A1-j cells as monitored by 3-day cell counts . . . . . p 106

TABLE 3.1

DNA synthesis in V-79 and A1-j cells as monitored by thymidine incorporation into TCA-precipitable material. . . . . p 107

TABLE 3.4A

The efflux of insulin from cell monolayers to the conditioning buffer expressed as a percent of cohort bound . . . . . p 108

TABLE 3.4B

Insulin degradation as monitored by TCA-soluble ^{125}I-labelled insulin in the conditioning buffer. . . . . p 109

TABLE 3.4C

Insulin degradation as monitored by TCA-soluble cell-associated ^{125}I-labelled insulin. . . . . p 109

TABLE 3.4D

The effect of adding inhibitors of the endosomal apparatus on 20-minute insulin degradation. . . . . p 110

TABLE 3.5

The effect of bpV(phen) on DNA synthesis as monitored by thymidine incorporation into TCA-precipitable material. . . . . p 111

ABBREVIATIONS:

IR/hIR	Insulin receptor/ human insulin receptor
IGF-I	Insulin-like growth factor-1
IGF-IR	Insulin-like growth factor 1 receptor
IRK	Insulin receptor tyrosine kinase
IRS-1	Insulin receptor substrate 1
FBS	Fetal bovine serum
CHO	Chinese hamster ovary cell
CHL	Chinese hamster lung fibroblast
FRTL-5	Follicular rat thyroid cell line #5
SH2/SH3	Src homology- 2 or -3 domains
SBS	Src homology binding sequence
SHC	Src homology and collagen-related protein
PI3K	Phosphatidyl inositol 3 kinase
PTPase	Phosphotyrosine phosphatase
MEK	MAPK/ERK kinase
MAPK	Mitogen activated protein kinase
GLUT4	Type 4 glucose transporter
GAPDH	Glyceraldehyde phosphate dehydrogenase
bpV(phen)	bisperoxo(1,10-phenanthroline)oxovanadate(v) anion
DTab	Whole diphtheria toxin containing both A and B subunits
DTaI	Insulin-diphtheria A-chain conjugate
2DG	2-deoxyglucose
EN	Endosomal network
DPM	Disintegrations per minute
SDS-PAGE	Sodium dodecylsulfate-polyacrylamide gel electrophoresis
kD	kilodalton(s)

INTRODUCTION:

Though written almost 40 years ago, Teilhard de Chardin's words (see page v) are as true today as they were when he wrote them in the 1959. To paraphrase, in order to fully comprehend the intricacies of human physiology, one must first gain a more complete understanding of its most fundamental unit: the cell. Nowhere is this more evident than in the study of insulin and the physiological effects that it mediates. Since its first discovery by Banting and Best in 1925, scientists have amassed a great deal of information about the structure and function of this hormone. We know how its produced, how its transported through the bloodstream, where its actions are directed, and how it is recognized and taken up by target tissues. Although much progress has been made in recent years to determine the mechanisms by which insulin exerts its pleiotropic effects, we have yet to explain exactly what happens inside the insulin-responsive cell once stimulated with an appropriate dose of insulin.

1 Insulin:

Human insulin is a heterodimeric peptide hormone with a molecular weight of approximately 6 kD. The "A" chain fragment consists of 21 amino acid residues, while the "B" chain contains 30 residues. The chains are connected by two disulphide bridges formed between Cys^{7}, Cys^{20} of the A chain and Cys^{7}, Cys^{19} of the B chain respectively. An additional disulphide linkage exists between Cys^{6} and Cys^{11} of the A chain. Figure I illustrates the 2-dimensional amino acid sequence (Fig. IA) and a 3-dimensional representation of the molecule (Fig. IB). Although insulin has demonstrated the potential for significant mitogenic activity[2,3,4,5,6,7,8,9], it is primarily considered as the dominant effector in the regulation of glucose homeostasis (reviewed in Moses AC, 1991[3], Moller, D., Flier, J., 1991[10]). Unlike related peptides IGF-I and IGF-II, insulin does not appear

to be bound to any serum carrier proteins (Clemmons, 1991[11]), and presumably travels freely through the bloodstream until it encounters an insulin-sensitive target tissue. Here it is recognized by specialized insulin receptors located on the plasma membrane surface of cells comprising the target tissue. Although insulin receptors are present in varying concentrations in nearly all vertebrate tissues (White, M., Khan C., 1994[12]), only three are physiologically relevant in regards to glucose homeostasis: liver, muscle and adipose (Fehlig, P., 1990[13]).

2 *The insulin receptor:*

2.1 Insulin Receptor Structure:

At the plasma membrane surface, the receptors are generally believed to be organized as heterotetramers with a $\alpha_2\beta_2$ structure although $[\alpha\beta]_{insulin}/[\alpha\beta]_{IGF\text{-}1}$ receptor hybrids (Christoffersen, C., *et al.*, 1994[14], Soos *et al.*, 1993[15]), have been reported. The α-subunits are approximately 125-135 kD in size, contain the insulin binding sites, and are located entirely on the extracellular surface of the plasma membrane. The size difference of the α chains is related to the tissue-specific alternative transcriptional splicing of a 36 base-pair sequence at the 3' terminus of exon 11 of the proreceptor gene (Seino *et al.*, 1989[16]). This yields two different insulin receptor isoforms: the A isoform which lacks the 12 N-terminal amino acids of the α-subunits, and the B isoform which possesses these residues. The β-subunits are transmembrane proteins of 95 kD molecular weight and contain a cytosolic tyrosine kinase domain which is activated upon insulin binding. Although each α/β half of the insulin holoreceptor complex contains 47 cysteine residues only five are believed to be involved in covalent linkages that maintain the quaternary structure (Finn *et al.*, 1989[17]). Data compiled from a number of different sources has suggested where these disulphide bonds may be located (Shoelson *et al.*, 1988[18]; Waugh *et al.*, 1989[19]; Shäffer and Ljungvist, 1992[20]; Cheatham and Khan,

1992[21]; Xu *et al.*, 1990[22]). These are depicted in Fig. IIA. along with potential N-linked (Hedo *et al.*, 1983[23]; Hedo *et al.*, 1981[24]) and O-linked (Herzberg *et al.*, 1985[25]; Collier and Gorden, 1989[26]) glycosylation sites.

2.2 *The extracellular domains:*

As mentioned above, the insulin binding sites of the insulin receptor are located within the α-subunits. Although two discrete regions (see Fig IIB) within each subunit have been implicated in the direct association with the ligand, there still remains no clear consensus among researchers as to exactly which amino acid residues comprise the ligand binding site(s) (Wedekind *et al.*, 1989[27]; De Meyts *et al.*, 1994a[28]; Kjeldsen *et al.*, 1994[29]). At physiological concentrations (0.1 - 1.0 nM), only 1 molecule of insulin is believed to bind per receptor although at higher concentrations (within the μM range) two (Lee and Pilch, 1994[30]; Shäffer, 1994[31]) or even three (De Meyts, 1994b[32]) molecules per receptor have been proposed. Binding of insulin to its receptor induces a conformational change which is believed to involve not only the α-subunits, but also the extracellular portions of the β-chains as well (White and Khan, 1994[12], Cheatham and Khan, 1992[21]; Leconte *et al.*, 1992[33]). In the unliganded state these extracellular domains of holoreceptor impose some sort of tonic inhibition upon their respective β-chain kinase counterparts. It has been suggested that the conformational change induced by ligand binding not only releases the tonic inhibition, as suggested by Shoelson *et al.*, 1988[18], but may also include a positive regulatory component which further enhances receptor kinase activity (Lee and Pilch, 1994[30]).

2.3 *The transmembrane region:*

One question that has long perplexed researchers is how the ligand-induced

conformational changes occurring in the extracellular domains of the insulin receptor were being transmitted across the plasma membrane to their cytosolic counterparts. Since the transmembrane domains of the β-subunits are relatively short in length (comprising merely 24 amino acids) and involve only one membrane-spanning region, it is difficult to envisage how enough movement could be generated here to effectively propagate a wave of allosteric modulation. A plausible hypothesis, however, has recently been proposed (Yamada *et al.*, 1995[34]) involving what is often referred to as "receptor oligomerization". In the absence of bound ligand, the α-subunits of the insulin receptors are somehow poised to prevent interactions between the transmembrane domains of the two adjacent β-subunits (perhaps by physically keeping them apart via steric hinderance). Upon insulin binding, conformational changes in the extracellular domains allows for homodimerization of the α-helical transmembrane regions (Fig III). This presumably places the cytosolic domains in closer juxtaposition with one another resulting in allosteric modulation and/or receptor kinase activation. Additionally, as suggested by data describing receptor activation through the inhibition of a membrane-associated phosphotyrosine phosphatase (PTPase), insulin-induced conformational changes may be activating the receptor β-subunits by releasing them from inhibitory interactions with negative regulatory elements (Posner *et al.*, 1994[156]).

2.4 *The insulin receptor tyrosine kinase (IRK):*

The cytosolic portion of the β chain (residues Arg^{941}- Ser^{1343}·), also referred to as the insulin receptor kinase (IRK) serves as the effector in insulin signalling (Fig. IIB). Once activated by the events described above, receptor β-chains undergo autophosphorylation which in turn activates their tyrosine kinase activity (reviewed in Cheatham and Khan, 1995[35]; Tavaré and Siddle, 1993[36]; Lee and Pilch, 1994[30]).

· The numbering of amino acid residues is based on the exon 11 minus form of the insulin receptor (missing the 12 N-terminal amino acids of the α-subunits).

Autophosphorylation is thought to be initiated by a *trans* mechanism whereby one β-subunit of the activated receptor binds ATP and phosphorylates the tri-tyrosine region in the adjacent β-subunit within the same holoreceptor (Frattali *et al.*, 1992[37]; Frattali and Pessin, 1993[38]; Lee *et al.*, 1993a[39]). The tri-tyrosine region (Tyr^{1146}, Tyr^{1150} and Tyr^{1151}) along with the ATP binding site (Gly^{991}-x-Gly^{993}-x-x-Gly^{996}-$(x)_{12}$- Lys^{1018}) are found within the IRK core domain. The kinase core lies within amino acid residues Val^{973}-Lys^{1271} (encoded by exons 17-22) and contains all of the peptide sequences necessary to retain fully functional enzymatic activity *in vitro* (Wei *et al.*, 1995[40]).

Two other important functional domains which are also autophosphorylated upon insulin binding have also been identified within each of the receptor β-chains. The first is the juxtamembrane region encoded by exon 16 of the proreceptor gene (amino acids Arg^{941} to Val^{978}) and includes two functionally important Tyr residues: Tyr^{953} and Tyr^{960}. Although the juxtamembrane domain is not required for exogenous kinase activity, the key role it plays in post-receptor signalling events is reflected by the fact that various deletions or point mutations within this region result in impaired biological responsiveness (White *et al.*, 1988[41]; Backer *et al.*, 1991[42]; Feener *et al.*, 1993[43]). Phosphorylation of Tyr^{960} has been shown to be essential in enabling IRK-mediated phosphorylation of its principle intracellular substrate: insulin substrate 1 (IRS-I). Furthermore, the consensus sequences $GPLY^{953}$ and/or $NPEY^{960}$ have been implicated in receptor endocytosis (Backer *et al.*, 1990a[44]; Backer *et al.*, 1992[45]).

The other functional domain of the insulin receptor β-chain is found in the C-terminal region (amino acid residues Leu^{1263}- Ser^{1343}). Of all of the domains comprising the insulin receptor, this one is perhaps the most enigmatic. Over the years a number of conflicting reports have been unable to clearly define a function for this region, but a consensus appears to be emerging that it is involved in negatively modulating mitogenic responsiveness of the receptor (reviewed in Tavaré and Siddle, 1993[36]). As in the other cytosolic domains, tyrosine phosphorylation, this time at Tyr^{1316} and Tyr^{1322}, has been implicated. A recent report has suggested that this region may play a key role in defining the signalling specificity of the insulin receptor versus that of the closely related

IGF-I receptor (Mothe *et al.*, 1995[46]). This is a particularly important observation since it currently not known how these two related receptors are able to produce such disparate responses even though they apparently mediate their effects through the same intracellular signalling network (Myers *et al.*, 1993[47]). Furthermore, another recent report has proposed a mechanism whereby an unknown intracellular protein somehow interacts with the C-terminus to dampen the autophosphorylation and kinase activity of the kinase core (Baron *et al.*, 1995[48]). Further examination of this putative protein interaction could hold the key to explaining why the insulin receptor mediates primarily metabolic responses and the IGF-I receptor mitogenic responses.

2.5 *Serine and threonine phosphorylation*

Although the activation of the IRK and subsequent biological activity has been associated with the phosphorylation of tyrosine residues on the receptor β-chains, insulin has also been shown to stimulate phosphorylation of Ser and Thr residues·. Interestingly, most of the insulin-stimulated Ser and Thr phosphorylation occurs in either the juxtamembrane or the C-terminal receptor domains (Feener *et al.*, 1993[43]; Lewis *et al.*, 1990a[49]; Lewis *et al.*, 1990b[50]). Since these domains appear to provide an interface between the kinase core of IRK with intracellular signal peptides, Ser and Thr phosphorylation presumably modulates the coupling of tyrosine kinase activity with subsequent signalling events. Furthermore, several studies have shown that receptors phosphorylated at Ser and Thr sites show decreased kinase activity and biological responsiveness (Takayama *et al.*, 1988[51]; Stadmauer and Rosen, 1986[52]; Chin *et al.*, 1993[53]). Taken together, these data imply that insulin-stimulated Ser and Thr phosphorylation may be involved in a negative feedback loop that serves to "switch off"

· The insulin receptor is also Ser/Thr phosphorylated, albeit to a lesser extent, under basal conditions.

phosphorylation may be involved in a negative feedback loop that serves to "switch off" the insulin signal following some critical intracellular event.

3 *The tyrosine phosphorylation cascade:*

The insulin receptor, like other members of the receptor tyrosine kinase family, is believed to modulate most if not all of its biological effects by initiating a phosphorylation cascade through a network of intracellular signal peptides. A number of reports, however, have surfaced which suggest that many of the biological effects may also be mediated through kinase independent pathways (Rafaeloff *et al.*, 1991[54]; Rolband *et al.*, 1993[55]; Gottschalk, W., 1991[56]; Moller *et al.*, 1991[57]; Wong *et al.*, 1995[58]). Since many of these claims are based on transfection studies, data from a recent report (Sasaoka *et al.*, 1995[59]) raises the possibility that reported kinase-independent signalling is in fact artifactual. Although such pathways may exist, no one to date has *convincingly* demonstrated their physiological relevance to insulin signalling.

Upon activation, most receptor tyrosine kinases, such as the EGF· and PDGF† receptors, form direct non-covalent complexes with their endogenous substrates. These protein-protein interactions are mediated through substrate SH2 (src homology 2) domains which strongly associate with Tyr-phosphorylated SBS‡ sequences within the activated receptor (reviewed in Schlessinger and Ullrich, 1992[60]; Fantl *et al.*, 1993[61]).

· EGF: epidermal growth factor

† PDGF: platelet derived growth factor

‡ SBS: SH2 binding site - a consensus sequence of 4-6 amino acids surrounding a critical tyrosine residue which often includes one or more C-terminal hydrophobic residues, e.g.: YXX*O* (*O* = a hydrophobic residue such as V, I or M). Phosphorylation of the Tyr residue activates binding, but the molecular specificity is defined by the other amino acids in the sequence. For example: the regulatory subunit of PI3K recognizes YXXM motifs, GRB2 - PXY(V/I)N(V/I), etc...

Even though the insulin receptor and the related IGF-I receptor do possess a single SBS motif within their C-terminal domains*, they are not thought to interface directly with their second messenger system through SH2 associations. Instead, both insulin and IGF-I signalling appears to be mediated by the phosphorylation of docking proteins which contain the SBS motifs necessary to mediate complex formation with downstream messengers of the signalling cascade. To date, two such docking proteins have been identified: insulin receptor substrate-1 (IRS-1) and SHC (*src homology and collagen related*).

3.1 Insulin receptor substrate- 1(IRS-1):

Although its predicted molecular weight based on amino acid composition is 131 kD, IRS-1 migrates at around 160 kD on SDS-PAGE and at 185 kD when phosphorylated in response to insulin and IGF-I (reviewed in Cheatham and Khan, 1995 [35]). It has been characterized as a soluble cytosolic protein (Sun *et al.*, 1991[62]) although cellular subfractionation studies have identified a membrane-associated population as well (Kelly and Ruderman, 1993[63]; Kublaoui *et al.*, 1995[64]). The molecule itself contains no SH2 or SH3† domains (Sun *et al.*, 1991[62]) but does contain a pleckstrin homology (PH) domain which may mediate an association with some as yet unidentified protein (Cheatham and Khan, 1995 [35]). A recent report describes a putative sequence SAIN (*S*HC *a*nd *I*RS-1 *N*PEY-binding) within IRS-1 that associates with the juxtamembrane region of both the insulin and IGF-I receptors (Gustafson *et al.*, 1995[65]; Craparo *et al.*, 1995[66]). Although the SAIN domain has been mapped to the amino terminal portion of IRS-1, it does not include the PH sequence. Fig. IVA depicts a one-dimensional structural map of the pertinent domains in IRS-1.

---

* Y^{1322}THM and Y^{1316}AHM are the putative SH2 binding sequences found in the C-termini of the insulin receptor and the IGF-I receptor respectively.

† SH3: src homology-3 domains which also mediate protein-protein interactions but associate with Pro-rich sequences rather than SBS motifs.

IRS-1 is not a kinase and has not been associated with any particular enzymatic activity even though a putative ATP-binding region has been identified near its amino terminus: Gly^{137}-x-Gly-x-x-Gly-$(x)_{12}$-Lys^{156} (Cheatham and Khan, 1995 [35]). Rather, it appears to mediate its effects by serving as a "docking" protein for downstream effector molecules. Of the 28 Tyr residues found in the IRS-1 molecule (Sun *et al.*, 1991[62]), about 21 are found within putative SBS-type binding sites (White and Khan, 1994[12]). Phosphorylation at some of these sites has been shown to promote protein-protein associations with a number of SH2 containing signal peptides. Some of these molecules (e.g.: PI3 kinase) possess intrinsic enzymatic activity which is activated upon association with IRS-1; others, such as GRB2, serve as adaptor molecules that couple IRS-1 phosphorylation to other intracellular messengers. Other proteins which have been shown to associate with activated IRS-1 include the tyrosine phosphatase Syp (Kuhne *et al.*, 1993[67]), and the adaptor protein Nck (Lee *et al.*, 1993b[68]). Fig. IVB illustrates the proteins that are currently known to be "docked" at IRS-1 upon insulin stimulation.

The use of IRS-1 as an intracellular messenger sets the insulin and IGF-I receptors apart from the other protein kinases which appear to be unable to effect its phosphorylation (Cheatham and Khan, 1995[35]). Conversely, attempts to correlate the phosphorylation pattern of IRS-1 with insulin *vs* IGF-I signal specificity have been less fruitful. It appears that not only do both insulin and IGF-I receptors elicit the same pattern of phosphorylation in IRS-1, but they also appear to involve many of the same downstream effectors. Stimulation with insulin and IGF-I also appears to stimulate Ser and Thr phosphorylation in IRS-1, the function of which remains unclear at the moment.

3.2 SHC:

Another, more recently discovered substrate for the insulin receptor is SHC. This protein, first characterized in 1992 (Pelicci *et al.*, 1992[69]), has three different isoforms:

p46, p52, and p66. The p46 and p52 isoforms appear to be differentially translated from the same mRNA while p66 comes from a distinct mRNA species whose origin is not entirely clear. Although the functional differences between the three isoforms has not been fully explored, it appears that the p52 isoform may be the one most relevant to insulin signalling (Yamauchi and Pessin, 1994[70]). Thus, like IRS-1, SHC is believed to function as a "docking" protein which activates downstream effectors by facilitating the formation of multi-component intracellular signalling complexes (see *The ras MAP kinase pathways* below). See Fig. V for a one-dimensional map of the functional domains and protein binding regions within SHC.

Tyrosine phosphorylation of the SBS sequence Y^{317}VNV (Skolnik *et al.*, 1993[76]) has been shown to induce association with GRB2 (Pronk *et al.*, 1993[71]; Pronk *et al.*, 1994[72]) thereby activating the ras-signalling cascade (see *The ras MAP kinase pathways* below). Due to the inability of researchers to co-precipitate SHC and IRS-1, it is currently believed that they do not associate with each other but rather form independent binding complexes upon activation (De Meyts, 1994b[32]; Gustafson *et al.*, 1995[65]). In fact, recent studies indicate that SHC and IRS-1 may compete for the same "active" site· on the insulin receptor. Both substrates contain a SAIN binding domain (described in *IRS-1* above) which reportedly recognizes the $NPEY^{960}$ consensus sequence within the juxtamembrane region of the insulin receptor† (Gustafson *et al.*, 1995[65]; Craparo *et al.*, 1995[66]).

Unlike IRS-1, which is confined to insulin and IGF-I mediated signalling, SHC has been implicated in the signalling pathways of a number of mitogens and cytokines including epidermal growth factor (EGF- Pelicci *et al.*, 1992[69]), platelet-derived growth

---

· In this case the term active site is used rather than binding site. This is to acknowledge the fact that neither the IR nor the IGF-IR form stable protein aggregates with these substrates following the appropriate stimulation. Presumably, the association exists to facilitate the enzymatic function of the receptor kinase which involves phosphorylation and subsequent release of the target substrate.

† As well as the corresponding $NPEY^{950}$ sequence of the IGF-IR.

factor (PDGF- Yokote *et al.*, 1994[73]), nerve growth factor (NGF- Obermeier *et al.*, 1993[74]), and interleukin 2 (IL2- Ravichandran and Burakoff, 1994[75]). Also contrary to IRS-1, the phosphorylation of SHC does not appear to initiate the docking of numerous effector molecules (Skolnik *et al.*, 1993[76]; Rozakis-Adcock *et al.*, 1992[77]). Rather, it is currently believed that all of the mitogenic actions mediated through SHC occur as a result of its interaction with GRB2.

3.3 The Phosphatidyl inositol-3 kinase (PI3K) pathway:

Phosphatidyl inositol 3 kinase, or PI3K, mediates the phosphorylation of D-3 position of the inositol ring (Whitman *et al.*, 1988[78]) of a family of phosphatidyl phosphoinositides (see Fig VIA). Functional PI3K has a heterodimeric structure consisting of a 110 kD catalytic subunit which actually catalyzes the above reaction, and an 85 kD regulatory subunit that serves as an ON/OFF switch for the catalytic subunit. The p85 subunit contains two SH2 domains and one SH3 domain (Escobedo *et al.*, 1991[79]; Skolnik *et al.*, 1991[80]). The binding of these SH2 domains to phosphorylated YXXM sequences in IRS-1 result in the allosteric activation of the p110 subunit (Shoelson *et al.*, 1993[81]). Both SH2 binding sites were found to be important for this interaction, with 4 possible putative YXXM binding sites being implicated NY^{460}ICMG, GY^{608}MPMS, EY^{939}MNMD, DY^{987}MTMQ (Sun *et al.*, 1993[82]). The demonstration of two p85 subunit isoforms (Otsu *et al.*, 1991[83]) raises the possibility that all four YXXM sites in IRS-1 may be involved in binding to PI3K: two to the p85α and two to the p85β subunit.

The following information briefly summarizes what is currently known about the PI3K branch of the insulin signalling cascade (please refer to Fig VIB for a diagrammatic representation). No phospholipase has been isolated which is capable of cleaving the

products of PI3K into DAG· and IP† moieties (Serunian *et al.*, 1989[84]) which implies that they don't enter the classical phosphoinositide signalling pathway. Instead, these metabolites, which include PI-3-P, PI-3,4-P, and PI-3,4,5-P (phosphatidyl inositol 3-phosphate, etc...), probably remain membrane bound and presumably exert their biological effects from this subcellular location. Although the physiological function of these phosphatidyl phosphoinositides is presently unknown, *in vitro* studies have demonstrated their ability in stimulating the ζ isoform of protein kinase C (Nakanishi *et al.*, 1993[85]). This provides a "switch"‡ kinase connection not only for downstream signalling events, but also for the putative negative feedback inhibition discussed above (see *Serine and threonine phosphorylation* page 6).

Insulin stimulates glucose transport in target cells primarily by increasing the activity of the GLUT4 hexose transporter. There are two principle mechanisms by which this occurs. One method is to enhance the activity of the transporters that are present at the plasma membrane surface, and the other is to increase the number of these transporters that are transferred to the cell surface from the endosomal compartment inside the cells (Lienhard *et al.*, 1992[86]). It has been demonstrated that the latter process, also referred to as GLUT4 translocation, is blocked upon the addition of specific inhibitors to PI3K (Cheatham *et al.*, 1994[87]). The mechanisms underlying the translocation process, and thus their connection to PI3K signalling, remains poorly understood. Subcellular fractionation experiments, however, have shown that 75% of activated PI3K is found in the endosomes of L1-3T3 adipocytes indicating that subcellular localization of the PI3K signal may be important to GLUT4 translocation in insulin-sensitive target cells (Kelly and Ruderman, 1993[63]). This would also explain why the

---

· DAG: Diacyl glycerol - the hydrophobic membrane-bound component

† IP: phosphoinositide - soluble cytosolic component: best represented by the second messenger IP_3 (inositol-1,4,5-tris phosphate).

‡ A switch kinase constitutes a point where upstream tyrosine kinase signalling events initiated by the insulin receptor are converted to downstream Ser and Thr phosphorylation events. Ras and Raf play a similar role in the Ras-MAPK cascade (see below).

activation of PI3K is in and of itself not sufficient to stimulate hexose transport - i.e., mitogens IGF-I, EGF, and PDGF are able to activate PI3K yet do not promote GLUT4 translocation.

Another downstream effector in the PI3K branch of the insulin signalling cascade is $pp70^{rsk}$ - a 70 kD phosphoprotein ribosomal S6 kinase (Blenis *et al.*, 1991[88]; Fingar *et al.*, 1993[89]). One principle physiological function of $pp70^{rsk}$ is to phosphorylate the S6 phosphoprotein in the 40S complex on multiple serine sites thereby stimulating protein translation (Palen and Traugh, 1987[90]). Thus, in addition to glucose transport regulation, PI3K has also been implicated in the mitogenic signalling cascade of insulin. Currently, little is known about the activation of the $pp70^{rsk}$ pathway other than the fact that it can be inhibited by the macrolide· rapamycin (Chung *et al.*, 1992[91]; Lartey *et al.*, 1994[92]).

3.4 The Ras - MAP kinase pathways:

Activation of the ras-MAP kinase pathway begins with the association of the adaptor protein GRB2† with either IRS-1 or SHC (see Fig VII). GRB2 is a small cytoplasmic protein with a predicted molecular weight of 23 kD essentially consisting of one SH2 domain flanked by two SH3 domains (Lowenstein *et al.*, 1992[93]). GRB2 binds to an SBS binding site in either IRS-1 ($PGEY^{895}VNIE$) or SHC ($PSY^{317}VNV$)‡, which then allows it to bind to mSOS through its SH3 binding domains (Skolnik *et al.*, 1993[76]; Li *et al.*, 1993[94]). The mSOS protein is the *mammalian* homolog of the Drosophila *son-*

· Macrolides comprise a large number of naturally occurring antibiotic compounds that are characterized as containing a lactone moiety within a large ring system, the best known representative being erythromycin. The antibacterial function of these compounds generally resides in their ability to selectively inhibit protein synthesis by binding to the bacterial 50S ribosomal subunit.

† The name GRB2 is derived from *gr*owth factor receptor *b*ound-2 as it was initially characterized as being able to bind to activated EGF receptors.

‡ The reported consensus sequence is PXY(V/I)N(V/I).

of-sevenless protein and functions as a guanine nucleotide-releasing factor. Its association with the activated protein complex presumably recruits mSOS to a submembrane region in the cytosol (De Meyts, 1994b[32]). Here, it is able to activate the membrane-bound G-protein $p21^{ras}$ by providing it with GTP in exchange for bound GDP (Marshall, 1993[95]). Activated $p21^{ras}$ is, in turn, able to bind to and activate a Ser/Thr kinase called Raf. Although the exact mechanism of Raf activation is currently not clear, other effectors, including the insulin receptor itself, may also be involved (MacDonald *et al.*, 1993[96]).

Raf, in turn, activates another kinase: MEK· by the phosphorylation of a critical Ser residue† (Huang *et al.*, 1993[97]). MEK is a dual-purpose kinase which activates its principle substrate MAPK (*m*itogen *a*ctivated *p*rotein *k*inase) by phosphorylation of both serine and tyrosine residues (Nishida and Gotoh, 1993[98]). MAPK actually comprises a family of related 42-63 kD Ser/Thr kinases also known as ERKs (Extracellular Signal-Regulated Kinases) whose intracellular substrates are many and varied (Pelech and Sanghera, 1992[99]). One key substrate $pp90^{rsk}$, not to be confused with $pp70^{rsk}$, has been implicated in both mitogenic signalling (see *Activation of early growth response genes* below) and control of glycogen synthesis. In the latter capacity, $pp90^{rsk}$ appears to act directly by phosphorylating PPG-1, a critical node in glycogen metabolism (Dent *et al.*, 1990[100]). PPG-1 (protein phosphatase-glycogen associated-1) mediates its effects through its phosphatase activity on two key proteins glycogen synthase and phosphorylase kinase. Dephosphorylation of a critical Ser residue leads to activation of glycogen synthase which catalyzes the transfer of UDP-glucose onto growing chains of glycogen (Stryer, 1995a[101]). Conversely, dephosphorylation inactivates phosphorylase kinase which activates the enzymes which catalyze phosphorolytic glycogenolysis.

· MEK is derived from *M*APK/*E*RK *k*inase and is so named for its principle substrate which is alternatively named MAPK (*m*itogen *a*ctivated *p*rotein *k*inase) or ERK (*e*xtracellular signal *r*egulated *k*inase).

† Although MEK is both Ser and Thr phosphorylated in vivo, Thr phosphorylation doesn't appear to be as important for activation.

As mentioned earlier GRB2, the most proximal effector in the Ras-MAPK pathway, can bind to *both* IRS-1 or SHC following insulin stimulation (Skolnik *et al.*, 1993[76]). One group of researchers has recently shown that overexpression of IRS-1 can partially inhibit insulin-regulated MAPK activity and downstream c-fos expression (Yamauchi and Pessin, 1994[70]). This suggests that the SHC-GRB2 pathway may in fact be more physiologically relevant than the IRS-1-GRB2 pathway in the activation of MAPK and its downstream effectors. Yamauchi and Pessin have further proposed that IRS-1 may in fact be competing with SHC for a limited pool of GRB2·. Although the physiological relevance of this observation has yet to be determined, it is doubtful that the relationship between SHC and IRS-1 is purely competitive given another recent report suggesting that both molecules are required in order to mediate the mitogenic effects of insulin (Cheatham and Khan, 1995[35]).

3.5 Activation of early growth response genes:

Once activated by phosphorylation, both $pp90^{rsk}$ and MAPK are able to translocate to the nucleus of the cell (Blenis, 1993[102]). Here, they in turn mediate the phosphorylation of a number of factors involved in transcriptional activation and ribosomal synthesis, as well as lamin-related proteins which presumably modulate the accessability of chromatin fibres during transcription and/or DNA replication. Among the transcriptional activators whose activity has been shown to be enhanced by insulin stimulation are c-Fos and c-Jun. Both of these proteins belong to the AP-1 family of transcriptional activators which also includes Fos-related proteins Fos-B, Fra-1, Fra-2, as well as Jun-related proteins Jun-B and Jun-D (Angel and Karin, 1991[103]). Insulin stimulation has been shown to modulate both transcriptional (Mohn *et al.*, 1990[104];

· N.B.: Since IRS-1 and SHC are activated through the same interaction with the juxtamembrane region of the ligand-bound insulin receptor, it is possible that the limiting factor is the activated ligand-receptor complex and not GRB2.

Weiland *et al.*, 1991[105]), and post-translational activation of these proteins through the Ser/Thr phosphorylation function of its downstream effectors (Kim and Khan, 1994[106]).

The *c-jun* gene encodes a 36-39 kD protein which is able to dimerize with c-Fos (55-62 kD) via leucine zipper to form the functional core of the AP-1· complex (Curran and Franza, 1988[107]). AP-1, which is also believed to comprise several other unidentified components, is able to recognize and bind to the palindromic TRE (TPA†-responsive element) consensus sequence: 5'-TGA(G/C)TCA-3' (reviewed in Angel and Karin, 1991[103]). Binding of AP-1 to its promoter induces the transcription of the protein-coding region directly downstream. The TRE promoter can be found upstream of a number of genes including the metallothionein IIa, collagenase, stromelysin, as well as certain genes involved in growth control: TGFα, TGFβ, and IL2. Although expression of both *c-fos* and *c-jun* has been correlated with the transition from G_1 to S, no genes whose products participate in this transition are directly regulated by AP-1. Furthermore, stemming from the observation that AP-1 activity has been associated with the opposing cellular processes of proliferation and terminal differentiation, it is currently believed that the AP-1 complex modulates these events indirectly in conjunction with other nuclear signals (Angel and Karin, 1991[103]).

It has been suggested that c-Fos serves as the molecular switch in the transcriptional activation of AP-1(Angel and Karin, 1991[103]). This hypothesis stems from the fact that its promoter region contains both a CRE (cAMP responsive element) and a DSE (dyad symmetry element). Induction of c-fos transcription by most mitogens is thought to be mediated through an interaction of the DSE sequence and the $p67^{SRF}$/$p62^{TCF}$ complex (Shaw *et al.*, 1989[108]). Phosphorylation of $p67^{SRF}$ by $pp90^{rsk}$ and/or $p62^{TCF}$ by MAPK has been shown to induce the activity of these transcription factors (Blenis, 1993[102]) providing a link to the insulin-signalling cascade. The role of c-Fos as a

---

· AP-1: activator protein-1.

† TPA: 12-O-tetradecanoyl phorbol 13-acetate. The TPA-response element is so named because it was first characterized in cells stimulated with this transforming factor.

molecular switch is further reflected by its transient expression. Not only is the mRNA of this protein rapidly degraded, but so is the c-Fos protein itself (Angel and Karin, 1991[103]). Furthermore, the c-Fos product is itself capable of repressing its own transcription. Thus AP-1 activity not only appears to be coupled to hormonal stimulatory pathways via c-Fos, but is also subject to negative feedback inhibition through this protein.

Conversely, the expression of *c-jun* does not appear to be regulated by externally mediated signals, nor is its expression subject to repression by its protein product (Angel and Karin, 1991[103]). On the contrary, the only known endogenous transcriptional activator of *c-jun* expression is the c-Jun protein itself. The current model holds that this relatively stable protein is present in the cell under basal conditions and is capable of mediating low levels of TRE-activated transcription (including its own transcription) through the formation of Jun:Jun homodimers. Upon external stimulation, increasing levels of c-Fos lead to the formation of active AP-1 which further enhances c-jun production through an autoregulatory feed-forward loop. Removal of the external stimulus is followed by rapid depletion of c-Fos and, by extension, AP-1 thereby restoring basal conditions.

The post-translational control mechanisms of c-Fos and c-Jun are not as well characterized. A recent report describes the transient phosphorylation of c-Fos and c-Jun in response to insulin stimulation in 3T3-442A cells (Kim and Khan, 1994[106]). Although phosphorylation of both proteins peaked within 1 minute, it only persisted for 5 minutes in c-Jun while c-Fos remained phosphorylated for up to 60 minutes post-stimulation. Although the authors were also able to show the insulin-dependent stimulation of AP-1 driven transcription in these cells, the relationship to the phosphorylation events is unclear. This is primarily due to the observation that the DNA-binding ability, and hence activity, of AP-1 is enhanced not by phosphorylation but by *de*phosphorylation of the peptide sequence: TPPLS[243]PIDMES· within c-Jun (Boyle *et al.*, 1991[109]). This apparent contradiction, however, may be simply due to the fact that

---

· The underlined sequences represent phosphorylation sites.

insulin stimulates an entirely different subset of Ser/Thr (or even Tyr) residues than those that negatively modulate DNA binding.

4 Insulin internalization and processing:

4.1 Endocytosis:

Not only does the binding of insulin to its receptor result in the activation of the tyrosine phosphorylation cascade, but also initiates a sequence of events leading to the internalization of the receptor-ligand complex. Currently it is believed that this process, referred to as receptor-mediated endocytosis, proceeds by a two-stage mechanism for the insulin receptor (Carpentier and Paccaud, 1994[110]).

The initial binding of insulin to its receptor is believed to occur preferentially on the microvilli of the cell. Prior to endocytosis, ligand-bound receptors aggregate into small clusters (see Fig. VIII). In the first stage of endocytosis, the receptor clusters migrate from the microvilli to clathrin-coated pits located in the non-villous regions of the cell surface (Carpentier and Paccaud, 1994[110]). This "ligand-dependent" stage requires the activation of the β-chain receptor kinase and autophosphorylation (Carpentier *et al.*, 1992[111]), which apparently leads to the release of a molecular constraint that holds unliganded receptors to the microvilli (Carpentier and McClain, 1995[112]). Although the nature of this molecular "brake" is unknown, it likely involves the interaction of a sub-membrane protein with a peptide sequence contained within the kinase core of the receptor β-subunit. Furthermore, it is not known whether release of the constraint involves the phosphorylation of an IRK substrate or whether the conformational changes induced by autophosphorylation are sufficient to free the activated receptor.

The second stage of endocytosis is characterized as being "ligand-independent" (Carpentier and Paccaud, 1994[110]). Here, cytoskeletal proteins associated with the clathrin-coated pits recognize the β-turn motifs of the NPEY and/or GLPY peptide sequences of the juxtamembrane region of the receptor β-subunit (Backer *et al.*, 1992[45]).

As demonstrated by truncated insulin receptors missing the tyrosine kinase core*, once receptors have migrated to non-villous regions, internalization is constitutive and no-longer requires insulin or autophosphorylation (Carpentier and McClain, 1995[112]). In contrast to these findings, a recent study using the B isoform of the insulin receptor showed that neither NPEY or GLPY sequences were necessary for insulin-mediated receptor internalization (Berhanu *et al.*, 1995[113]). Although this contradictory finding may be specific to the B isoform of the insulin receptor†, there remains the possibility that other sequences within the receptor β-chains may play an equally important role in mediating this stage of endocytosis. A subset of adaptin molecules (AP2) has recently been implicated in stage 2 endocytosis of the EGF receptor via interaction with an as of yet unidentified sequence in the carboxy terminus of the receptor (Nesterov *et al.*, 1995[114]). It remains to be seen if these adaptins play an equally important role in the receptor-mediated endocytosis of insulin.

The current model is based largely on the studies of a limited subset of cells - namely fibroblasts and/or adipocytes. It is important to note that other cells, such as the physiologically relevant hepatocytes, have demonstrated clathrin-independent endocytosis of insulin-IR complexes (Smith *et al.*, 1991[115]). Presently it is unclear exactly what effect these cell-specific variations may have on the internalization of insulin, although several reports have described unimpaired insulin internalization in hepatocytes depleted in intracellular ATP‡ (Backer *et al.*, 1989a[116]; Smith and Jarrett, 1990[117]). This observation is, however, consistent with Carpentier's model in the sense that in bypassing the requirement for aggregated receptors to migrate to and concentrate in coated pits, internalization would no longer require energy to release the receptors from villous cell surface regions. Given that liver, in addition to being a target tissue for insulin action,

---

* The hIRΔex17-22 contains only the juxtamembrane domain of the β-subunit and is therefore not held on the microvilli in the unliganded state.

† Most other internalization experiments employed the hIRA isoform.

‡ The implication here is that receptor IRK activity is not required for endocytosis since ATP is required to activate the receptor β-chain.

is a clearance site for plasma-borne insulin, this clathrin-independent mechanism may represent a constitutive endocytic pathway whose primary function is to assist in the clearance of blood-borne molecules.

4.2 Intracellular routing of insulin:

Internalization of the receptor-complex involves the invagination and "pinching off" of the clathrin-coated plasma membrane region to which they have migrated (Fig. VIII). Within 1- 2 minutes the clathrin coating is shed from the resulting vesicle through the function of an uncoating ATPase (Rothman and Schmid, 1986[118]; Pearse and Bretscher, 1981[119]). The uncoated vesicles then fuse with a network of larger vesicular and tubular structures comprising the endosomal compartment (reviewed in Berg *et al.*, 1995[120]). As the internalized ligand-receptor complexes traverse the endosomal apparatus they are subjected to a gradual drop in pH (from 7.4 to 5) causing insulin to dissociate from its receptor (reviewed in Mellman *et al.*, 1986[121]). The insulin is subsequently degraded while the receptor is generally recycled back to the plasma membrane surface for another round of insulin binding and endocytosis (see *Control of insulin receptor expression* below). Although the molecular mechanisms underlying the degradation of insulin are not clear at present, the prevailing opinion is that degradation occurs entirely within the endosomal compartment and not in the lysosomes as previously believed (Berg *et al.*, 1995[120]). An acidic thiol metalloproteinase has been proposed as the probable effector in this process (Authier *et al.*, 1994[122]). It is interesting to note, however that several reports document the existence of a cytosolic insulin degrading enzyme with a pH optimum of 7.4 (reviewed in Berg *et al.*, 1995[120]). Since it appears very unlikely that such an enzyme could participate in endosomally mediated activity, it would be very interesting to determine what role it plays in insulin processing.

4.3 The role of endosomes in insulin signalling:

One of the principle functions of the endosomal apparatus appears to be the uncoupling of insulin from its receptor and the subsequent sorting of these components into distinct metabolic pathways. The receptor is directed to a retroendocytic pathway back to the cell surface, while unbound insulin is degraded and the proteolytic fragments expelled into the extracellular fluid (Berg *et al.*, 1995[120]). This molecular sorting is presumably facilitated by the fact that the receptor is membrane-associated while the unbound ligand floats freely in the lumen. Another important function of the endosome is the actual degradation of the internalized insulin thus providing the first level of control over signal termination, i.e., the elimination of the stimulatory ligand.

In addition to its function in insulin clearance, the endosomal network has also been implicated in the propagation of the tyrosine phosphorylation cascade. It has been demonstrated that the activation of IRK along with concomitant phosphorylation of membrane-associated IRS-1 is maximal in the endosomal compartment suggesting that the internalized receptor complexes are the principle effectors of the signalling cascade and not those present in the plasma membrane (Bevan *et al.*, 1995[123]; Khan *et al.*, 1989[124]). Furthermore, the activation of PI3K was found to occur exclusively within the endosomal network of rat adipocytes (Kelly and Ruderman, 1993[63]). A model has recently been proposed suggesting that the activation of GLUT4 translocation in target cells involves the phosphorylation of a sub-population of EN·-associated IRS-1 (Kublaoui *et al.*, 1995[64]). According to this model, activated IRK at the plasma membrane surface associates with, and initiates the phosphorylation of, EN-IRS-1 (see Fig. IX). This, in turn promotes the recruitment of cytosolic PI3K to the submembrane region of the cell. As the activated insulin-receptor complexes are internalized, further phosphorylation of IRS-1 results in the activation of PI3K. It has been shown that activated IRS-1/PI3K are localized to a different subset of vessicles than those that contain IR and those that

---

· EN: endosomal network

contain GLUT4 (Kelly and Ruderman, 1993[63]). The translocation of GLUT4 vessicles is therefore presumably stimulated by an inter-vesicular cross activation mechanism similar to that described above for PI3K.

The rapid uncoupling and elimination of insulin (within 4-5 min following internalization) provides the potential for a correspondingly rapid termination of IR signalling (Kublaoui *et al.*, 1995[64]). Although studies in hepatoma cells indicate that receptor phosphorylation appears to persist for almost 20 min following insulin-receptor dissociation (Backer *et al.*, 1989b[125]), a more recent study using rat adipocytes reports a very rapid dephosphorylation of endosomally associated insulin receptors which occurs within the time-frame of ligand uncoupling (Kublaoui *et al.*, 1995[64]). Furthermore, in the latter report receptor dephosphorylation correlated perfectly with both a decrease in exogenous kinase activity and IRS-1 phosphorylation. In liver cells, however, the phosphorylation state of endosomal IR did not correlate with its kinase function (Burgess *et al.*, 1992[126]). Assuming that these discrepancies are the result of tissue-specific differences, it is tempting to speculate that differential handling of the insulin-receptor complex in the endosome could constitute a potential point of divergence in the insulin signalling pathway. In this respect, tighter coupling of insulin degradation to IR inactivation in adipocytes versus liver cells reflects the different biological effects insulin exerts in these cells and may even be involved in routing the insulin signal to a different set of biological effectors. Although the inactivation of endosomal IRK is believed to be mediated by dephosphorylation via membrane-associated phosphotyrosine phosphatase (PTPase), its potential connection to ligand uncoupling remains obscure (Faure *et al.*, 1992[127]).

Another potential point of signalling divergence lies in the phosphorylation of cytosolic IRS-1. It has been demonstrated that dephosphorylation of this IRS-1 fraction is not very tightly coupled to the inactivation of IRK (Kublaoui *et al.*, 1995[64]) suggesting that it would be best suited for the modulation of long-term bioeffects such as mitogenesis. This idea is further supported by the fact that PI3K, a key metabolic effector, is not associated with this population of IRS-1 in physiological target cells

(Kelly and Ruderman, 1993[62]). Although this supports the idea that the Ras - MAPK pathway is the principle effector for the mitogenic signalling of insulin, the role of PI3K has not been ruled out (Cheatham and Khan, 1995[35]). Furthermore, other groups have detected cytosolic PI3K activity in response to insulin (Lavan and Lienhard, 1993[128]). Thus, while PI3K may not in and of itself constitute a branching point in insulin signalling the subcellular localization of its activation may. Although research into the role of subcellular localization in insulin signalling is still in its infancy, it is becoming increasingly evident that herein lies the key to elucidating the enigma of intracellular signal sorting and possibly the generation of signal specificity.

5 *Control of insulin receptor expression:*

The hIR is encoded in a single gene approximately 150 kB in length which is located on the short arm of chromosome 19 (Seino *et al.*, 1989[16]). The coding region of the hIR gene is comprised of 22 exons which are spliced together to give a 4.2 kB cDNA sequence. Human insulin receptors are synthesized as single chain preproreceptor molecules either 1370 (isoform A) or 1382 (isoform B) amino acids long. The preproreceptor is secreted into the lumen of the rough ER followed by cleavage of the a 27 amino acid N-terminal signal sequence, a series of disulphide isomerizations leading to the activation of the ligand binding domain, and proreceptor dimerization (Olson *et al.*, 1988[129]). N-linked glycosylation is also initiated here and has been postulated to be essential for correct post-translational processing presumably by stabilizing the correct protein folding patterns during cystine isomerization (Olson *et al.*, 1989[130]). Maturation of the N-glycosidic linkages (Hedo *et al.*, 1983[23]; Hedo *et al.*, 1981[24]), as well as fatty acylation (Hedo *et al.*, 1987[131]; Magee and Siddle, 1988[132]) and O-linked glycosylation (Herzberg *et al.*, 1985[25]; Collier and Gorden, 1989[26]) occur in the Golgi apparatus, but their exact function remains unclear at present. It is in the Golgi where the tetrabasic

sequence $Arg^{720}Lys^{721}Arg^{722}Arg^{723}$· is cleaved resulting in the mature receptor which is expressed at the plasma membrane surface (Yamada *et al.*, 1995[34]). Expression of the mature insulin holoreceptor at the cell surface has been shown to be regulated by both transcriptional, post-transcriptional and post-translational means.

The promoter region of the insulin receptor gene contains four GC-rich sequences with the Sp1 binding homology (Seino *et al.*, 1989[16]). This together with the absence of a TATA box strongly indicates that the insulin receptor is expressed constitutively like a typical housekeeping gene (Stryer, 1995b[133]). In contrast, however, several studies have reported the ability of glucocorticoids to enhance the expression of the insulin receptor apparently by stimulating its transcription (Rouiller *et al.*, 1988[134]; Saad *et al.*, 1995[135]). More recently, characterization of the 350 base pair promoter region -692 to -345 has revealed a glucocorticoid response element along with promoters for two novel *trans*-acting elements insulin receptor nuclear factors I and II (IRNF-I and IRNF-II: Lee *et al.*, 1992[136]). Due to the presence of four polyadenylation sites at the 3' end of the receptor gene, an equal number of mRNA species (5.4, 6.9, 8.0, 9.4 kB) result (Goldstein *et al.*, 1989[137]). A recent report has suggested that the post-transcriptional control of IR mRNA is mediated by a labile RNA degrading enzyme (Levy and Hug, 1992[138]). Interestingly, these researchers report that degrading activity is increased as cells undergo proliferation and that IR mRNA appears to be most stable during quiescence.

Other studies have shown that chronic exposure of cultured cells to insulin results in the reversible downregulation of insulin receptors without affecting mRNA expression (Saad *et al.*, 1995[135]; Blake *et al.*, 1987[139]; Treadway *et al.*, 1989[140]; Arsenis and Livingston, 1986[141]). Furthermore, it appears that increased inactivation and/or degradation of insulin receptors, rather than decreased proreceptor processing, is the principle means of this post-translational control (Knutson, 1991a[142]; Knutson, 1991b[143]; Knutson, 1992[144]). Though very little is known about the receptor inactivation process,

---

· The numbering of this and subsequent amino acid sequences is based on the exon 11 minus isoform of the insulin receptor.

loss of insulin binding activity did not correlate with increased receptor degradation (Knutson, 1991a[142]). Upon interpreting her results, Knutson suggested that degradation is preceded by some other structural modification leading to receptor inactivation. She also found that while receptor inactivation appeared to be independent of endosomal acidification, subsequent proteolysis was not (Knutson, 1991a[142]).

Although a couple of recent reports have documented the involvement of protein kinase C (PKC) in insulin-induced receptor down-regulation, the findings initially appear to be contradictory (Torrosian *et al.*, 1993[145]; Seedorf *et al.*, 1995[146]). In the latter study, chronic exposure to PKC is reported to induce receptor down-regulation, while in the former PKC had no effect by itself and was in fact inhibitory to insulin-stimulated down-regulation. While these discrepancies can be accounted for by the differential expression of undefined cell context factors, taken together the results raise the possibility that insulin and PKC regulate IR proteolysis through mutually exclusive mechanisms. Furthermore, direct association between PKC and the β-chain kinase of the insulin receptor along with a concomitant inhibition of protein tyrosine phosphatase (PTPase) activity was observed by Ullrich's group (Seedorf *et al.*, 1995[146]). Since the PTPase responsible for deactivation of the insulin receptor tyrosine kinase (IRK) is believed to form an intimate association with the insulin receptor (Faure *et al.*, 1992[127]), the observed inhibition of PTPase activity may be the result of a disruption of this association through the formation of IRK-PKC complexes. Whether or not PTPase is directly involved in the intracellular trafficking of the insulin receptor, as suggested by the above interpretation, remains to be seen.

6 The A1-j mutant:

6.1 Isolation and initial characterization:

The A1-j / V-79 system was developed in our lab as the result of a clonal

selection process involving the isolation of Chinese hamster lung fibroblasts resistant to the killing effects of a toxic insulin molecule. The toxic construct chosen was a hybrid peptide (DTaI) comprising the A-chain fragment of diphtheria toxin (DTa) linked to purified porcine insulin (I) - (Leckett and Germinario, 1992[1]; Leckett, 1991[147]). The 21 kD A-chain of Diptheria toxin, or DTa, is the enzymatically active portion and exerts its effects by inhibiting the function of elongation factor-2 (EF2) which is essential for protein synthesis (Stryer, 1995b[133]). Subsequent characterization of the A1-j mutant cell line revealed that they were all still as sensitive to whole Diptheria toxin as the parental V-79 strain (Leckett and Germinario, 1992[1]; Leckett, 1991[147]). It was therefore concluded that the resistance of A1-j cells to DTaI was not conferred by alterations at the target site (i.e., by somehow blocking the action of DTa on EF2), but rather by differential processing of the DTaI conjugate through the insulin receptor signalling system (Leckett and Germinario, 1992[1]).

Although the ability of insulin to stimulate glucose transport in A1-j cells appears to be unimpaired, growth curves and 3-day growth experiments demonstrated that the mutant is not able to grow in the presence of insulin as the sole mitogen while the parental V-79 cell line exhibited significant growth under identical conditions (Leckett and Germinario, 1992[1]; Leckett, 1991[147]). A similar pattern was observed when IGF-I was used as the sole mitogen. Interestingly, the A1-j cell line grew just as well as V-79 cells in 5% FBS. Furthermore, as illustrated in Table I, the mitogenic block in A1-j cells appears to be confined to insulin and IGF-I as growth responses to both α-thrombin and EGF were unimpaired. Binding studies revealed that A1-j cells express 50 - 60% fewer insulin receptors at the plasma membrane surface than do their V-79 counterparts yet both cell lines possess equal numbers of IGF receptors. The fact that both insulin and IGF-I mediated signalling has been affected equally and the receptor binding properties differentially, strongly suggests that the causal lesion has occurred at some post-receptor step where the insulin and IGF-I pathways converge. Finally, despite the lower number insulin receptors expressed at the cell surface, the kinetics of receptor-mediated endocytosis appear to be unaffected in the mutant cell line (see Fig X).

6.2 *Experimental objectives:*

The objectives of the current study were twofold: 1) To further characterize the observed mutant phenotype; 2) To attempt to locate the lesion in the A1-j cell line responsible for the mitogenic blockade. In order to meet the first objective a group of experiments were designed to assess the mitogenic and metabolic responsiveness of A1-j cells to insulin. Three day growth and hexose uptake assays were performed in order to corroborate previous findings. Additionally, insulin-stimulated glycogen synthesis was measured to determine if this metabolic pathway also remained unaffected. Next, the ability of insulin to stimulate DNA synthesis in the A1-j cell line was measured in order to localize the genetic lesion to a $G_1 \rightarrow S$ effector. The ability of a novel insulinomimetic agent to rescue mitogenic signalling in the mutant was determined placing the A1-j mutation at a post-receptor step in the insulin signalling cascade. We then looked for differential expression patterns, in the early growth gene response as well as in substrate Tyr-phosphorylation, that may place the A1-j lesion either proximally (closer to the receptor) or distally (closer to the biological endpoint) along the cascade. Finally, the role of insulin processing was examined by measuring cell-mediated insulin degradation both in the absence and presence of endosomal inhibitors.

MATERIALS:

Culture flasks and Petri dishes were obtained from Falcon. The culture media, antibiotics, fetal and newborn bovine serum, amino acid supplements, AEBSF, and radio-labelled biochemicals were supplied by ICN Biomedicals Canada Ltd.. The media was re-constituted from powder and filter sterilized using the Millipak 20 0.22 μm filter from Millipore Corporation (a 1 μm glass fibre filter, also supplied from Millipore, was used as a pre-filter). The Sigma Chemical Company provided the glycogen, protease inhibitors used in western analysis, Coon's F-12 media, bovine insulin, and human apo-transferrin. Trypsin was supplied by Difco. The versene was formulated using Fisher Scientific reagents and double deionized water, and sterilized by autoclaving for 45 min. at 250°F (liquid cycle). Buffers and other reagents used for RNA extraction and northern analysis were supplied by BDH Chemicals. Aldrich Chemiclas provided the NaF and Na_2VO_4 used in protein extraction. The Folin-Cialcteau reagent used for the Lowry assay was purchased from A&C American Chemicals Ltd.. Wild type V-79 cells were a gift from Dr. Scheffler (Department of Biology, University of California, San Diego). Isolation of the A1-j mutant cells is described in a previous report (Leckett and Germinario, 1992[1]).

METHODS:

1 Tissue culture:

The V-79 and A1-j cell lines were maintained at constant temperature (37°C) and humidity (100%) in an atmosphere of CO_2:air (5:95). Both cell lines were grown in Dulbecco's modification of Eagles essential media (DMEM) supplemented with 5% fetal bovine serum (Cellect Gold FBS), 100 international units/mL penicillin and 100 μg/mL streptomycin. The cells were passaged in either 75-mm culture flasks or 100-mm plastic petri plates. The cells were harvested in 10 mL 0.02% (w/v) EDTA following a 1-min treatment with 0.04% (w/v) trypsin (both trypsin and EDTA were made up in phosphate-buffered saline). They were then centrifuged 5 min at 300xg and resuspended in an appropriate volume of culture medium.

2 Lowry protein determination:

Protein determination employed a modification of the Lowry assay (Lowry *et al.*. 1951[148]). Cell monolayers were dissolved in 1N NaOH followed by addition of Lowry reagents as described previously. When the color was fully developed (~30 min following the addition of the final reagent), sample and standard aliquots were transferred to a 96-well plate and analyzed on a Titertek Multiskan spectrophotometric multi-well plate reader using a wavelength of 650 nm.

3 Hexose transport:

Hexose transport was monitored using tritiated 2-deoxyglucose ([^{3}H]-2DG) as a

radio-labelled non-metabolizable substrate (Germinario *et al.*. [149,150]). Cells were grown to 80% confluence in 35-mm plastic petri plates (Falcon) and then serum starved 18-24 hours in serum-free DMEM (DMEM-S). Plates were rinsed twice at 37°C in DMEM-S and various hormonal stimuli added for 30 min. After the required treatment time, 0.8 mL of 0.05 mM [^{3}H]-2DG (specific activity 50 μCi/ μmol) was added for a period of 5 min. Plates were then rinsed 4 times at 4°C in 2 mL PBS. The cell monolayers were dissolved in 1 mL 1N NaOH and 200 μL aliquots taken for liquid scintillation counting and Lowry protein determination.

4 Glycogen synthesis:

In determining glycogen synthesis, the incorporation of [U-^{14}C] D-glucose into glycogen was monitored (Lawrence *et al.*, 1977 [151]). Cells were grown to 80% confluence in 35-mm plastic petri plates (Falcon) and then serum starved 18-24 hours in serum-free Eagles minimal essential medium (EMEM-S). Cells were exposed to insulin or control medium for 4 hours at 37°C. The treatment was then replaced with 0.8 mL 2 μCi/mL [U-^{14}C]- D-glucose in PBS and 1.0 mg/mL D-glucose. Following a 1-h incubation at 37°C, the cells were rinsed 4 times in PBS at 4°C and solubilized in 0.8 mL 60% KOH containing 1.0% (w/v) glycogen. The extracts were transferred to 15-mL glass centrifuge tubes, boiled for 30 min and precipitated overnight at 4°C using 10 volumes of 95% ethanol. The precipitates were centrifuged at 4°C for 15 min at 2000xg and the unincorporated label washed away with two rinses of refrigerated 95% ethanol. Each pellet was then solubilized in 1 mL 1N NaOH and a 200 μL aliquot taken for liquid scintillation counting.

5 Growth curves and 3-day growth assays:

Cells were plated in 35-mm culture plates at 60,000 cells per plate in

DMEM+5% FBS and allowed to adhere overnight 12-18 hours). The medium was then replaced with basal medium (DMEM+0.2%FBS with 60 nM apo-transferrin), DMEM+5% FBS, or basal medium containing varying concentrations of insulin. After various time intervals (1-6 days), cells were either harvested in 0.02% EDTA and counted, or dissolved in 1N NaOH and analyzed for protein content using the Lowry procedure.

6 Thymidine incorporation studies:

In order to monitor DNA synthesis, the incorporation of tritiated thymidine into TCA precipitable material was measured (Perez-Rodriguez, R., *et al.*., 1981[152]). Cells were serum deprived overnight (12-18 hours) using DMEM +0.2% FBS. At various times following stimulation by insulin or control medium, the plates were pulsed for 1 h at 37°C with 0.8 mL 2.5 μCi/mL [methyl-^{3}H]-Thymidine in PBS containing 4.5 mg/mL D-glucose. The plates were then rinsed 4 times with PBS, 1 mL 10% (w/v) TCA was added, and the plates incubated at 4°C for 45 min. Following 2 rinses with 2 mL 5% (w/v) TCA at 4°C, the precipitate was solubilized in 1 mL 1N NaOH for Lowry determination and liquid scintillation counting.

7 Insulin binding studies:

Cells were grown to 80% confluence in 35-mm culture plates and serum starved overnight (12-18 hours) in DMEM-S + 0.1% (w/v) BSA (dialyzed fraction V). The plates were rinsed twice at room temperature with 2 mL Hank's HEPES-buffered saline with 0.2% BSA (**HHBSA**: 1X Hanks Balanced Salts, 20mM HEPES, 0.85 mM $NaHCO_3$, 0.2% (w/v) dialyzed (molecular weight cut-off: 10 kD) fraction V BSA, pH 7.4). One set of plates was then treated with 0.8 mL of 1 ng/ mL ^{125}I-Insulin in HHBSA. To control for non-specific binding, the remaining plates were treated with 1

mL ^{125}I-Insulin containing an additional 40 μg/mL of non-radioactive insulin. The plates were incubated for at least 4 hours at 4°C followed by 4 rinses with Hanks HEPES-buffered saline (HHBS: no BSA added) at 4°C. The plates were solubilized in 1N NaOH and analyzed for ^{125}I using an LKB model 1282 Compugamma γ-counter.

8 Assay for secreted insulin binding proteins/proteases:

Cells were cultured to confluence using 20 mL DMEM+5%FBS in 100-mm culture plates. The plates were subsequently rinsed and 5 mL DMEM-S was added for overnight conditioning (12-18 h). The conditioned media was then transferred to 15-mL polystyrene tubes, cellular debris removed by centrifugation at 500xg for 15 min, and assayed for its ability to inhibit insulin-stimulated thymidine incorporation in FRTL-5 cells (a follicular rat thyroid cell line). FRTL-5 cells were cultured to confluence in a 24-well plate at 37°C in a 5% CO_2 atmosphere using Coon's F-12 medium supplemented with 0.2% newborn bovine serum (NBS) and a mixture of 6 hormones: 167 mU thyroid stimulating hormone (TSH), 0.83 mg/mL apo-transferrin (95% iron-free), 1.67 μg/mL Glycyl-Histidyl-Lysine acetate, 1.67 μg/mL Somatostatin, 0.83 mg/mL insulin, 0.783 μg/mL hydrocortisone phosphate (Ambesi-Impiombato *et al.*, 1980[153]). The confluent monolayers were deprived of growth factors overnight (12-18 hours) in Coon's F-12 + 0.2% NBS. This was followed by the addition of 1 mL of mitogenic stimulus: 6.7 nM insulin and 1.0 nM TSH in Coon's F-12 along with varying volumes of control or conditioned DMEM-S. After 10 hours of incubation, thymidine incorporation into TCA precipitable material was determined using the procedure described above (see page 31).

9 Insulin degradation studies:

Insulin degradation was monitored using a modification of a temperature shift assay described elsewhere (Backer *et al.*, 1990b[154]; Kuo *et al.*., 1991[155]). Cells were

grown to 80% confluence in 35-mm culture plates and then serum deprived overnight (12-18 hours) in DMEM+0.1% dialyzed BSA. The plates were rinsed twice with 1 mL HHBSA at 4°C (see insulin binding protocol for the formulation, page 31). A 0.8-mL quantity of 1ng/mL ^{125}I-insulin in HHBSA was added to each plate followed by incubation for a minimum of 4 hours at 4°C to allow for receptor-ligand equilibration. Unbound label was rinsed away using 2 X 1 mL HHBSA at 4°C.

Degradation was initiated by adding 0.8 mL 37°C HHBSA to each plate for varying periods of time. After the required degradation time, the conditioned HHBSA was transferred from each plate to an appropriately labelled microtube containing an equal volume of 10% (w/v) TCA at 4°C. Corresponding monolayers were rinsed twice with 1 mL HHBS (see insulin binding protocol for the formulation, page 31) and dissolved for 1 hour at 4°C in a solubilization buffer (20 mM Tris, 1% NP-40, 150 mM NaCl, pH 8.0 containing 0.5 mM AEBSF, 5 μg/mL Leupeptin, 500 I.U./mL Aprotinin). Cell lysates were then transferred to another set of microtubes containing an equal volume of 10% (w/v) TCA. Following a 45-min incubation at 4°C, samples were microfuged at 14,000 RPM for 5 min. Both TCA-soluble (supernatant) and TCA-precipitable (pellet) were assayed for ^{125}I counts. The results are expressed as the percent soluble ^{125}I counts.

10 Peroxovanadium rescue studies:

Bis-peroxovanadyl phenanthroline or bpV(phen) is an insulin-mimetic agent that was developed in Dr. B. Posner's lab (Department of Medicine, McGill University, Montreal)[156]. This compound was tested to determine if its insulin-mimetic properties could induce a normal mitogenic response in A1-j both in the presence or absence of insulin. The compound was added at a final concentration of 1.0 μM both in the absence and presence of 667 nM insulin or 5% FBS and mitogenesis monitored by the incorporation of thymidine into TCA-precipitable material (see Thymidine incorporation studies, page 31).

11 Tyrosine phosphorylation of endogenous substrates:

PY-20 (ICN), a commercially available mouse IgG_2 antibody raised against phosphotyrosine residues, was used in order to examine the protein extracts of V-79 and A1-j cells to determine if any differences existed on the level of endogenous substrate phosphorylation. Of particular interest was the level of insulin-stimulated autophosphorylation of insulin receptor β-chain, and the concomitant phosphorylation of an important primary substrate: insulin receptor substrate 1 (IRS-1). This being the case, induced 3T3-L1 cells were used as a positive control as they have previously been shown to exhibit strong phosphorylation of both the insulin β-chain and IRS-1 in response to insulin stimulation (Keller *et al.*, 1993[157]).

11.1 Cell culture and protein extraction

3T3 cells were grown at 37°C in a 5:95 CO_2:air atmosphere using 100-mm culture plates containing DMEM + 10% FBS. Upon reaching 80% confluence they were induced to differentiate into adipocytes (Reed, B.C., *et al.*., 1981[158]). Typically, greater than 95% induction was obtained. In preparation for an experiment, 2 h of serum deprivation in DMEM-S was found to be sufficient to achieve a stable baseline response in 3T3 cells (unpublished observation). A1-j and V-79 cells were grown to 80% confluence in 100-mm culture plates in DMEM + 5% FBS, and serum starved overnight (12-18 hours) prior to experimentation.

Following serum deprivation, 5 mL of control media (DMEM-S), or media containing varying concentrations of insulin, were added to the plates and incubated at 37°C for a specified amount of time (usually 2 min). The protein extraction protocol used in this assay is based on a technique provided by Dr. Shula Katzav (Terry Fox Cancer Center, Jewish General Hospital). After the required treatment time, each plate was placed on ice, rinsed twice and the monolayers harvested in 1-mL PBS containing

100 mM NaF, 1 mM Na_2VO_4 using a rubber policeman. The monolayers were collected into 2-mL microtubes and pulse-microfuged at 14,000 RPM. The supernatants were discarded. The pellets were resuspended in 300 μL lysis buffer (20 mM Tris, 150 mM NaCl, 1% NP-40, 50 mM NaF, 2 mM Na_2VO_4, 2.5 I.U./mL Aprotinin, 10 μg/mL Leupeptin, 1 mM AEBSF, 4% SDS) and homogenized by sequentially passing them through a 17- and then a 23-gauge needle. The resulting lysates were boiled 5 min and then kept at room temperature. Protein content was determined by performing a Lowry assay on a 10-μL aliquot from each sample.

11.2 Western blotting

Based on the Lowry protein determination, 200 μg of protein were taken from each sample, mixed with an equal volume of 4X reducing Laemmli sample buffer (240mM Tris, 8% SDS, 400mM dithiothreitol, 0.04% bromphenol blue, 40% glycerol, 4mM EDTA, pH 6.8), boiled 5 min., and cooled to room temperature. Sample proteins were size fractionated using a modified Laemmli SDS-PAGE method (Okajima *et al.*., 1993[159]). Briefly, a 6% polyacrylamide resolving gel: 6% total (acrylamide and bis-acrylamide), 2.7% crosslinker (bis-acrylamide), 0.75 M Tris-HCl pH 8.85, 0.1% SDS, 0.18% ammonium persulphate, 0.06% TEMED, was cast into a Protean II gel apparatus. This was overlaid with a 5% stacking gel: 5% total (acrylamide and bis-acrylamide), 2.7% crosslinker (bis-acrylamide), 0.125 M Tris-HCl pH 6.8, 0.1%SDS, 0.12% ammonium persulphate, 0.1% TEMED. The gel was run at 60-V for approximately 4 hours in 0.05 M Tris-HCl pH 8.3, 0.38 M Glycine, 0.1% SDS. The resulting protein bands were then transferred to 0.2-μm nitrocellulose paper (Schleicher and Schuell BA-83) using a Bio Rad Trans-Blot 200 transblotter with plate electrodes. The aqueous transfer system was run at 100 mA (15 V) overnight in the following transfer buffer: 50 mM Tris pH 8.3, 300mM glycine, 20% methanol. The transfer efficiency was qualitatively assessed by staining the nitrocellulose membrane with Ponceau Red (Harlow, E., 1988[160]).

The membrane was blocked for 2 h in 100 mL Tris-Buffered Saline with Tween and BSA (**TBSTA:** 10 mM Tris - pH 7.4, 150 mM NaCl, 0.05% Tween 20, 5.0% Fraction V BSA) using slow rotation on an orbital shaker. The PY-20 antibody was diluted 1:1500 in 40 mL TBSTA containing 15 μg/mL gentamycin, added to the blot in a heat-sealable bag, and incubated 2 h with medium rotation. This was followed by three 5-min rinses in Tris-Buffered Saline with Tween (**TBST**: no BSA added). The secondary antibody, GαM:HRP (goat anti-mouse conjugated to horse radish peroxidase), was prepared by diluting the stock solution 1:4000 in 40 mL TBSTA containing 15 μg/mL gentamycin. The blot was placed in a heat-sealable bag and probed with GαM:HRP for 1 h. Following another 3 rinses in TBST, protein banding patterns were detected using an enhanced chemiluminescence kit developed by Boehringer Manheim Canada Ltd..

12 Early growth gene expression:

Northern blotting was used to monitor growth gene expression in V-79 and A1-j cells at various times following stimulation with 667 nM insulin or 5% FBS to determine if any differential patterns could be detected. Two well-characterized early growth-response genes were selected for study: c-fos and c-jun (reviewed in Angel and Karin, 1991[103]). Glyceraldehyde phosphate dehydrogenase (GAPDH) expression was used as a loading control (Maniatis, T., *et al.*, 1982[161]).

12.1 Plasmids:

All plasmids used in this study were generously provided by Dr. Lorraine Chalifour (Bloomfield Center for Research in Aging, McGill University, Montreal). Human c-fos cDNA (1.8 kB) was obtained in the form of pBK28 (ATCC # V01512), and JAC.1 (ATCC # J04115) contained murine c-jun cDNA (2.6 kB). A 0.6 kB cDNA fragment of murine GAPDH was also obtained as a pGEM-4Z subclone. All plasmids

were grown and replicated in the *E. Coli* DH5α strain (a gift from Dr. Lawrence Panasci, Department of Oncology Jewish General Hospital, Montreal). Techniques used for plasmid replication and purification are described elsewhere (Maniatis, T., *et al.*, 1982[161]). Plasmid inserts were cut out using Pharmacia's One-Phor-All restriction enzymes generously provided by Dr. Lawrence Kleiman (McGill Aids Research Center, Jewish General Hospital, Montreal). The excised cDNA was purified using a Sephaglas bandprep kit obtained from Pharmacia.

12.2 Cell culture and RNA extraction/purification:

HeLa cells were cultured to provide a positive control for the expression of the early growth genes (Angel *et al.*, 1988[162]). The cells were grown in 75-mm culture flasks using RPMI 1640 medium supplemented with 10% FBS. Once 80% confluence was established, the medium was removed and total RNA was extracted and purified using a rapid acid-phenol extraction technique described previously (Chomczynski and Sacchi, 1987[163]). V-79 and A1-j cells were grown to 80% confluence followed by overnight serum deprivation (12-18 hours). 5 mL of control or insulin-containing media were then added to the plates for varying amounts of time. At the required time intervals, the medium was removed and total RNA extracted using the Chomczynski / Sacchi method. Sample RNA concentrations were determined by measuring OD_{260} on a 1:100 diluted aliquot using the Hewlett Packard model 8451A diode-array spectrophotometer. OD_{260}:OD_{280} and OD_{260}:OD_{230} ratios were generally found to be above 1.7 indicating that samples were free of protein contamination and excessive salinity. Furthermore, sample aliquots were run on a TBE-agarose gel revealing no significant RNA degradation or DNA contamination (Maniatis, T., *et al.*, 1982[161]).

12.3 Northern blotting:

The techniques used for performing northern analysis are based on protocols detailed in the literature (Maniatis, T., *et al.*, 1982[161]). Sample aliquots containing 10 μg RNA were adjusted to a 10μL volume and added to an equal volume of Formaldehyde Gel Loading Buffer (55% deionized formamide, 1.1X MOPS, 7.2% formaldehyde, 0.03% bromophenol blue, 0.03% xylene cyanol, 6.9% glycerol, 0.05 μg/mL ethidium bromide). The sample aliquots were then denatured by incubating 15-20 min. at 60°C followed by snap cooling on ice. Samples were loaded onto a 400-cm^2 formaldehyde-agarose denaturing gel (1% agarose, 1X MOPS, 1% formaldehyde), and run at 100-V until the bromphenol blue dye front was 8-cm from the origin (3-4 h) using 1X MOPS as the running buffer. After cutting away unused portions, the gel was rinsed twice for 20 min in 10X SSC. Sample RNA was transferred overnight to a 0.2-μm nitrocellulose membrane (Schleicher and Schuell BA-83) using a standard capillarity transfer set-up and 10X SSC as the transfer solution. The RNA was then cross-linked to the membrane via 5-min exposure to a transilluminator followed by baking 1 h at 80°C in a vacuum oven.

Prior to probing, the blot was placed in a heat sealable bag and incubated for 2 -4 hours at 42°C with the following pre-hybridization solution: 50% v/v formamide, 6X SSPE, 5X Denhardt's solution, 250 μg/mL Salmon sperm DNA, 0.5% SDS, 10% dextran sulphate. Amersham's random priming kit was used to make double-labelled probes from the cDNA inserts purified above (see Section 12.1 page 36). α-^{32}P-dCTP and α-^{32}P-dATP, specific activity 3000 mCi/mmol, were provided by ICN. Labelled probes were adjusted to a 300-μL volume in TE buffer (pH 8.0) and purified by elution at 500g through a Sephadex G-50 spin column. A 2-μL sample was taken from the eluate and analyzed for ^{32}P on the liquid scintillation counter. A 2.0x10^6 CPM quantity of labelled probe per mL pre-hybridization solution was then carefully added to the blot. Following overnight hybridization at 42°C, the probe was removed and the blot rinsed with: two 5-min rinses in 1X SSC, 0.1% SDS at room temperature, two 15-min rinses in 0.1X SSC, 0.1% SDS at 42°C, and two 45-min rinses in 0.1X SSC, 0.5% SDS at 42°C. Rinse volumes varied according to the surface area of the blot (2-4 mL/ cm^2)

RESULTS:

The results are presented in four sections each representing the particular experimental direction taken. The first series of experiments, entitled "Characterization of the metabolic signalling pathway", were designed to examine the effect of insulin stimulation in the A1-j mutant cell line with regards to only those responses related to homeostatic or metabolic control (e.g.: hexose transport, glycogen synthesis). Since the growth-promoting effects of insulin are generally believed to operate through a distinct signalling pathway (reviewed in De Meyts, 1994b[32], White and Khan, 1994[12]), these were examined in a separate series of experiments: "Characterization of the mitogenic signalling pathway". Having established a distinctive phenotypic response pattern for A1-j from the first sets of experiments, the third section: "Insulin signalling cascade", was devoted to determining the approximate location of the lesion(s) within the insulin-signalling cascade of the mutant. This was done by examining various known points along the cascade to determine if their signalling mechanisms are being in any way interfered with. Finally, the last group of experiments, entitled "Early Growth Gene Expression", examined the potential role of two well-characterized early growth response genes, c-fos and c-jun, in insulin-stimulated mitogenesis.

1 Characterization of the metabolic signalling pathway:

1.1 Hexose transport:

In characterizing the A1-j mutant, the first cellular response that was examined was the ability of insulin to stimulate hexose transport (see Table 1.1). A 2-way ANOVA revealed that, insulin stimulated a significant increase in transport in both cell lines at all concentrations used ($P<0.01$), with no significant difference observed between the two cell lines ($P>0.25$). In both V-79 and A1-j cells, the concentration-dependent effect appears to plateau between 6.7 nM and 67 nM insulin and treatment with 5% FBS was able to elicit a maximal response. Furthermore, the basal uptake values were virtually identical for both cell lines: 1954 ± 168 and 1992 ± 453 pmol 2DG/ mg protein/ 5 min for the V-79 and A1-j cell lines respectively (student's t-test: $P>0.80$). These findings are in complete agreement with those reported in an earlier study (Leckett and Germinario, 1992[1]).

1.2 Glycogen synthesis:

A series of time-course experiments revealed that glycogen synthesis, as monitored by incorporation of [U-^{14}C]-D-glucose into glycogen, peaked at 4 hours post-stimulation with 667 nM insulin in both V-79 and A1-j cell lines (Table 1.2A: Leckett *et al.*., 1993[164]). A 2-way ANOVA revealed a significant time dependence ($P<0.05$), yet the V-79 and A1-j responses were not significantly different ($P>0.05$).

Table 1.2B represents the concentration dependence profiles of insulin-stimulated glycogen synthesis in both cell lines at 4 hours post-stimulation. In the absence of hormonal stimulus, glycogen synthesis was found to be $1.83\pm0.34\times10^4$ DPM/ mg protein in V-79 cells and $1.76\pm0.53\times10^4$ DPM/ mg protein in A1-j cells revealing no significant difference by the student's t-test ($P>0.75$). As seen in table 1.2B and Fig. 1.2, both cell

lines exhibited a significant concentration dependent effect (2-way ANOVA: $P<0.001$). Interestingly, the difference between the mutant and parental responses was also found to be significant (2-way ANOVA: $P<0.05$). Furthermore, this difference was interactive with the concentration dependence (2-way ANOVA: $P<0.001$). The ED_{50} of the A1-j response to insulin was estimated from Fig. 1.2 and found to be 19nM which was almost half that seen in the parental V-79 strain: 34 nM ($P<0.001$). At 667 nM insulin, however, both cell lines respond equally: 1.56 ± 0.05 *vs* 1.58 ± 0.10 relative to basal synthesis (student's t: $P>0.77$).

2 *Characterization of the mitogenic signalling pathway:*

2.1 Growth curves:

The data depicted in Fig. 2.1 represent the results of a typical growth curve experiment wherein both cell lines were cultured under optimal conditions (i.e., in the presence of 5% FBS - Leckett and Germinario, 1992[1]). The doubling times were read from the linear, or log-phase, portion of the graph. The average doubling times from 3-4 separate experiments were determined to be 10.8 ± 0.25 and 10.6 ± 0.45 hours for V-79 and A1-j cells respectively. A student's t-test revealed no significant differences between the two cell lines ($P>0.60$). A number of workers in our lab have corroborated these findings reporting doubling times between 10-13 hours (unpublished data).

2.2 3-day growth assays:

For the 3-day growth assays, cells plated at 6.0×10^4 per plate were cultured for 3 days using various hormonal stimuli and then counted. Even in the absence of hormonal stimuli, both cell lines exhibited increases in numbers over the three day period

- the resulting basal counts being 3.6 $\pm$1.2 x10^5 and 3.9$\pm$1.5 x10^5 cells/plate for V-79 and A1-j cells respectively. A student's t-test revealed no significant difference between these two values ($P > 0.67$). In the presence of insulin, the V-79 cell line experienced a 2-fold stimulation of growth above basal levels which was found to be significant by the students t-test ($P < 0.01$). The results shown in Table 2.2 and Fig. 2.2 are expressed relative to basal growth levels· (average $\pm$ S.E.M.). Unlike their V-79 counterparts, the A1-j cells showed no significant response to insulin within this time frame (student's t-test: $P > 0.10$).

3 *Insulin signalling cascade:*

3.1 Thymidine incorporation studies:

Since the growth-promoting effects of insulin appear to be ineffective in the A1-j mutant, the next step was to determine if the mitogenic block had occurred early (i.e., at the G_1-S boundary) or late (i.e., the G_2 - M transition) in the cell cycle. Since DNA synthesis occurs in the S phase, increased transition from G_1 to S, following hormonal stimulation, would be manifested by an increase in thymidine incorporation into TCA-precipitable material. Fig 3.1A. displays the results from a single preliminary time course experiment (expressed relative to basal thymidine incorporation at each time point). Using both 667 nM insulin, and 5% FBS, maximal incorporation occurred between 8-10 hours post-stimulation reaching a stable plateau for up to 20 hours post-stimulation in both cell lines. A1-j cells, however, exhibited a diminished response to both stimuli relative to V-79 cells.

To investigate further, replicate experiments were performed at both 10 and 20

· This represents the number of cells grown in the presence of the various mitogens divided by the number of cells present in the basal medium for that same day.

hours following stimulation with either 667nM insulin or 5% FBS. The results, expressed relative to basal incorporation, represent the average of 3-4 replicate experiments (Table 3.1 and Fig. 3.1B). At both 0 hours and 20 hours post stimulation, insulin had no significant effect on thymidine incorporation in the mutant (student's t-test, 10h: $P>0.12$, 20h: $P>0.82$). The V-79 cell line, on the other hand, showed a greater than 2-fold increase at both times which was found to be significant by the student's t-test ($P<0.001$). Although both cell lines also exhibited significant responses to stimulation with 5% FBS (student's t-test: $P<0.001$), at 20 h, the A1-j response was markedly lower than that of the V-79 cells: 2.89 ± 0.63 *vs* 6.81 ± 1.38 (student's t-test: $P<0.01$). The fact that thymidine incorporation is affected in the mutant suggests that the A1-j phenotype may be attributable to a block at the G_1-S boundary in its cell cycle.

In addition to the lack of responsiveness to insulin, A1-j cells also exhibited a substantial increase in basal thymidine incorporation at both times. At 10 h, the V-79 cell line incorporated $3.81\pm0.62\times10^5$ DPM thymidine per mg protein *vs* $10.09\pm0.80\times10^5$ DPM/mg protein in A1-j cells. This represents a 2.64 ± 0.47-fold difference (student's t-test: $P<0.001$). At 20 h, basal thymidine incorporation was measured at $2.66\pm0.45\times10^5$ DPM/ mg protein and $5.36\pm1.11\times10^5$ DPM/ mg protein for V-79 and A1-j strains respectively, representing a 2.02 ± 0.54-fold difference (student's t-test: $P<0.001$).

3.2 Insulin binding studies:

Upon isolating the A1-j mutant cell line, among the first characteristics to be identified was a decreased number of insulin receptors available at the cell surface for binding insulin relative to the parental V-79 cell line (Leckett and Germinario, 1992[1]). These researchers also found that the V-79 cells specifically bound 11.2 ± 1.2 fmol ^{125}I-labelled insulin per mg protein while the A1-j strain bound only 4.0 ± 0.4 fmol/ mg protein (a 64.3 ± 9.1% decrease in binding). The results obtained in the current study support the observed decrease in specifically bound ^{125}I-insulin in A1-j cells:

12.00±1.44 *vs* 19.99±2.40 fmol/ mg protein in V-79 cells (a 40.0±10.2% decrease). Discrepancies between the two sets of results can be accounted for by differences in the protocols used to obtain the data. In the current study, binding was done at 4°C (instead of room temperature as done previously); and the BSA used to block non-specific binding was dialyzed prior to use in order to eliminate contaminating cell monolayers with unlabelled insulin. Furthermore, when undialyzed BSA was used and the assay performed at room temperature, the results were virtually identical to the earlier findings (unpublished observation).

3.3 Release of autocrine insulin binding proteins/ proteases:

One possible explanation for the non-responsiveness of the A1-j mutant cell line to the growth-promoting effects of insulin is the interference of a secreted autocrine factor. There are two mechanisms by which such a factor could conceivably achieve this end. The factor could represent an insulin-specific protease which, once released into the extra-cellular environment, proceeds to degrade any free insulin in the media before it can be bound and internalized by the target cells. The factor could also simply be a protein capable of binding to the extra-cellular insulin with enough affinity to effectively sequester it from its site of action on the cell surface. In either case, the presence of inhibitory autocrine factors can be tested by determining if culture media exposed to confluent monolayers of V-79 or A1-j cells is capable of suppressing an insulin-sensitive reporter system.

In this case, the insulin-sensitive reporter system that was monitored was the stimulation of DNA synthesis in FRTL-5 cells. Fig 3.3A shows the synergistic effect of adding insulin together with thyroid stimulating hormone (TSH) on DNA synthesis in FRTL-5 cells. Thymidine incorporation into TCA-precipitable material, at 10 h post stimulation, was considerably higher ($2.54\pm0.27\times10^5$ DPM/mg protein) following the combined stimulation with 6.7nM insulin and 1.0nM TSH than when basal conditions were used ($0.36\pm0.05\times10^5$ DPM/mg protein (a greater than 7-fold increase). Taking

$2.54 \pm 0.27 \times 10^5$ DPM/mg protein to be the maximal stimulation possible in this system ($100.0 \pm 10.6\%$), the addition of TSH alone only produced a $34.4 \pm 3.7\%$ maximal signal (Fig 3.3B).

When DMEM, conditioned overnight (12-18 h) with either V-79 or A1-j cell monolayers, was added to the insulin/TSH mixture, there was a slight decrease in the FRTL-5 response. At all three volumes used (50, 100, and 200 μL) the average signal obtained ranged from 70.5 ± 14.0 to $85.0 \pm 9.5\%$ of the maximum (Fig 3.3B). If an autocrine inhibitor were being secreted by A1-j cells in sufficient numbers to neutralize a 667 nM quantity of insulin (as used in the growth assays) one would expect a much more pronounced suppression of the FRTL-5 response upon addition of media conditioned with these cells relative to their V-79 counterparts. In fact, the response should approach that of TSH alone ($34.4 \pm 3.7\%$ of maximal) as the amount of available free insulin in the assay falls to zero. Furthermore, since the observed suppression is not maximal, one would expect to see a concentration-dependent effect, i.e., an increasing amount of suppression with increasing quantities of suppressor (in this case: volumes of conditioned media). However, 2-way ANOVA revealed that increasing the sample volumes had no significant effect ($P > 0.44$). Also, the decrease in signal obtained with the conditioned samples was not significantly different from that obtained when the same volumes of unconditioned DMEM were added (2-way ANOVA: $P > 0.46$). Taken together, these data suggest that the observed decrease is not due to the presence of an autocrine factor in the conditioned media samples, but is rather the result of dilution with the DMEM itself. It is also possible that one of the compounds comprising DMEM may be in some way interfering with the assay.

3.4 Insulin degradation:

Preliminary data obtained on insulin degradation suggested that the defect in the A1-j cell line may lie at the level of intra-cellular insulin processing. In order to investigate this further, the ability of V-79 and A1-j cells to degrade insulin was monitored by the appearance of TCA-soluble ^{125}I counts in both cell monolayers and the conditioning buffer following the binding of a cohort of ^{125}I-labelled insulin to cell monolayers.

Fig 3.4A demonstrates how rapidly insulin is processed and then quickly released into the conditioning buffer. As the degradation assay progresses, the amount of ^{125}I-insulin (soluble and precipitable) found in the cell monolayers steadily decreases with a concomitant increase in the amount found in the conditioning buffer. Within 15 min, greater than 50% of the label has been expelled into the conditioning buffer: $51.5\pm12.4\%$ and $53.4\pm9.7\%$ from V-79 and A1-j cell monolayers respectively. By 120 min, these values increased to $87.2\pm13.0\%$ and $83.5\pm17.5\%$ respectively. The data shown in Table and Fig 3.4A indicate that the efflux rates of insulin are virtually identical in the V-79 and A1-j cell lines (2-way ANOVA $P>0.77$). These results represent the average $\pm$ S.E.M. from 3-8 experiments.

Throughout the assay, the total amount of insulin in each cohort (i.e., the sum of insulin found in the conditioning buffer and that found in the cell monolayers) remained a constant 16.8 ± 2.1 fmol/ mg protein in V-79 cells and 13.2 ± 1.5 fmol/ mg protein in A1-j cells. For the A1-j cell line, this number reflects the amount of insulin initially bound to the cell monolayer (12.0 ± 1.44 fmol/mg protein) within the limits of experimental error. The value of 16.8 ± 2.06 fmol/mg protein for the V-79 strain, however, is significantly smaller than the amount of insulin initially bound: 20.0 ± 2.4 fmol/mg protein (student's t test: $0.005<P<0.001$). Since cells are otherwise treated identically in both binding and degradation assays, the 16% of insulin unaccounted for must have been removed during the second rinse with HHBS following the degradation assay (see Methods page 32).

Table 3.4B and Fig 3.4B display the amount of degraded insulin (as %TCA soluble counts) present in the conditioning buffer. After 20 min or less there was no significant difference between the degradation profiles of the 2 cell lines (2-way ANOVA: $P>0.12$). At times greater than 20 min however, degradation in A1-j cells was found to be significantly lower than that of V-79 cells (2-way ANOVA: $P<0.01$). This difference was also reflected by the insulin degradation observed within the cell monolayers (Table and Fig 3.4C) where A1-j cells showed significantly reduced degradation only after 20 min (2-way ANOVA - 20 min or less: $P>0.31$, greater than 20 min: $P<0.002$).

Although there is considerable controversy over the mechanisms underlying the intracellular degradation of internalized insulin, evidence is mounting that much of this degradation is occurring within the endosomal compartment of the cell (Berg *et al.*, 1995[120]). The three compounds: Bacitracin, Chloroquine, and Monensin, have been previously been shown to inhibit insulin degradation presumably by disrupting the normal functioning of endosomes. Bacitracin is a protease inhibitor whose principle mode of action is to directly inhibit insulin degrading activity (Gansler *et al.*, 1986[165]) presumably within the endosomal lumen. Chloroquine is an acidotropic agent that accumulates within acidified vacuoles (e.g.: lysosomes, some endocytic compartments), and inhibits the function of constituent acidophilic enzymes by raising the intralumenal pH. Similarly, carboxylic ionophores, such as Monensin, function as pores in the vacuolar membrane which dissipate the pH gradient across the membrane by allowing the free exchange of monovalent cations (i.e., K^+ for H^+). The effects of Chloroquine and Monensin have been reviewed by Mellman *et al.*, 1986 [121].

Based on their reported effectiveness in hepatocytes, these compounds were used in a number of preliminary experiments at the following concentrations: 100 U/mL Bacitracin, 100 μM Chloroquine, 25 μM Monensin (Backer *et al.*, 1990b[154], Blackard *et al.*, 1986[166], Hamel *et al.*, 1987[167]). Table 3.4D represents the average $\pm$ S.E.M. from two replicate 20-min degradation assays. The data are expressed as the percent of

the insulin cohort that was rescued by the inhibitor·. At the concentrations used, Chloroquine appeared to be most effective in both cell lines rescuing a total of 26.4 ± 1.4% of the cohorts bound to V-79 cells and 18.4 ±1.5% of those bound to A1-j cell monolayers. Conversely, 100 U/mL Bacitracin seemed to have a negligible effect in both cell lines: 7.93±5.34% and 3.04±5.26% insulin rescued from V-79 and A1-j cells respectively. Monensin had an intermediate effect: 9.0±3.2% and 12.5±1.6% for the V-79 and A1-j strains respectively. In the Monensin and Bacitracin-treated plates, there were no significant differences observed between the V-79 and A1-j responses (student's t: $P>0.20$). The A1-j response to Chloroquine, however, was significantly reduced relative to that observed in V-79 cells (student's t: $P<0.05$).

3.5 Peroxovanadium rescue studies:

The insulin-mimetic agent bpV(phen) was used to determine if the defect in the A1-j cell line lies within the insulin receptor itself. This compound has been previously shown to produce insulin-like responses in a number of different cell lines, by acting at a post-receptor step in the insulin signalling cascade - i.e., through the inhibition of an insulin receptor-associated phosphotyrosine phosphatase (Posner, B. *et al.*., 1994[156]). The ability of bpV(phen) to "rescue" the mitogenic response in A1-j cells would indicate that the defect had occurred at the level of the insulin receptor since this appears to be the only stage that is bypassed by the compound. The data in Table 3.5A and Fig 3.5A do not support this hypothesis.

· The term cohort designates the entire complement of ^{125}I-labelled insulin molecules that were prebound onto a cell monolayer during the 4 hour incubation period at 4°C (see materials and methods). The total amount of insulin degraded was expressed as the percentage of the sum of degraded insulin in the conditioning buffer and cell monolayers over the total amount of insulin in the cohort at each time point. The % cohort rescued represents the difference between % total insulin degraded in untreated plates and those treated with inhibitor.

At 10 hours following the addition of 1 μM bpV(phen) to V-79 cells, stimulation of thymidine incorporation into TCA precipitable material was 1.78$\pm$0.34-fold over basal conditions (student's t: $P<0.025$). Stimulation with 667 nM insulin had a comparable effect: a 2.34$\pm$0.42-fold increase over basal thymidine incorporation (student's t: $P<0.005$). When added together, these concentrations of insulin and bpV(phen) produced a signal only 2.28$\pm$0.41-fold greater than basal which was not significantly different from the effect of insulin alone ($P>0.25$). Neither of these compounds, added separately or together, was able to stimulate DNA synthesis above basal levels in the A1-j mutant cell line (student's t: $P>0.25$). Similar results were obtained at 20 h post-stimulation (Table 3.5B). Since bpV(phen) was unable to rescue the mutant phenotype, the results suggest that the A1-j defect lies at a post-receptor stage in the insulin signalling cascade.

3.6 Tyrosine phosphorylation of endogenous substrates:

One of the first steps following the binding of insulin to its receptor is the autophosphorylation of the receptor's β-chain and activation of its tyrosine kinase function. Once activated, this insulin receptor kinase (IRK) is capable of phosphorylating the tyrosine residues of a number of endogenous substrates within the target cell. The most important of these is a 170-180 kD protein known as insulin receptor substrate-1 (IRS-1). Using an antibody raised against phosphotyrosine residues, western blotting was performed on V-79 and A1-j cell extracts in order to determine if these early phosphorylation events are somehow being disrupted in the mutant. The results of a typical western blot are shown in Fig 3.6A. Swiss 3T3 cell extracts were loaded in lanes 1-3 as an experimental control. Given the relatively non-specific nature of the antigen, the anti-phosphotyrosine antibody was able to pick up a number of protein bands in each sample. Many of these, however, exhibit a stable phosphorylation pattern regardless of the stimulating conditions. In fact, the major band at 120 kD has been previously shown to be constitutively phosphorylated in rat liver cells (Rothenberg *et al.*, 1991[168]), Fao

Hepatoma cells (White *et al.*, 1985[169]), CHO cells (Sun *et al.*, 1991[62]), and NIH 3T3 HIR 3.5 cells (Goren and Boland, 1991[170]); and may serve as an internal loading/phosphorylation control for the current V-79/a1-j system. As a caveat for the general use of the pp120 band in this manner, there have been reports of insulin-stimulated phosphorylation of HA4, a sialylated 120 kD membrane-associated glycoprotein in rat liver cells (Rees-Jones and Taylor, 1985[171]; Perotti *et al.*, 1987[172]; Margolis *et al.*, 1988[173]).

Of particular interest are the bands at 95 kD and 180 kD: representing IRK and IRS-1 respectively. When 3T3 cells were stimulated 2 min with either 67 nM or 667 nM insulin (lanes 2 and 3), there is a substantial increase in the phosphorylation of these two bands relative to basal-stimulated extracts (lane 1). Interestingly, although a 2-min treatment with 5% FBS did appear to mildly stimulate the autophosphorylation of pp95 (the 95 kD band), there was no observable increase in the 180 kD band (data not shown). Lanes 4 and 5 contain V-79 cell extracts -/+ 2-min stimulation with 667 nM insulin, while lanes 6 and 7 contain similarly treated A1-j cell extracts. In both cell lines there is an insulin-stimulated increase in phosphorylation of the pp95 and pp180 bands (lane 5 *vs* lane 4 and lane7 *vs* lane 6) even though this increase is much less pronounced than that seen in the 3T3 controls.

In comparing the insulin-treated extracts in lanes 5 and 7, it appears that the insulin-responsive tyrosine-phosphorylation of pp95 and pp180 is noticeably weaker in A1-j than in V-79 even though both cell lines appear to be loaded equally (the pp120 bands are of equal intensity). This difference can, however, be accounted for by the lower number of functional insulin receptors in A1-j cells (40.0 ± 10.2 less than in V-79s). When V-79 cell samples were loaded at 2/3 the A1-j amount to account for this difference in receptor numbers, the insulin-stimulated phosphorylation pattern in A1-j cell extracts matched that seen in the V-79 cell extracts (Fig 3.6B lane 4 *vs* 2). Since there were no significant anomalies observed in the tyrosine-phosphorylation pattern of the A1-j mutant cell line, it appears that the lesion responsible for its lack of responsiveness to the mitogenic effects of insulin involves a step in the intra-cellular insulin signalling

cascade which lies beyond receptor autophosphorylation and tyrosine kinase activation.

4 Early growth gene expression:

Since insulin fails to stimulate the kind of growth in the A1-j mutant cell line as it does in the parental V-79 strain, we wanted to determine how this lack of responsiveness relates to the expression of genes that regulate the passage through the cell division cycle. The results of the thymidine incorporation data (see page 42) place the defect near the G_1-S boundary which falls under the purview of the early growth response genes. A number of such genes (e.g.: c-fos, c-jun) have been implicated in the mitogenic response to insulin. Northern analysis was performed on the extracts of both V-79 and A1-j cells at various times following stimulation with 5% FBS or 667 nM insulin. Unfortunately, insulin-stimulated cell extracts from both cell lines failed to produce a detectable signal at any of the time points examined. The following results were obtained using V-79 and A1-j mRNA extracts following stimulation with 5% FBS.

4.1 Expression of c-fos:

Total RNA from both V-79 and A1-j cell lines was extracted at 0, 1, 2, and 4 hours following stimulation with 5% FBS. These samples were probed with the *c-fos* probe resulting in the banding pattern shown in Fig 4.1A. The bands are located at approximately 2.2 kB which is the size of the murine *c-fos* transcript (Weiland *et al.*, 1991[105]). Maximal stimulation occurred at 1 hour post-stimulation with earlier time points (i.e., 10, 20, 30 min) displaying sub-maximal responses in both cell lines (data not shown). Furthermore, expression of *c-fos* in the control HeLa extract was significantly greater (greater than 5-fold above the maximal signal seen in V-79 cells) than in either of the other two cell lines (data not shown). Below the *c-fos* band, is displayed another at 1.4 kB which resulted when the same blot was probed for GAPDH

(Bhatia *et al.*, 1994[174]). Since GAPDH is constitutively expressed (Maniatis, T., *et al.*, 1982[161]) any differences observed between the samples can be attributed to inaccuracies in sample loading. Note that the 0 and 1 hour time points for V-79 cells (lanes 1 and 2) appear to be underloaded relative to the other samples. Following quantification of the bands using an optical densitometer, differences in sample loading were accounted for by dividing each *c-fos* reading by that of GAPDH. The results, expressed as a percent of the maximal stimulation in V-79 cells, are shown in Fig 4.1B. Although both cell lines show maximal expression at 1 hour post-stimulus, the signal in A1-j cells is 46.4% that of the V-79 strain (a greater than 2-fold difference).

4.2 Expression of c-jun:

As was the case with *c-fos*, *c-jun* expression peaked at 1 hour post-stimulus in both V-79 and A1-j cell lines. Messenger RNA transcripts of the *c-jun* proto-oncogene were observed as a 2.7 kB band on the blot (Fig 4.2A). This is in agreement with its reported molecular weight (Ryder and Nathans, 1988[175]). The GAPDH loading control is displayed directly below. Fig 4.2B shows the normalized optical density readings for both cell lines. At 1 hour post-stimulus, the maximal *c-jun* signal in A1-j cells represents only 9.1% of that observed in their V-79 counterparts. Since the hormonally induced expression of *c-jun* has been previously shown to be dependent upon the level of c-Fos protein present (Angel and Karin, 1991[103]), it is not surprising to find that the reduction in *c-fos* transcription: 46.4% relative to V-79 levels, leads to an even greater reduction in *c-jun* transcription: 9.1% relative to V-79 levels. Interestingly, although the expression of both *c-fos* and *c-jun* mRNA is reduced in A1-j cells relative to V-79 cells at every other time point measured, mRNA levels of both proto-oncogenes appears to be slightly elevated at the 4 hour time point. Since sufficient data was lacking for statistical analysis of these results, the significance of this observation is unclear at present.

DISCUSSION:

The mitogenic block is specific to insulin and IGF-I:

After having isolated the DTa-resistant mutants, one of the first properties that was measured was their ability to grow and divide in serum-supplemented media (R. Germinario - pers. comm.). A few of the mutants, such as VI-A3-b, VI-A4-d and VI-A5-d, exhibited a generalized suppression in mitogenic signalling as manifested by increased doubling times when grown in 5% FBS (Leckett, 1991[147]; A. Spurmanis - unpublished observation). This, however, did not appear to be the case with the IV-A1-j mutant which grew as well as the parental V-79 strain (T_D = 12 - 13 hours) when grown in FBS (Leckett *et al.*, 1993[164]). What was interesting about A1-j was its inability to grow in the presence of insulin as the sole mitogen. Although both cell lines were able to grow and divide comparably (about 6-fold over a 3 day period) under basal conditions, the addition of insulin was able to elicit a further 2-fold stimulation of growth where none was seen in the A1-j mutant. The same results were obtained when protein and DNA content was measured (data not shown). Furthermore, cell growth could be qualitatively confirmed by visual inspection of the phenol red indicator in the culture media. When grown under basal conditions, the media in the plates containing either V-79 or A1-j cells appeared red due to the limited production of acidic metabolic waste by-products. Conversely, the media from plates containing actively growing cells in 5% FBS were yellow due to a drop in the extracellular pH caused by lactate production (R. Germinario - pers comm). Insulin-stimulated V-79 cells, showing intermediate growth, produced orange-colored media while media exposed to A1-j cells, showing no growth above basal levels, remained red.

The fact that A1-j could grow as well in serum as the parental V-79 strain, yet was non-responsive to the mitogenic effects of insulin suggested that the latter effect is specific to the insulin signalling pathway. This was supported by the observation that

two unrelated mitogens, α-thrombin (α-THR) and epidermal growth factor (EGF), were able to stimulate growth in the mutant (The results for insulin, α-THR and EGF are summarized in Table I). In the absence of insulin or IGF-I, both cell lines exhibited equal responses to α-THR and EGF representing about 40-50% of serum stimulated growth when added alone or in combination (Leckett *et al.*, 1993[164]). Further addition of insulin or IGF-I resulted in the apparent reconstitution of the serum-induced response in V-79 cells (101±3% FBS-stimulated growth), but had no effect in the A1-j cell line. Interestingly, when added alone, IGF-I was also unable to stimulate mitogenesis in the A1-j mutant cells even though its effects on the V-79 strain were comparable to those seen with insulin (Leckett *et al.*, 1993[164]). Thus the mitogenic block in the A1-j mutant appears to be confined to a signalling pathway shared by insulin and IGF-I but not by the other two growth factors tested. This is not surprising considering that not only are these ligands able to cross-react with each other's receptors (Werner *et al.*, 1991[176]), but also appear to mediate their biological effects through the same intracellular signalling cascade (Melmed, 1993[177]).

Metabolic signalling in A1-j:

In both V-79 and A1-j cell lines, an increase in hexose transport of approximately 25-30% was observed following stimulation with 6.7 nM insulin. Furthermore, a similar concentration dependent increase (to 60% stimulation above basal) was seen in both cell lines when the insulin concentration was raised to 67 nM insulin. Increasing the insulin concentration to 667 nM had no further effect producing a 60% stimulation in 2-DG uptake in both V-79 and A1-j cell lines.

The findings with glycogen synthesis essentially parallel those seen with hexose uptake in that no reduction of the insulin stimulated response was observed in A1-j cells relative to measurements in V-79 cells. Furthermore, both cell lines exhibited the same temporal response patterns (Table 1.2A), and were maximally stimulated with 667 nM insulin to levels 55-60% above basal (Table 1.2B, Fig 1.2). The A1-j cell line was in

fact more responsive to insulin stimulation than their V-79 counterparts vis-a-vis glycogen synthesis. The ED_{50} of the A1-j response in Fig. 1.2 was 19 nM, almost half that seen in V-79 cells (34 nM - $P<0.001$). This latter finding was unexpected considering that A1-j cells were originally selected to be resistant to the stimulatory effects of insulin. In light of the fact that the mitogenic signalling pathway of insulin is blocked in the A1-j cell line, one possible explanation for the above observations is that some of the post-receptor events in the insulin signalling cascade exhibit a responsiveness that is somehow balanced between two, or possibly more, signalling pathways and that the abrogation of one of the branch points results in the diversion of signalling potential to the remaining functional branches. This interpretation is supported by earlier studies involving the stable transfection of C-terminally truncated insulin receptors into Rat-1 cells (Thies *et al.*, 1989[178]). Here, the authors observed that enhanced mitogenesis was accompanied by decreased metabolic responsiveness (ie.: stimulation of glucose transport and glycogen synthesis).

Interestingly, several other reports (reviewed in Tavaré and Siddle, 1993[36]) have also described enhanced mitogenic signalling by truncated insulin receptors although the parallel effects on metabolic signalling were variable·. One likely source of this variation is the requirement of other cell context factors in order to mediate the intracellular routing of the insulin signal. Since these factors have not been defined as of yet, their expression may be subject to cell-specific or clonal variation† resulting in the kind of discrepancies reported in the literature. Nonetheless, it appears that the C-terminal region of the IR does play a role in this regard. This is corroborated by the finding that

---

· Some studies reported that truncation had no effect on metabolic signalling although mitogenesis was enhanced, while still others reported that the mutation had no effect on either signalling pathway (Tavaré and Siddle, 1993[36]).

† The term cell-specific variation is used to describe diffrences in gene expression between cell lines of dissimilar origin (e.g., rat hepatocytes *vs* rat adipocytes, or human adipocytes and 3T3 adipocytes). Clonal variation pertains to differences in gene expression observed when comparing different colonies of cells isolated from the same source or different passages of a cultured cell line.

the IR C-terminus was able to mediate enhanced glycogen synthesis when included as part of a IR/IGF-IR hybrid (Tartare *et al.*, 1994[179]). A more recent report suggests a potential molecular connection between the C-terminus and at least one potential context factor. Baron and co-workers discovered that an acidic portion (residues 1270-1280) of its C-terminus was able to modulate the exogenous kinase activity of the insulin receptor upon association with histone *in vitro* (Baron *et al.*, 1995[48]). Due to its nuclear localization, histone is not likely to be involved in a physiologically relevant association with the insulin receptor. The identity of the corresponding endogenous peptide is not currently known. If it were found that the C-terminus of the insulin receptor is implicated in the A1-j phenotype, it would be tempting to speculate that this domain is somehow involved in endosomal trafficking or processing of insulin or its receptor. The latter hypothesis is based on the observation that the current data collected on the mutant are consistent with endosomal re-routing of insulin and its receptor (see *The involvement of insulin- and insulin receptor-processing* below).

The G1→S transition is uncoupled from hormonal stimulation in A1-j:

The inability of insulin to stimulate thymidine incorporation into TCA precipitable material in A1-j cells, where the corresponding V-79 response was greater than 2-fold (Table/Fig 3.1B), places the mitogenic defect at the boundary between G_1 and S. The straight forward explanation for this observation is that the initiation of DNA synthesis has somehow become uncoupled from the signalling mechanisms controlled by insulin. This partial uncoupling from hormonal stimulation may also explain why basal thymidine incorporation levels are elevated 2-fold in A1-j cells relative to V-79 cells ($P < 0.001$). In the latter case, uncoupling of the DNA synthesizing machinery from negative regulatory elements in the insulin signalling cascade, would presumably be unleashing an intrinsically elevated basal activity. Also, the higher basal activity in the A1-j cell line does not entirely account for the observed reduction of the 5% FBS-stimulated signal at 20 h since absolute thymidine incorporation values were also significantly different at

this time point: $1.81 \pm 0.20 \times 10^6$ *vs* $1.55 \pm 0.11 \times 10^6$ DPM/ mg protein in V-79 and A1-j cells respectively ($P < 0.004$).

The idea that the A1-j defect is related to a partial uncoupling from hormonal regulation is further supported by observed differences in the expression of *c-fos* and *c-jun* proto-oncogenes between V-79 and A1-j cells grown in 5% FBS. Curiously, the literature generally reports maximal stimulation of both genes within 15-30 min following hormonal stimulation. In the current system, however, expression of *c-fos* and *c-jun* at times earlier than 1 hour resulted in sub-maximal expression (data not shown). As shown in Fig 4.1B, the expression of *c-fos* is significantly blunted in the A1-j cell line demonstrating only 46.4% of the level seen in the V-79 strain. Since an important role of the c-Fos protein is to link the activation of the AP-1 complex to hormonal stimulation (Angel and Karin, 1991[103]), reduced *c-fos* transcription would, among other things, have the effect of weakening this link. This is reflected by an even greater reduction in *c-jun* mRNA levels seen in the mutant (showing only 9.1% of the maximal expression seen in V-79 cells at 1 hour post-stimulus).

How the altered expression of *c-fos* and *c-jun* in A1-j relate to the stimulation of DNA synthesis is not clear especially since no known enzymes which participate in the latter process are regulated by AP-1 binding (Angel and Karin, 1991[103]). Furthermore, the elevated basal thymidine incorporation observed in the mutant cannot be attributed directly to enhanced *c-jun* expression since *c-jun* mRNA levels are actually decreased in A1-j cells relative to their V-79 counterparts in the absence of hormonal stimulation (see Fig 4.2B - 0 h). It is also interesting to note that, even though basal DNA synthesis is elevated in the A1-j cell line, this does not translate to increased growth in basal medium since both cell lines display the same 6-fold increase in cell numbers when grown for 3 days in DMEM alone. This, however, can readily be accounted for by the fact that growth is dependent upon the transition not only through the $G_1 \rightarrow S$ interface, but also through other stages of the cell cycle as well. Therefore, even if the mutant were traversing the $G_1 \rightarrow S$ boundary more readily than the V-79 cell line, growth may be held back at some other stage: the $G_2 \rightarrow M$ transition for example. Alternatively, the possibility

cannot be entirely excluded that the elevated basal thymidine incorporation in the mutant represents some alteration in thymidine metabolism (e.g.: a reduction intracellular thymidine pools). Yet another possibility is that the observed increase in basal DNA synthesis in the A1-j cell line does not relate to genomic duplication but may rather reflect the activation of a futile nucleotide sythesis process which is unrelated to cell division.

The known functions of the insulin receptor appear to be intact in A1-j:

Given the insulin-specific nature of the mitogenic block in A1-j cells, one obvious candidate for the causative genetic lesion is the insulin receptor itself since it acts in linking the specific recognition of the peptide hormone to subsequent intracellular events. As the evidence detailed below suggests, the insulin receptor appears to function normally in the mutant. It should be noted, however, that these experiments were designed to test previously well-characterized functions of the insulin receptor such as ligand binding or tyrosine kinase activity. Since the function of some portions of the receptor are not entirely clear (particularly the C-terminus), one cannot rule out the possibility that the causative lesion may still be found here.

Scatchard analysis (Leckett and Germinario, 1992[1]) revealed that although the receptor binding affinities were the same (ED_{50}=0.5 nM), the A1-j cell has up to 50% fewer insulin receptors expressed at its plasma membrane surface than does the V-79 cell (800 *vs* 1500 respectively - Leckett and Germinario, 1992[1]). ^{125}I-insulin displacement studies also showed a 40 - 50% decrease in specific binding thus corroborating these earlier findings. Although it is presently unclear how this observation relates to the mitogenic block in the A1-j cell line, there is evidence against a causal relationship (see *The involvement of insulin- and insulin receptor-processing* below). Furthermore, in addition to binding affinity, several other features of the mutant receptor were tested and found to be normal. Others have found that, when normalized to receptor number, both cell lines demonstrated identical internalization kinetics (Leckett and Germinario, 1992[1])

suggesting that both lateral translocation and endocytosis are occurring normally. Fig. X shows that internalization rises rapidly in both cell lines (within 5-7 min) followed by a slower but steady decrease in internalized ligand. These data are in general agreement with the internalization pattern observed for Fao hepatoma cells (Backer *et al.*, 1990b[154]). In the latter study, the amount of internalized insulin peaked within 3-5 min followed by a rapid decrease. In the above cases, the decrease in internalized insulin can be attributed to rapid intracellular degradation and subsequent expulsion into the extracellular fluid (Backer *et al.*, 1990b[154]).

Under basal conditions, the insulin receptor is believed to run a futile cycle whereby its β-subunits undergo continual rounds of autophosphorylation rapidly followed by dephosphorylation via tightly associated phosphotyrosine phosphatase (PTPase - Bevan *et al.*, 1995[123]; Kublaoui *et al.*, 1995[64]). The compound bpV(phen) is able to stimulate phosphorylation of the β-subunits by inhibiting the activity of PTPase and thereby bypasses the requirement of insulin binding. In fact, bpV(phen) alone was found to be almost as effective as insulin in stimulating the incorporation of thymidine into TCA precipitable material in V-79 cells: 1.78 ± 0.34 *vs* 2.34 ± 0.42 fold over basal respectively (Fig/Table 3.5A). This is in agreement with a previous report which attributed the slightly lower effectiveness of bpV(phen) to the fact that *insulin*-stimulated activation of IRK probably involves more than just the release of PTPase-induced suppression (Posner, B. *et al.*, 1994[156]). The fact that bpV(phen) was unable to produce a comparable response in A1-j cells, either alone or together with insulin indicates that bypassing the ligand binding step has no effect on the mutant phenotype. Thus, the genetic lesion in the A1-j cell line must therefore lie beyond the level of the insulin-receptor interaction.

Even though the evidence suggests that the ligand binding domain and internalization sequences remain intact in the mutant, there is still the question of the receptor's tyrosine kinase activity. To this end, insulin-stimulated phosphorylation of the receptor β-chain and the phosphorylation of endogenous substrate IRS-1 were measured by anti-phosphotyrosine western analysis. Both were found to be decreased in the mutant

relative to V-79 cells when extracts were loaded equally (Fig. 3.6A lane 6 *vs* 8). However, when cell extracts were loaded to correct for differences in receptor number (i.e., 2/3 the amount of V-79 cell extracts were loaded relative to A1-j cell extracts since the latter were observed to express 60.0$\pm$10.2% the number of active surface receptors), both cell lines appear to generate identical banding patterns (Fig 3.6B lane 2 *vs* 4). Thus, although the absolute amount of tyrosine phosphorylation is decreased in the mutant, IRK and IRS-1 phosphorylation were proportionate to the number of functional receptors found in each cell line. This indicates that both autophosphorylation and kinase activity are not affected in the mutant.

Evidence for a post-receptor mutation:

The above data suggest that the causative genetic lesion in the A1-j mutant cell line does not lie within the insulin receptor itself. This is further supported by the observation that both insulin and IGF-I were able to stimulate growth in V-79 cells but were unable to do so in the A1-j cell line (see below). Conversely, the finding that basal thymidine levels, which would presumably not be directly related to insulin-stimulated activity, were elevated in A1-j cells (see *The G1→S transition is uncoupled from hormonal stimulation in A1-j* above) does not necessarily preclude a receptor mutation. Considering that both C-terminal and juxtamembrane regions of the receptor appear to be involved in coupling the receptor to downstream signalling events, a mutation in either of these domains could conceivably result in the observed mitogenic uncoupling. Similarly, the altered induction of serum-stimulated *c-fos* and *c-jun* transcription may represent secondary effects which may not be directly related to the causative lesion.

Even though neither insulin nor IGF-I was able to stimulate growth in the mutant, only the surface expression of insulin receptors was affected (Leckett and Germinario, 1992[1]). IGF-I binding was the same in V-79 and A1-j cells: 19.8$\pm$1.2 *vs* 18.7$\pm$2.2 fmol/ mg protein respectively (Leckett and Germinario, 1992[1]). One way to account for

the finding that signalling has been affected similarly by both hormones, while the corresponding receptors have been affected differentially, is that the genetic lesion involves a post-receptor event common to both insulin and IGF-I. In support of this hypothesis, it was subsequently discovered that all of the downstream effectors implicated in insulin signalling to date are also reported to be involved in the IGF-I signalling cascade (Cheatham and Khan, 1995[35]; Melmed, 1993[177]).

It can also be argued, however, that a mutation in one of the two receptors could be sufficient to produce the A1-j phenotype if both hormones were mediating their mitogenic effects through that particular receptor. To this effect, the probability that IGF-I is exerting its mitogenic effects in V-79 cells solely through insulin receptors is highly unlikely considering that IGF-I receptors are present in comparable numbers· at the cell surface. Not only is the IGF-IR considered to be a dominant mitogenic effector in relation to the IR from the standpoint of β-chain signalling activity (Cheatham and Khan, 1995[35]; De Meyts, 1994b[32]; Lee and Pilch, 1994[30]), but IGF-I also possesses a 100- to 500-fold greater affinity for its own receptor than for IR (Werner *et al.*, 1991[176]). Conversely, it is possible that insulin can be mediating its mitogenic effects through IGF-I in the V-79 cell line. Even though the affinity of insulin for IR is 100 to 500 times greater than that for IGF-IR, most of the assays performed in the current and previous studies used insulin concentrations that exceed physiological levels by up to 700-fold raising the potential for a significant amount of receptor "cross-activation". Although impairment of the IGF-IR could possibly account for the mitogenic block in the A1-j cell line, it is difficult to envisage how such a mutation could result in the altered expression of the insulin receptor that was observed.

· Given that both IR and IGF-IR have similar affinities for their respective ligands (Kd = 1nM- Werner *et al.*, 1991[176]), the fact that ^{125}I-IGF-I binding (19.8$\pm$1.2 fmol/ mg protein) was found to be similar to ^{125}I-insulin binding in V-79 (11.2$\pm$1.2 fmol/ mg protein) means that these receptors are present in similar proportions on the cell surface.

The involvement of insulin- and insulin receptor-processing:

Although the data collected thus far cannot formally exclude the possibility that the causative genetic lesion in the A1-j cell line exists at the level of the insulin receptor, ligand binding, endocytosis, autophosphorylation, and tyrosine kinase activity do not appear to be involved. Neither is the secretion an inhibitory autocrine factor since media conditioned by exposure to A1-j cell monolayers was unable to disrupt the synergistic stimulation of DNA synthesis of insulin + TSH in a FRTL-5 reporter system (Fig. 3.3 A and B). It is, however, very likely that the mutant phenotype is related to an alteration in the intracellular trafficking of insulin and/or the insulin receptor following internalization. The reason for this is that the mutants were originally selected for their resistance to a toxic diphtheria A-chain/ insulin conjugate (Leckett and Germinario[1]). Considering that its endosomal network hasn't developed a way to directly inactivate DTa·, the only way to overcome DTaI toxicity would be to prevent its entry into the cytosol by re-routing it to another compartment. One way would be to selectively target it to the lysosomes for destruction.

In both cell lines, insulin degradation, as monitored by the appearance of TCA-soluble counts in the conditioning buffer, was found to follow biphasic kinetics (Fig. 3.4B). In order to understand how this occurs, it is important to first realize that the proteolytic processing of insulin is mediated through several "cycles" of insulin-receptor internalization, ligand dissociation, and receptor recycling. The first kinetic phase ($t \leq$ 15-20 min), represents the first wave of receptor internalization whereby a large proportion (about 30%) of the pre-bound ^{125}I-insulin cohort is rapidly internalized, degraded, and expelled back into the conditioning buffer. At this stage, the A1-j and V-79 cells exhibit similar activity ($P > 0.12$). The second kinetic phase ($t >$ 20 min) is slower and represents subsequent endocytic cycles where the number of active insulin-receptor complexes at the cell surface are becoming increasingly scarce. As a result, the

---

· Otherwise A1-j would be less sensitive to whole DT than V-79 which is not the case (Leckett and Germinario, 1992[1]).

stochastic process of receptor aggregation into clathrin-coated pits becomes increasingly less likely eventually limiting the amount of insulin internalization and degradation. Meanwhile, empty receptors are being recycled back to the cell surface (Backer *et al.*, 1990b[154]).

Interestingly, the proteolytic activity of the A1-j cell line appears to be consistently reduced relative to V-79 cells during the second phase ($P<0.01$). This could be due to the fact that the intracellular processing of insulin has been in some way altered in the A1-j strain. Interestingly, it has been previously reported that mutant CHO cells exhibiting defective acidification of the endosomal compartment were found to be resistant to the killing effects of whole diphtheria toxin (Merion *et al.*, 1983[180]). Although the cytosolic penetration of DT has been shown to require processing through an acidic compartment, this has been mainly attributed to conformational changes induced in the carrier B-chain portion of the toxin which is absent in DTaI (Madshus, 1994[181]). There is, however, evidence that endosomal acidification is required to induce unfolding of the A fragment in order to allow for its translocation into the cytoplasm (Falnes *et al.*, 1994[182]). Since insulin degradation has also been associated with endosomal acidification (reviewed in Berg *et al.*, 1995[120]), it is likely that a perturbation in endosomal processing of insulin represents a common mechanism for the observed DTaI resistance and decreased insulin proteolysis in A1-j.

Comparable results were obtained by monitoring TCA-soluble ^{125}I counts within the cell monolayer lysates although the kinetics in this case were further complicated by the rapid expulsion of degraded insulin following proteolysis (Fig. 3.4C). Earlier time points show parallel degradation kinetics ($P>0.31$), while at later time points degradation appeared to be diminished in A1-j ($P<0.002$). A lag of 5 min or less was observed prior to the initiation of degradation which is consistent with an endosomal mode of

degradation (Backer *et al.*, 1990b[154]). Interestingly, when Chinese hamster ovary cells (CHO)· were stably transfected with 80,000 surface-expressed human insulin receptors, a 20-minute lag time was observed before the onset of degradation (Backer *et al.*, 1990b[154]). Although the authors attributed their findings to the innate tendency of these cells to process insulin through a lysosomal pathway, it is possible that their observation is simply an artifact caused by the transfection. It could be that the endogenous endocytic machinery of the CHO cells was simply overwhelmed by the surplus of human receptors resulting in delays and/or other perturbations in the normal intracellular routing mechanism. Alternatively, the different handling of insulin by CHO and the CHL† cell lines studied here could also be the result of cell-specific or clonal variation.

While it was suggested that the slight reduction in insulin proteolysis in A1-j at time points greater than 20 min could be attributed to a perturbation in endosomal processing of the internalized ligand-receptor complex, one could speculate on another possibility. The decreased number of insulin receptors expressed at the plasma membrane surface could simply be limiting proteolysis by reducing the availability of active insulin-receptor complexes for the formation internalizable aggregates. To further explore the ability of A1-j to process intracellular insulin, the effect of a number of endosomal "inhibitors" was explored. The results reported in Table 3.4D are based on the addition of concentrations previously reported to be effective in other cell lines (see *Insulin degradation* in the Results section above). Since an earlier report indicated that the inhibitors would be maximally effective at earlier time points (Backer *et al.*, 1990b[154]), the inhibition assays were all performed at 20 min. At 100 U/mL, bacitracin had almost no effect in inhibiting proteolysis in either cell line, while 25μM monensin was only marginally effective resulting in the rescue of 9-12% of the pre-bound insulin cohort. Chloroquine at a concentration of 100 μM was the most effective being able to

---

· Not only do these cells originate from the same animal species as V-79 but also express comparable numbers (3000) of endogenous insulin receptors at the plasma membrane surface.

† CHL: Chinese hamster lung (i.e., V-79 and A1-j).

rescue 26.4 ± 1.4% of the V-79-bound insulin cohort and 18.4± 1.5% of the A1-j-bound cohort. At this point, however, it is not possible to assess the relative effectiveness of these agents since optimal concentrations were not rigorously established for the current system. In fact, a preliminary concentration-dependence profile demonstrated that increasing the concentrations of bacitracin and chloroquine 10-fold (to 1000 U/mL and 1 mM respectively) significantly enhanced cohort rescue, while a similar increase had little impact on the effectiveness of monensin (data not shown).

Of the three agents tested, only the response of A1-j cells to chloroquine was significantly reduced relative to that of the V-79 cell line ($P<0.05$). Since this compound acts as an acidotropic agent that disrupts endosomal function by raising the intralumenal pH, resistance to chloroquine suggests that insulin proteolysis in the A1-j cell line is being shifted to a process less dependent on, or possibly independent of, acidification. Precedence for such a mechanism does exist in the literature in the discovery of a cytosolically expressed specific insulin protease whose pH optimum is 7.4 (Kuo *et al.*, 1991[155]). Furthermore, an independent group of researchers reported significant endosomally-mediated insulin degradation in the absence of acidification (Hamel *et al.*, 1991[183]). Thus the endosomal processing of insulin may not be simply defined by a single molecular pathway, but rather by a combination of overlapping and possibly redundant processes.

Although the existence of multiple endosomal processing mechanisms clearly has implications regarding the processing of ligand-receptor complexes, it may play an equally important role in directing the post-receptor signal if it can be shown to be directly related to the mitogenic block in A1-j. In support of this hypothesis, a group of researchers in Japan has recently reported that when endosomal acidification was blocked in mouse embryonic liver cells, growth in DMEM+12% FBS was significantly compromised (Manabe *et al.*, 1993[184]). Additionally, Bergeron and co-workers have amassed a significant body of evidence establishing the importance of endosomes in insulin signalling (Bevan *et al.*, 1995[123]). Their work, in addition to ground-breaking studies by Kelly and Ruderman (Kelly and Ruderman, 1993[61]) and Pilch and co-workers

(Kublaoui *et al.*, 1995[64]), suggest that sub-cellular localization may play a key role in the routing of post-receptor signalling events to different biological endpoints.

Another interesting feature of the A1-j mutant cell line is the presence of fewer insulin receptors at its plasma membrane surface than seen in the parental V-79 strain. Although this could be the result of suppressed transcription and/or post-translational modifications, or of increased degradation of IR mRNA, two lines of evidence suggest that receptor proteolysis is enhanced in the mutant. Firstly, although decreased mRNA expression has been shown to result in decreased surface receptor numbers, this type of receptor down-regulation has been found to correlate with increased mitogenic potential (Levy and Hug, 1992[138]) which runs contrary to the observed behaviour in A1-j. Secondly, the above data are strongly suggestive of a perturbation in the endosomal trafficking of insulin-receptor complex. Although the importance of endosomal trafficking to insulin receptor expression is well established (Knutson, 1991a[142]; Knutson, 1991b[143]), the underlying molecular mechanisms are poorly understood.

The observation that insulin processing is less sensitive to chloroquine in the mutant suggests that insulin-receptor complexes may have been re-routed to a degradation pathway which is less dependent upon endosomal acidification. Such a pathway could involve the cytosolically located 110 kD insulin degrading enzyme (IDE) which operates at a pH optimum of 7.4 (Kuo *et al.*, 1991[155]). Recent characterization of IDE has revealed that it is tightly associated with a large multicatalytic proteinase complex (MCP) which has been localized to a cytoplasmic organelle called the prosome· (Bennett *et al.*, 1994[185]). Furthermore, the association of insulin with IDE has been shown to inhibit some of the proteolytic activity in MCP (Duckworth *et al.*, 1994[186]). Aside from ascribed roles in both ubiquitin-dependent and independent proteolytic pathways, MCP has also been implicated in cell growth and proliferation (Amsterdam *et al.*, 1993[187]). It is therefore conceivable that the A1-j mutation somehow involves the re-routing of the insulin-receptor complex from normal endosomal pathways to the prosome (see Fig XI). In this instance it not difficult to envisage how the insulin receptor, as well as insulin or

---

· The prosome is characterized as a ubiquitous cylindrical cytoplasmic organelle.

DTaI, may fall prey to the multiple proteolytic activities of MCP.

The proposed model also suggests possible roles for both the insulin receptor PTPase and PKC which have also been implicated in insulin receptor trafficking (see **Introduction** page 25). In this model, the association of the insulin receptor with PTPase is broken by allosteric changes brought about by ligand binding. Subsequent uncoupling of insulin from its receptor in the endosome triggers the re-association of the latter with PTPase resulting in receptor inactivation and recycling to the plasma membrane surface. Under conditions of chronic insulin exposure, this pathway may somehow become overloaded, possibly due to the limited availability of PTPase. PKC, on the other hand may either promote or inhibit re-association depending upon other cell context factors. When receptor recycling is prevented in this manner the receptors are targeted for destruction. It appears likely that final proteolysis of insulin and/or its receptor into component amino acids involves lysosomal participation although the involvement of the prosome in insulin- or PKC-induced IR destruction remains an open question.

Summary:

The current body of research details the characterization of a mutant Chinese hamster fibroblast line, A1-j, which was selected for its resistance to a toxic insulin-diphtheria A-chain conjugate. Although an insulin-resistant phenotype was anticipated, here we report that two important metabolic effects, namely stimulation of glucose transport and glycogen synthesis, remained intact in the mutant. Further examination revealed that the A1-j cell line was unable to respond to the mitogenic effects of insulin or the related peptide IGF-I like its parental V-79 strain. Although the mutation was localized to an early event (i.e., the $G_1 \rightarrow S$ boundary) in the insulin signalling cascade, most of the functions associated with the receptor, namely: ligand binding, internalization, autophosphorylation and tyrosine kinase activity, were unaffected. The possibility that the mutation involves either the insulin and/or IGF-I receptors could not

be formally excluded but is considered unlikely because the biological effectiveness of both hormones was abrogated even though the expression of their respective receptors was affected differentially in A1-j cells. In addition to a decrease in the number of surface-expressed insulin receptors, the mutant also demonstrated insulin proteolysis which appears to be less dependent upon endosomal acidification than its V-79 counterparts. Taken together, the data suggest that the mutation in the A1-j cell line has resulted in the re-routing of internalized insulin-receptor complexes from the normal endocytic pathway leading to receptor recycling, to one which mediates receptor inactivation/proteolysis. Although the nature of this re-routing is not known at present, extrapolation from other studies in the literature suggests that the prosome may somehow be involved.

Future directions:

Since the first inception of this project many discoveries have been made regarding the post-receptor events in insulin signalling leaving many new avenues open to explore. For instance, now that effectors in the tyrosine phosphorylation cascade have been identified, one could conceivably develop an entire research project around determining how these second messengers have been affected by the A1-j mutation. Naturally, the Ras-MAPK pathway would be of particular interest since it is believed to be central in mediating insulin's mitogenic response. In a complementary set of experiments, one could further characterize the metabolic pathway by exploring the PI3K pathway or by examining other potential biological endpoints such as pyruvate dehydrogenase activity (Gottschalk, 1991[56]).

Although such studies could potentially be fruitful in helping to elucidate the inter-relationship between the various components and pathways of the intracellular insulin signalling cascade, the key to finding the causative lesion in A1-j most likely lies in the exploration of its endosomal processing mechanisms. This subcellular process provides the only common link between the seemingly disparate features observed in the mutant

thus far namely: lower receptor numbers, acidification-insensitive insulin degradation, DTaI insensitivity, and insulin-specific mitogenic blockage. Although there is ample precedence in the literature connecting these observations to endosomal trafficking, evidence is lacking. One could devise a series of experiments to test the hypothesis presented in Fig XI. For instance, is the decrease in receptor number really due to enhanced degradation as suggested, or is it due to a decrease in transcription or translation? Maybe post-translational alterations are involved. These questions could all be answered using techniques such as RNase protection, nuclear run-on assays as well as subcellular fractionation experiments.

An acidification-insensitive mechanism of insulin processing in A1-j was proposed based on indirect evidence (i.e., a relative insensitivity to chloroquine). This finding could be readily verified by directly measuring endosomal pH with acridine orange and co-localizing it with internalized ^{125}I-labelled insulin or DTaI (Hamel *et al.*, 1991[183]). The use of subcellular fractionation, sucrose or Percoll density gradient centrifugation, or sub-cellular markers would be used to identify the sub-cellular structures involved in insulin processing. The effect of PKC and PTPases can be characterized by monitoring the effects of phorbol esters and bpV(phen) on insulin and/or insulin receptor degradation in both cell lines. One could also test to see if the inhibition of MCP activity plays a role in the mitogenic block of the A1-j cell line by determining if any of its known functions (Duckworth *et al.*, 1994[186]) are preferentially blocked by insulin stimulation relative to their V-79 counterparts. Although the model presented in Fig XI is based upon highly speculative interpretation of data presented in the current body of work as well as the literature, confirmation (and possibly even disproof) of one or more of its aspects could lead to significant new insights on how insulin and insulin receptor trafficking are linked to the phosphotyrosine signalling cascade and/or other post-receptor signalling events.

FIGURES:

Fig I: The insulin molecule

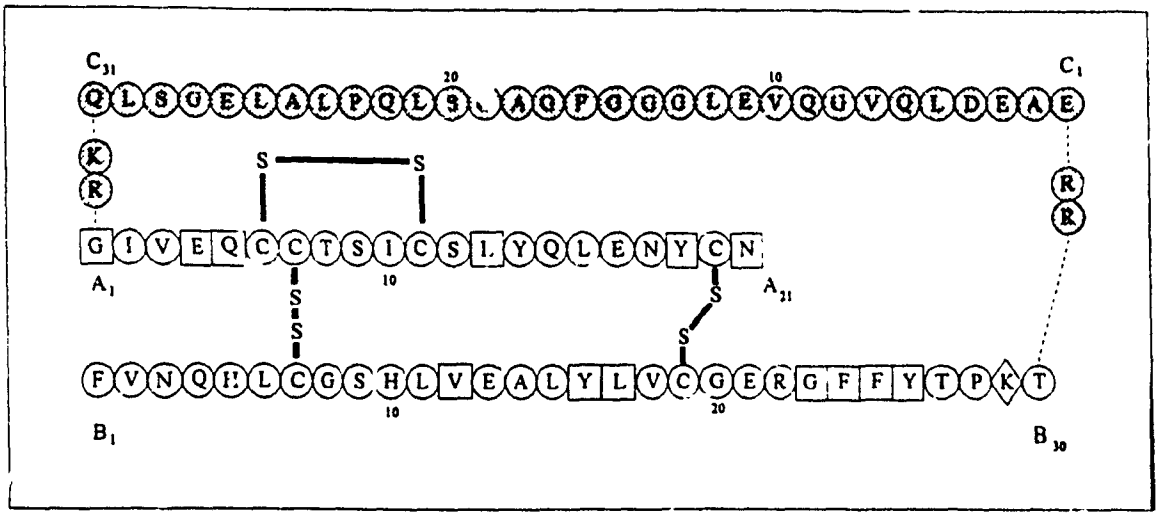

Fig IA: The amino acid sequence of human proinsulin. The A, B and C chains have been appropriately labelled with the shaded area comprising residues that are cleaved away from the mature peptide. The Lys[B29] residue represented by the diamond figure is the site of attachment for the Diphtheria A-chain in the toxic DTaI conjugate. Squares represent residues thought to be critical for receptor binding. Compiled from data found in Schuldiner *et al.*, 1991[188]; Leckett and Germinario, 1992[1]; De Meyts, 1994b[32].

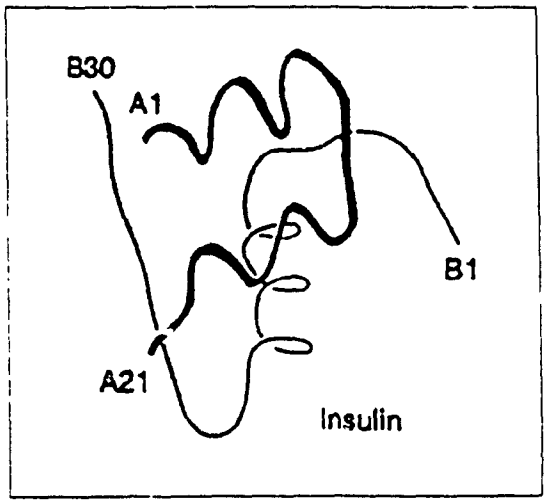

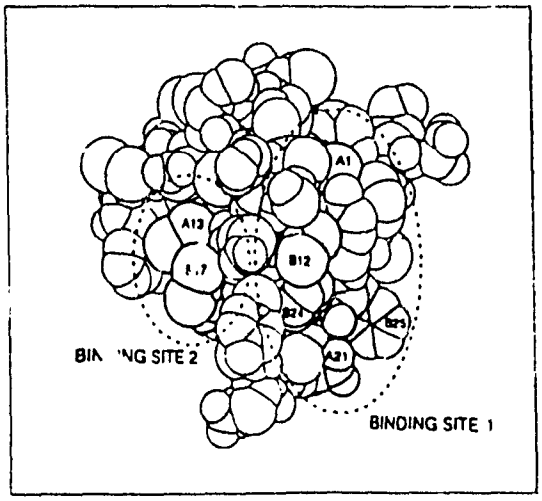

Fig IB: The 3-dimensional structure of insulin. The ribbon diagram displays basic secondary and tertiary structural characteristics (Blundell *et al.*, 1978[189]) while the space filling model depicts the two putative receptor binding regions (Shaffer, 1994[31]).

Fig II: The insulin receptor

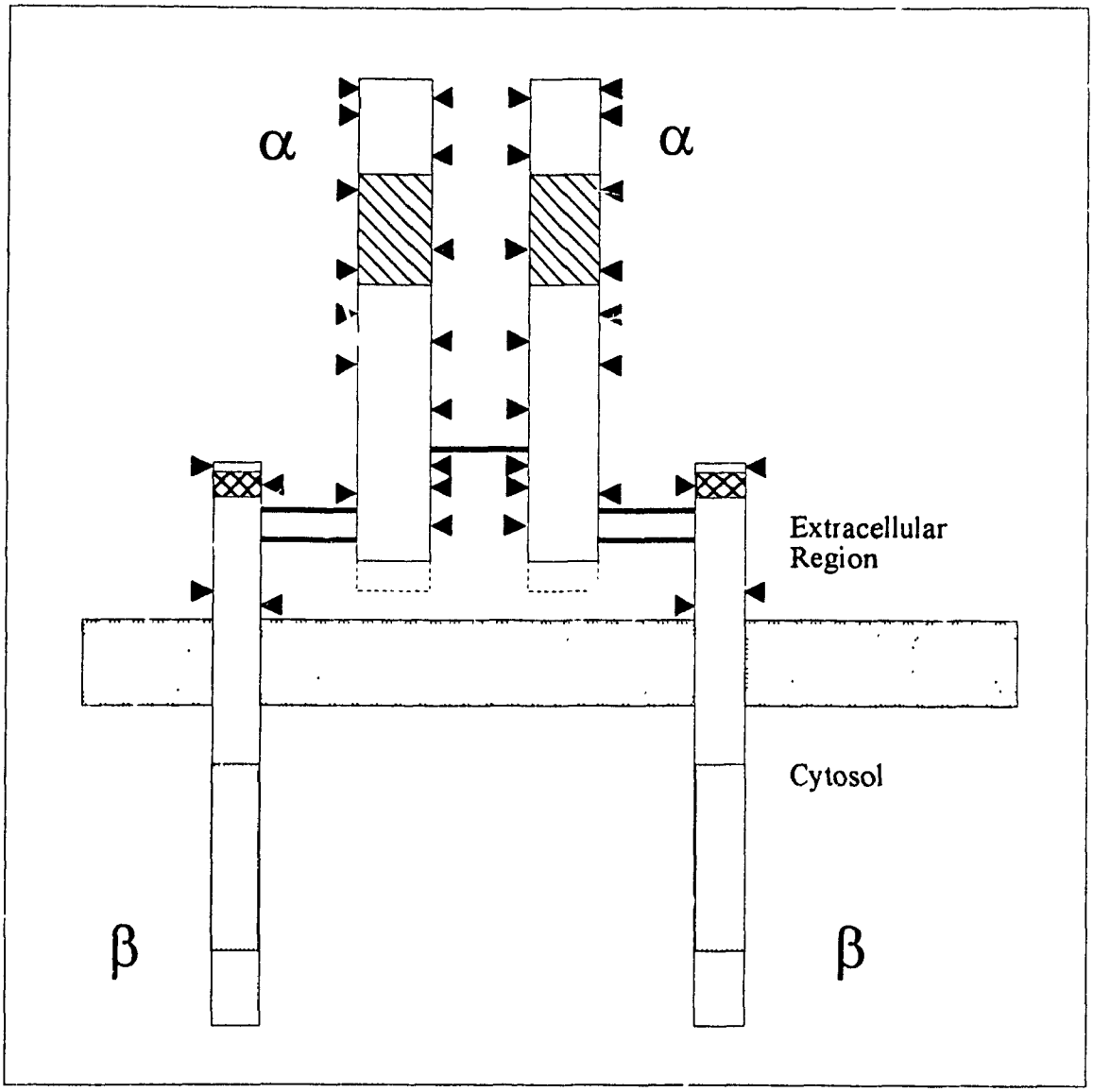

Fig IIA: Principle structural features. The hatched areas represent the cysteine-rich domains of the α-subunits. Potential N-linked glycosylation sites are designated by "◀" while O-linked sites are believed to be concentrated within a cluster of Ser and Thr residues (Thr^{756}-Ser^{764}) indicated by the cross-hatched area on the extracellular portion of the β-chains. The shaded area represents the tyrosine kinase core and the broken lines the alternatively spliced 11 amino acids differentiating the A and B receptor isoforms. The α-α disulphide link between adjacent Cys^{524} residues is also indicated along with 2 putative links between $Cys^{(\alpha)647}$, $Cys^{(\alpha)683}$ and 2 of the 4 available cysteines in the extracellular portion of the β-subunits. Compiled from data reviewed in Taylor, 1991[190]; De Meyts, 1994b[32]; Cheatham and Khan, 1995[35].

Fig II: The insulin receptor (...continued)

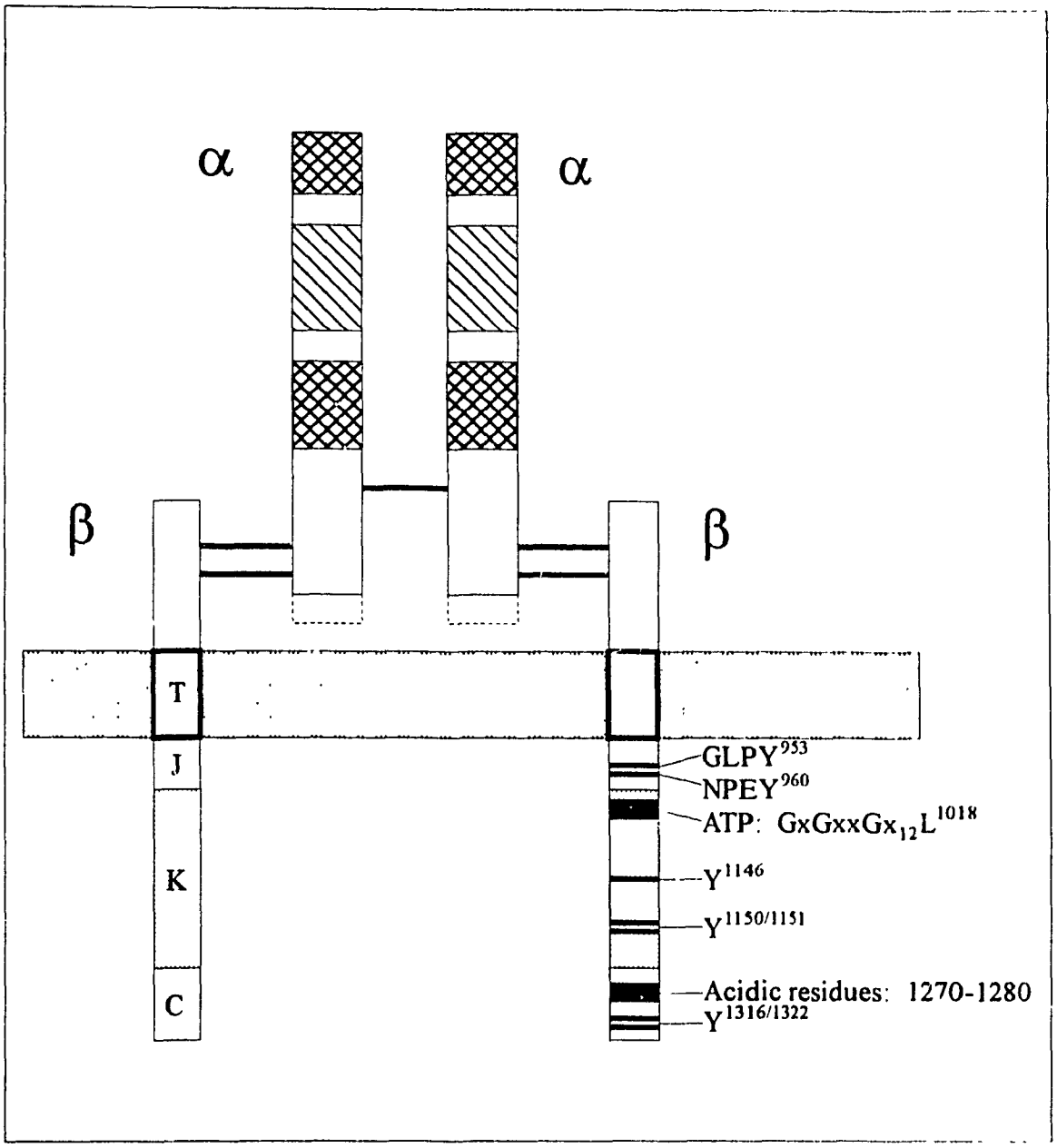

Fig IIB: Map of the functional domains. The hatched areas represent the cysteine-rich region while cross-hatched areas are believed to contain residues essential for insulin binding and recognition. The transmembrane domain, the juxtamembrane region, the tyrosine kinase core (shaded area), and the carboxy terminal tail are represented by the letters T, J, K and C respectively. Critical amino acids within the β-subunit have also been indicated (see text for details)

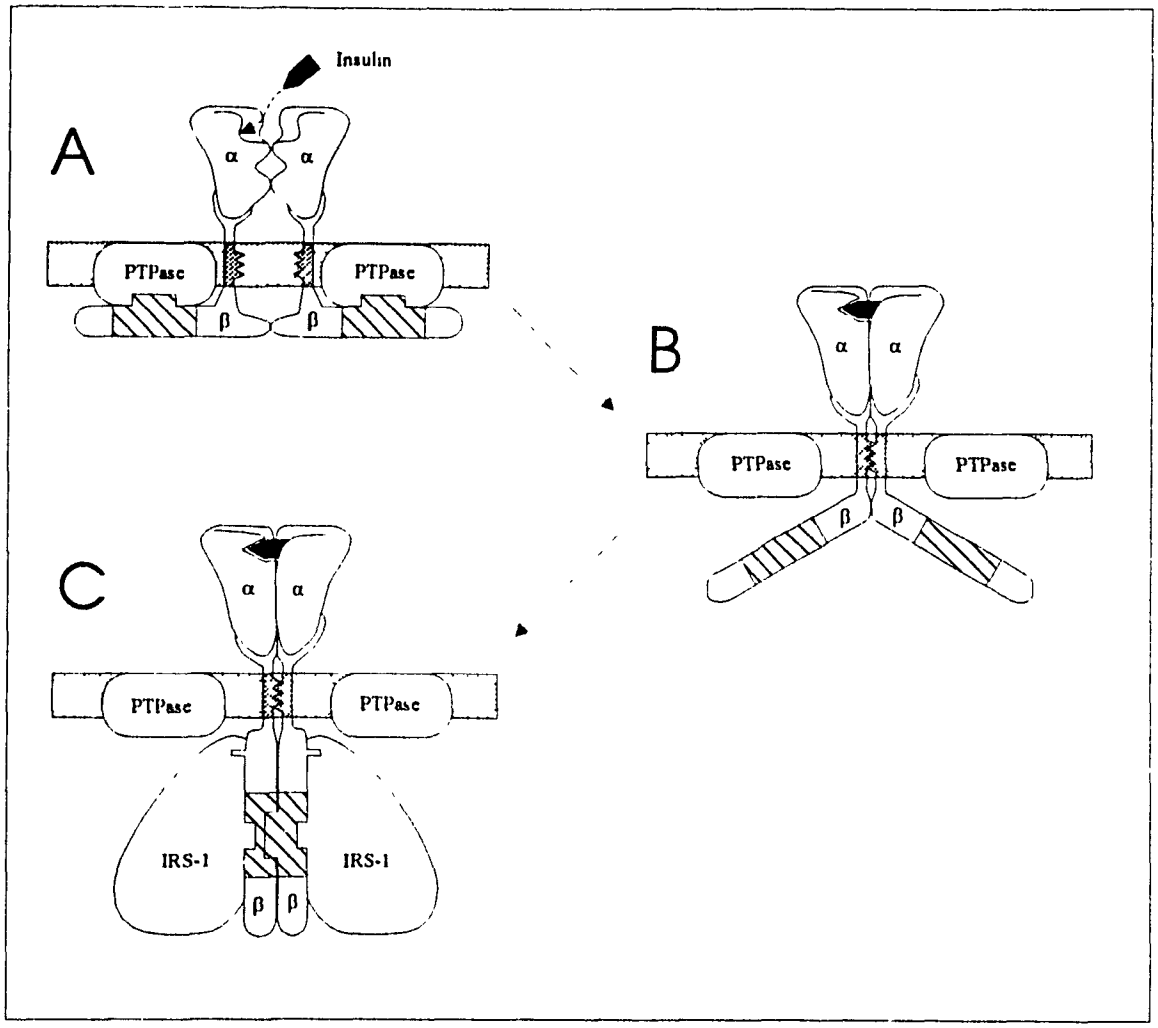

Fig III: Model for insulin receptor activation by dimerization of the transmembrane domain. In the unliganded state the extracellular regions are poised to keep the transmembrane domains (shaded region) apart (A). Insulin binds and cross-links the α-subunits resulting in a conformational change which permits the association of the membrane-spanning regions (B) This, in turn, induces conformational changes in the cytosolic domains of the β-chains resulting in autophosphorylation and tyrosine kinase activation (C). The allosteric changes in the β-subunits are also likely to be involved in mediating enhanced association with endogenous substrates like IRS-1 (White and Khan, 1994[12]), while at the same time promoting the dissociation from negative regulators like phosphotyrosine phosphatase (Posner, B. *et al.*, 1994[156]). The hatched area represents the tyrosine kinase core of the receptor β-chain.

Fig IV: Insulin receptor substrate 1 (IRS-1)

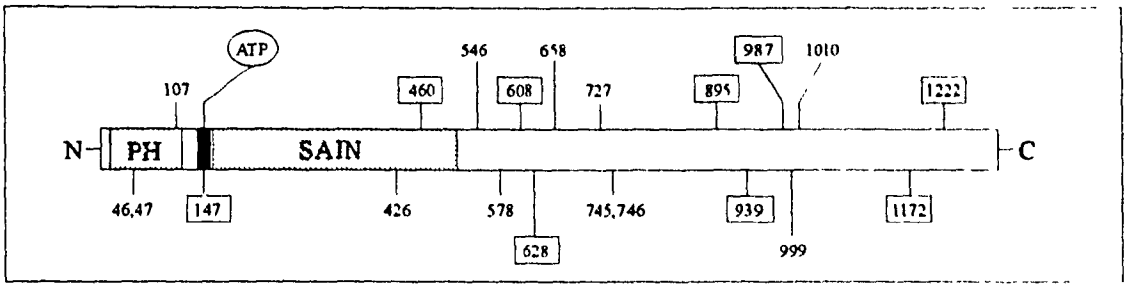

Fig IVA: Map of the functional domains of IRS-1. The pleckstrin homology (PH) and SAIN domains are shown along with a consensus ATP-binding site ($GXGXXGX_{12}L$[156]) between them (Sun *et al.*, 1991[62]; Craparo *et al.*, 1995[66]) The numbers indicate potentially phosphorylatable Y residues with boxed numbers representing confirmed phosphorylation sites*.

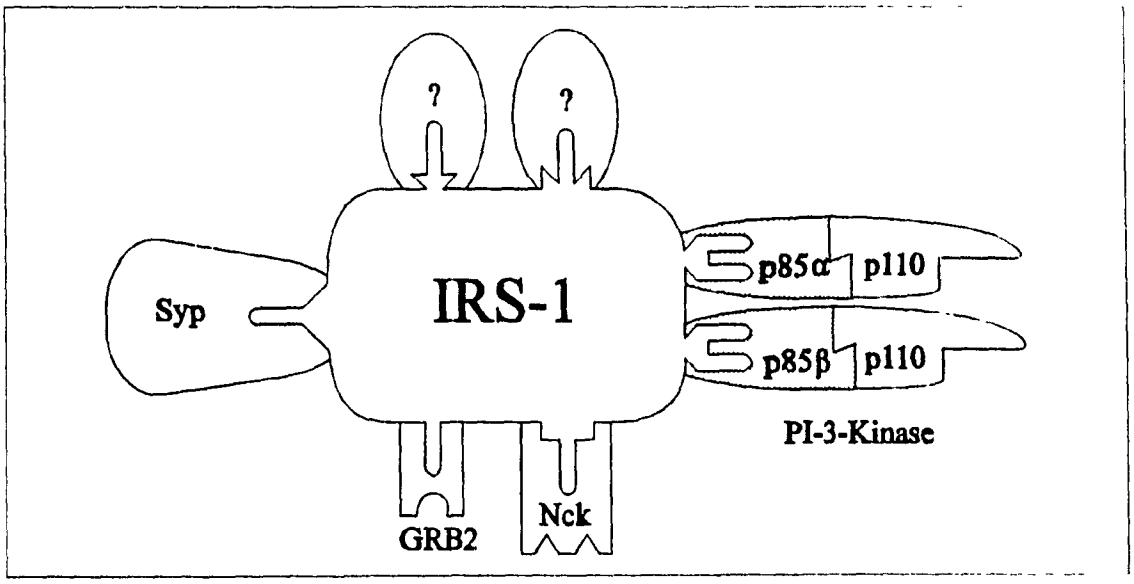

Fig IVB: SH2 binding sites. 7 of the 9 tyrosine residues shown to be phosphorylated by insulin have been implicated in an association with an SH2 region of a downstream effector protein. GRB2 binds to Y^{895}VNIE, while Nck and Syp associate with Y^{147}DTG and Y^{1172}IDL respectively. The p85 subunit of PI3K associates preferentially with 2 of 4 possible sites. Y^{460}ICM, Y^{608}MPM, Y^{939}MNM and/or Y^{987}MTM No protein has as yet been identified for the docking sites Y^{628}MPM and Y^{1222}ASI (Lee *et al.*, 1993b[68], Cheatham and Khan, 1995[35]).

---

* Phosphorylation of the Y^{147}DTG site has been shown indirectly through association with Nck (Lee *et al.*, 1993[39]).

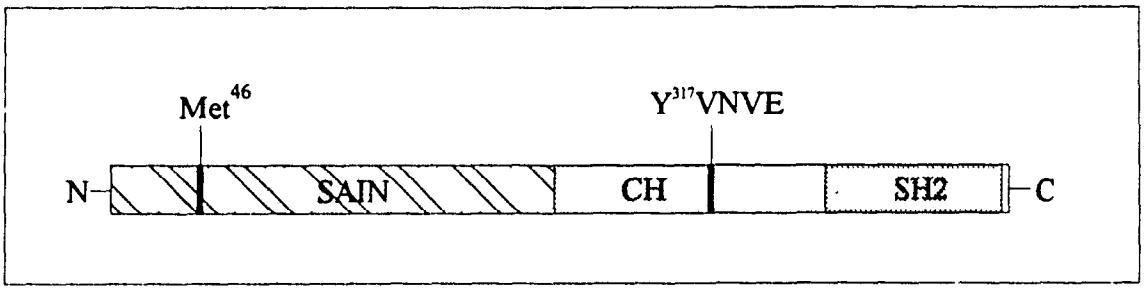

Fig V: Map of the functional domains of SHC. Only two regions of SHC have been identified as having sequence homology to previously characterized proteins. The 378-471 amino acid stretch shows greatest similarity (60%) to the SH2 region of Src, while the 233-377 sequence bears 50% homology to human α-collagen (Pelicci *et al.*, 1992[69]). The hatched region (amino acids 1-238) represents the putative SAIN motif which may be involved in an interaction with the insulin receptor (Gustafson *et al.*, 1995[65]). The GRB2-binding SBS site (Y^{317}VNVE) is also shown.

Fig VI: PI3 kinase

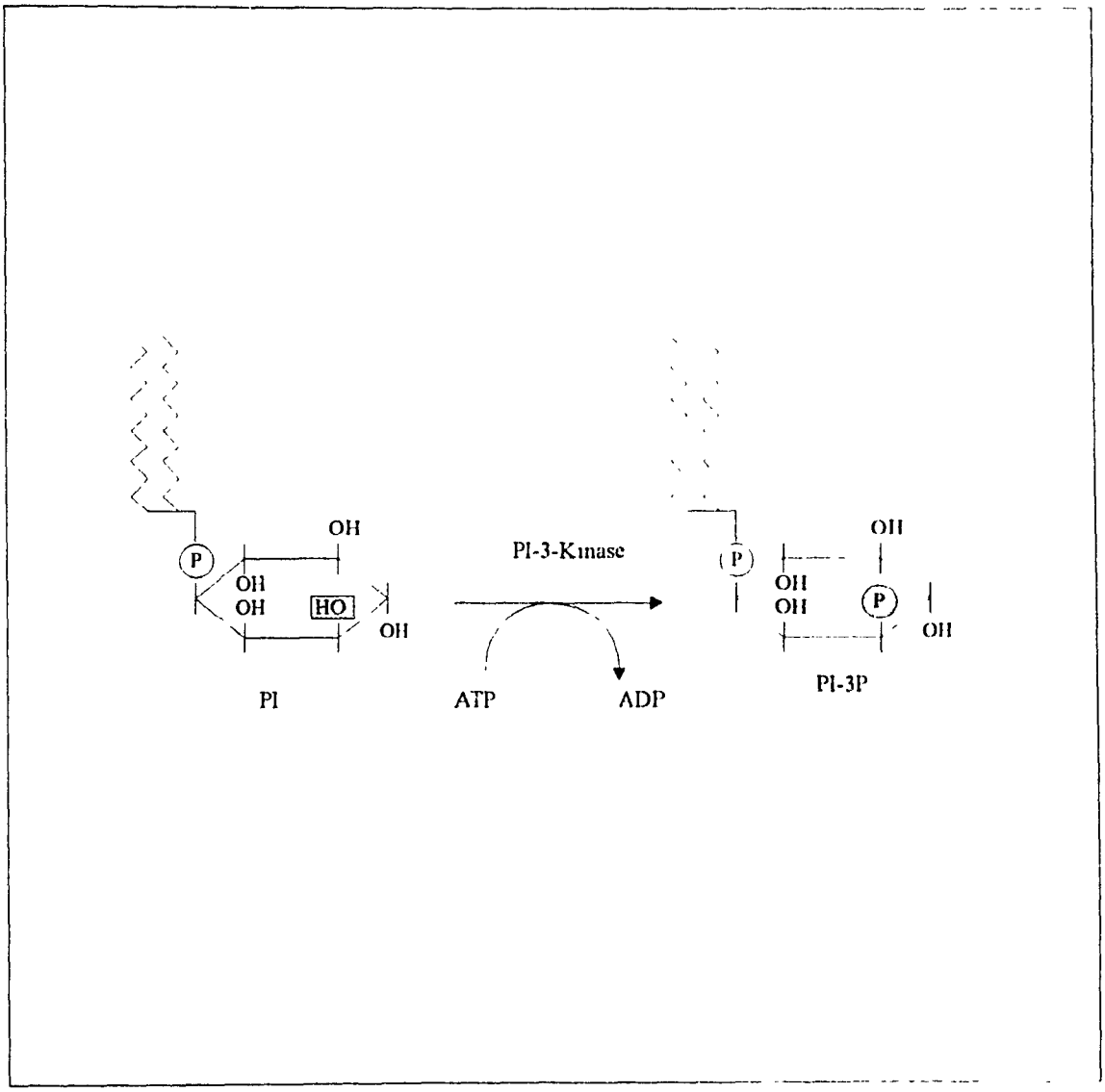

Fig VIA: The phosphatidyl phosphoinositide phosphorylation reaction. PI3K catalyzes the phosphorylation of the OH group in the D-3 position of the inositol ring of phosphatidyl inositol (PI) or related molecules PI-4P, PI-4,5P (phosphatidyl inositol 4-phosphate, etc...) to give PI-3P, PI-3,4P, or PI-3,4,5P respectively. The reaction occurs at the expense of 1 ATP molecule. Unlike the related PIP_2 intermediates however, the products of the PI3K reaction are not subsequently cleaved at the D-1 phosphate into polar inositol phosphates and non-polar diacyl glycerol moieties and thus do not participate in classical IP_3 second messenger signalling (Stryer, 1995c[191]).

Fig VI: PI3 kinase (...continued)

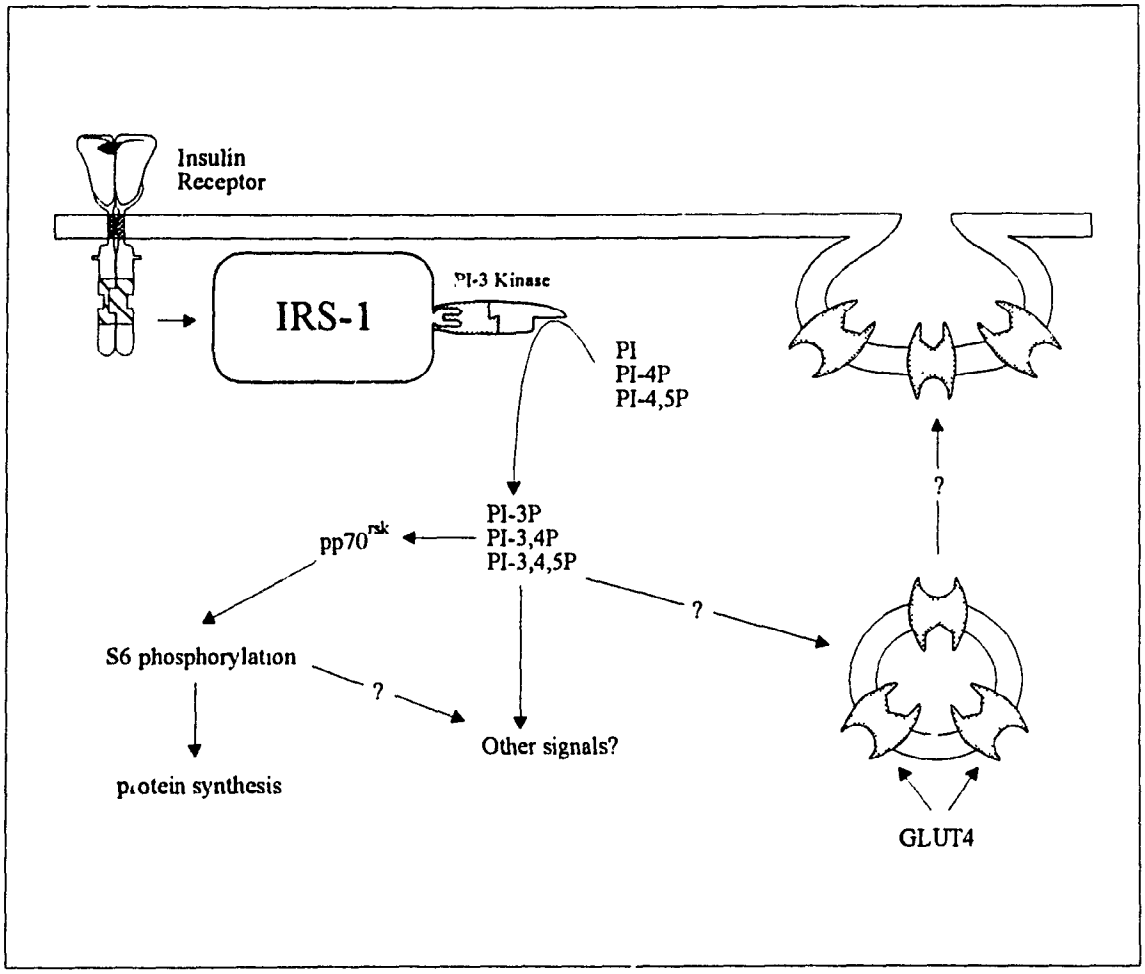

Fig VIB: The PI3K cascade. Following autophosphorylation, the active β-chain kinase of the insulin receptor phosphorylates the tyrosine residues of YXXM motifs within IRS-1 thereby stimulating association of the latter with the p85 regulatory subunit of PI3K. This allosterically activates the p110 catalytic subunit of the kinase which mediates the reaction described above (Fig VIA). Since the metabolic products of the PI3k reaction remain membrane-bound they presumably mediate downstream effects from this sub-cellular location. Subsequent signalling events include GLUT4 translocation, and activation of $pp70^{rsk}$ which in turn stimulates protein synthesis by phosphorylating the S6 protein of the ribosomal 40S subunit. Molecular connections to these downstream events, however, remain to be elucidated. "Other signals" include potential links to lipid metabolism, amino acid uptake, DNA synthesis, ion transport, activation of nuclear kinases and transcription factors (Ref: Cheatham and Khan, 1995[35]).

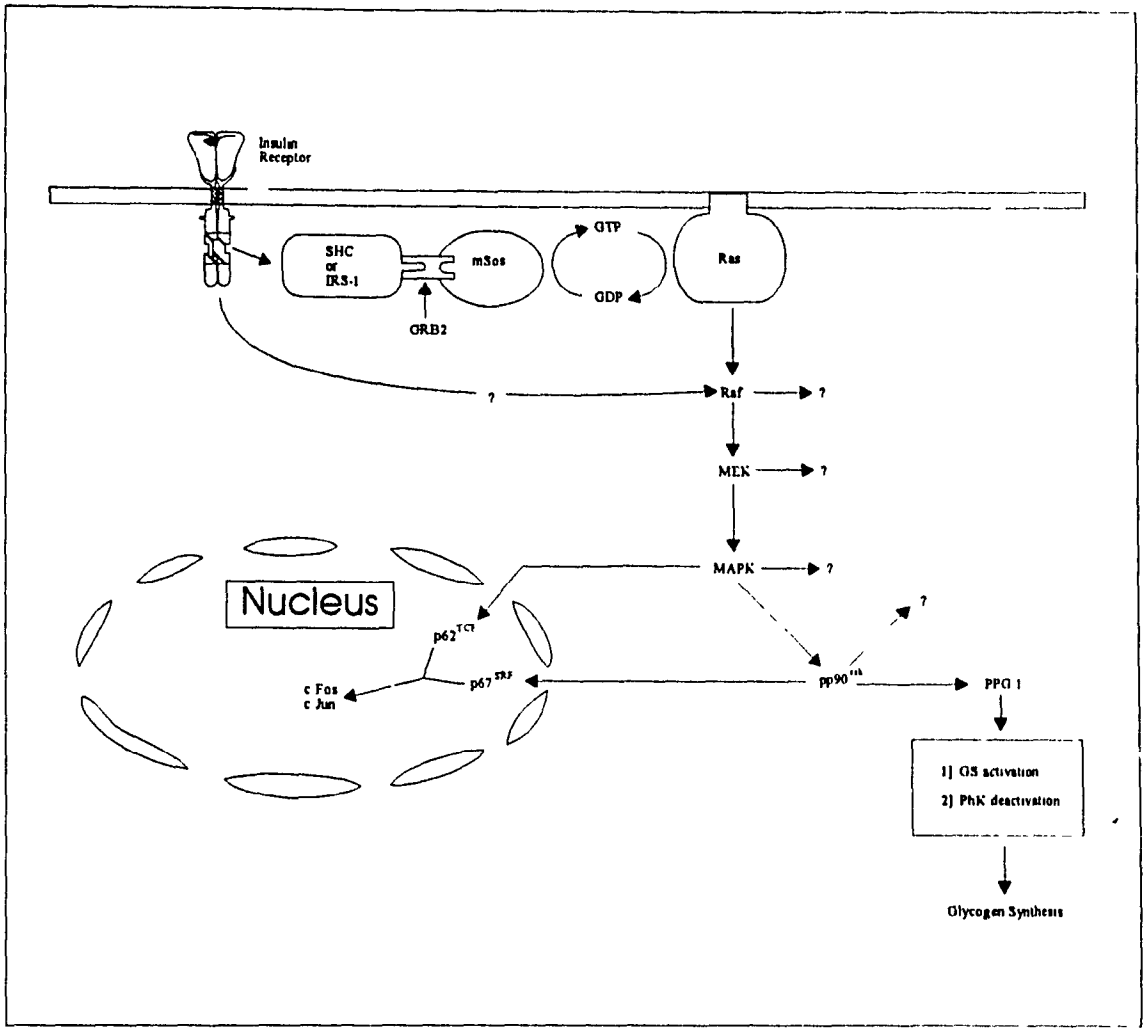

Fig VII: The Ras-MAPK cascade. GRB2 forms a non-covalent association with activated IRS-1 and/or SHC which in turn stimulates binding of mSos to the two SH3 regions of GRB2. In this manner, mSos is recruited to the sub-membrane region of the cell where it stimulates the activity of membrane-associated Ras by serving as a GTP exchange factor. Through a mechanism which is not entirely clear, Ras activates the Ser/Thr kinase Raf and thereby sets off a phosphorylation cascade involving MEK, MAPK and $pp90^{rsk}$. The two latter proteins are able to translocate to the nucleus whereupon they stimulate a variety of nuclear kinases and transcription factors. As an example, the transcription of proto-oncogenes c-fos and c-jun proceeds through the activation of $p62^{TCF}$ and $p67^{SRF}$ intermediates. Meanwhile, in the cytosol, $pp90^{rsk}$ stimulates glycogen synthesis by phosphorylating PPG-1 (protein phosphatase glycogen-associated -1) which in turn activates glycogen synthase (GS) and shuts down glycogenolysis by deactivating the phosphorylase kinase cascade (PhK). The "?" symbols indicate potential branch-points to unidentified signalling pathways (Ref: Cheatham and Khan, 1995[35]).

Fig VIII: Receptor-mediated endocytosis. Upon ligand binding insulin receptors undergo aggregation in a villous region of the cell surface (A). This is followed by the first of a two-stage endocytic mechanism whereby the aggregated receptors migrate to a clathrin-coated pit within a non-villous region of the cell surface (B). This is the ATP-dependent stage of endocytosis. In the second ATP-independent step, proteins within the coated pit recognize specific internalization sequences within the juxtamembrane region of the insulin receptor which triggers the invagination of the coated pit region (C and D). Eventually the coated pit pinches off from the plasma membrane forming a coated vesicle (E). Within 1 to 2 min, an uncoating ATPase removes the clathrin coat and recycles it back to the cell surface (F). The uncoated vesicle then fuses with a component of the endocytic network (G). As the endosome is acidified, insulin is released from its receptor (H). The insulin is targeted for degradation (I) while the receptors are separated and recycled back to the cell surface (J). Compiled from data presented in: Carpentier and Paccaud, 1994[110], Berg *et al.*, 1995[120], and Carpentier and McClain, 1995[112].

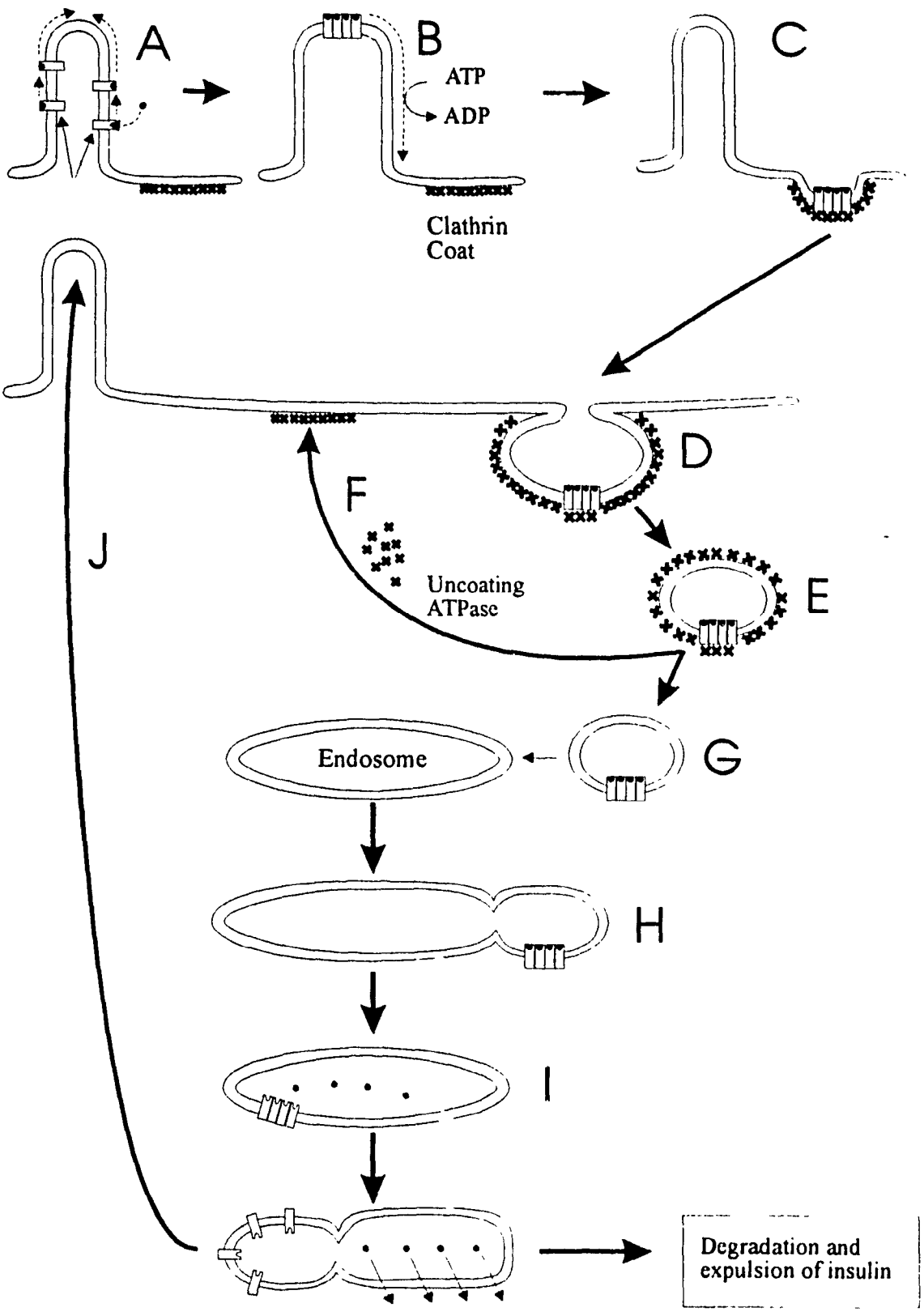
A
B
ATP
ADP
C
Clathrin
Coat
D
F
J
Uncoating
ATPase
E
Endosome
G
H
I
Degradation and
expulsion of insulin

Fig IX: The role of endosomes in insulin-regulated GLUT4 translocation. As the liganded insulin receptors begin undergoing endocytosis, the activated insulin receptor kinase begins phosphorylating endosomally-associated IRS-1 (A). Phosphorylation of one of the YXXM SBS sites in IRS-1 promotes association with the p85 regulatory subunit of PI3K but does not activate the p110 catalytic subunit of PI3K. Although IRS-1 has been shown to be associated with a particular subset of endosomal vesicles (labelled I), the nature of the association is unknown (Kelly and Ruderman, 1993[63]). At the same time a cytosolically localized subset of IRS-1 molecules are propagating the insulin signal to other pathways possibly including the Ras-MAPK phosphorylation cascade (B). As the internalized insulin-receptor complexes are directed to their own subset of endosomal organelles (labelled II), further phosphorylation of IRS-1, possibly at another YXXM site, induces the activation of PI3K (C). Activated PI3K associated with I-endosomes propagates the insulin signal to yet another group of vesicles (labelled III) which contain GLUT4 (D). How the message is propagated is unclear at present, although it likely involves the phosphorylation of lipid components of the III-vesicle membrane. The result is translocation to, and fusion of the III-vesicles with, the plasma membrane (E). Complied from data reported in Kelly and Ruderman, 1993[63] and Kublaoui *et al.*, 1995[64].

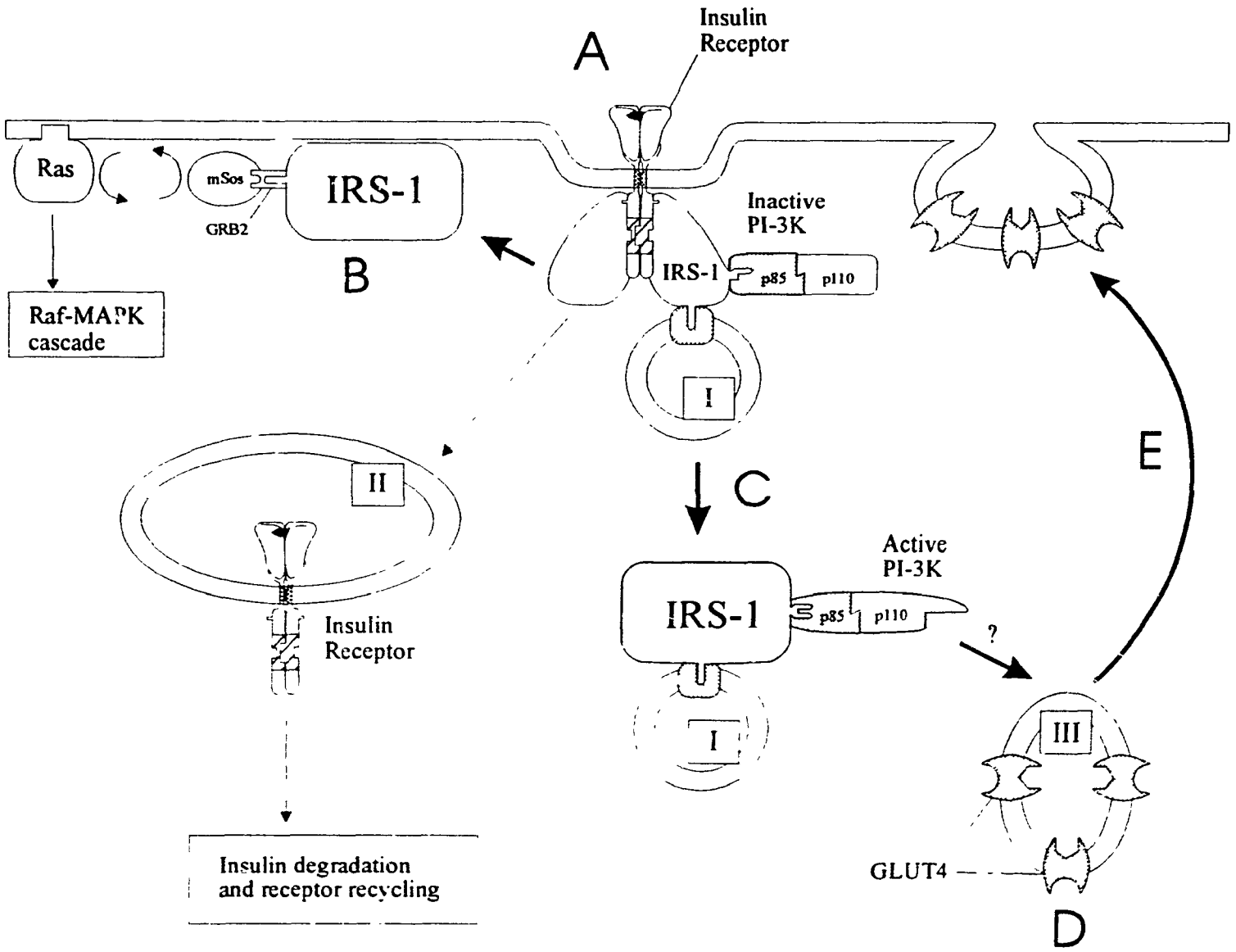
A
Insulin
Receptor
Ras
mSos
GRB2
IRS-1
B
Raf-MAPK
cascade
Inactive
PI-3K
IRS-1
p85
p110
I
C
II
Insulin
Receptor
Active
PI-3K
IRS-1
p85
p110
?
I
III
E
GLUT4
D
Insulin degradation
and receptor recycling

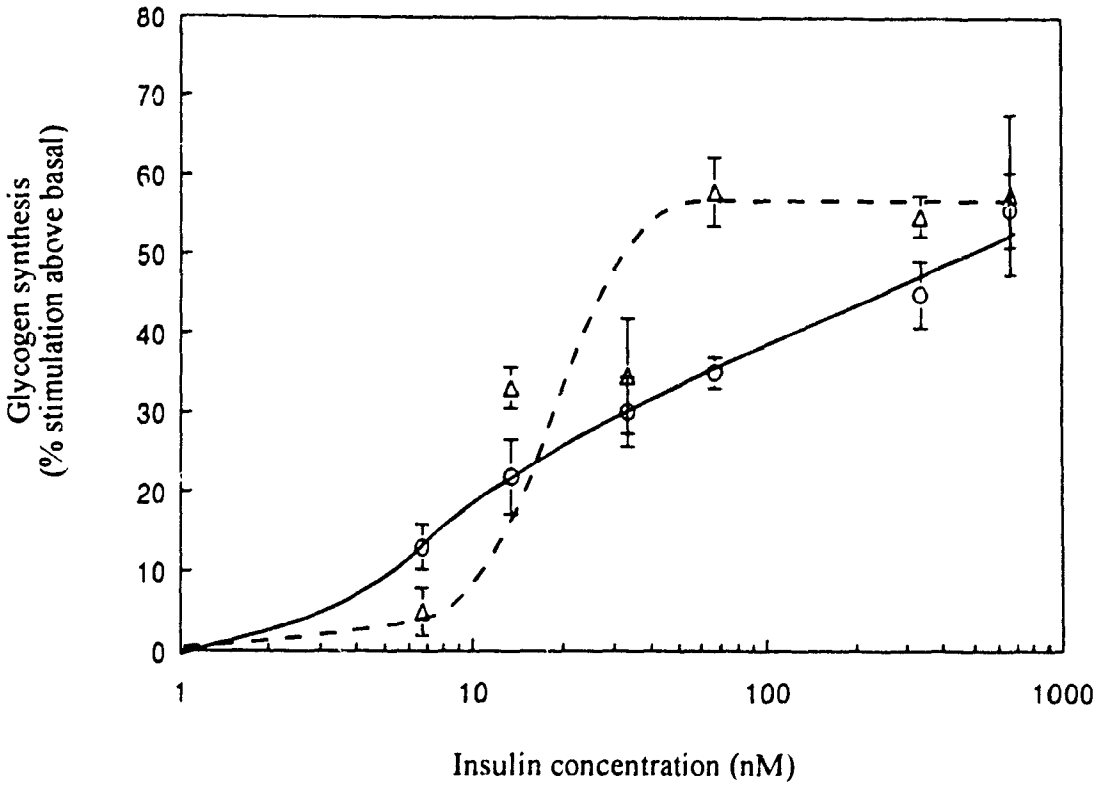

Fig 1.2: The effect of insulin concentration on glycogen synthesis in V-79 and A1-j cells. Glycogen synthesis was monitored in V-79 (O) and A1-j (Δ) cells by measuring the amount of ^{14}C-labelled glucose incorporated into KOH-precipitable material 4 hours following stimulation with varying concentrations of insulin The results represent the average of triplicate determinations ± S.E.M. from 3 separate experiments The ED_{50} for insulin was determined to be 34 and 19 nM for V-79 and A1-j cell lines respectively ($P<0.001$).

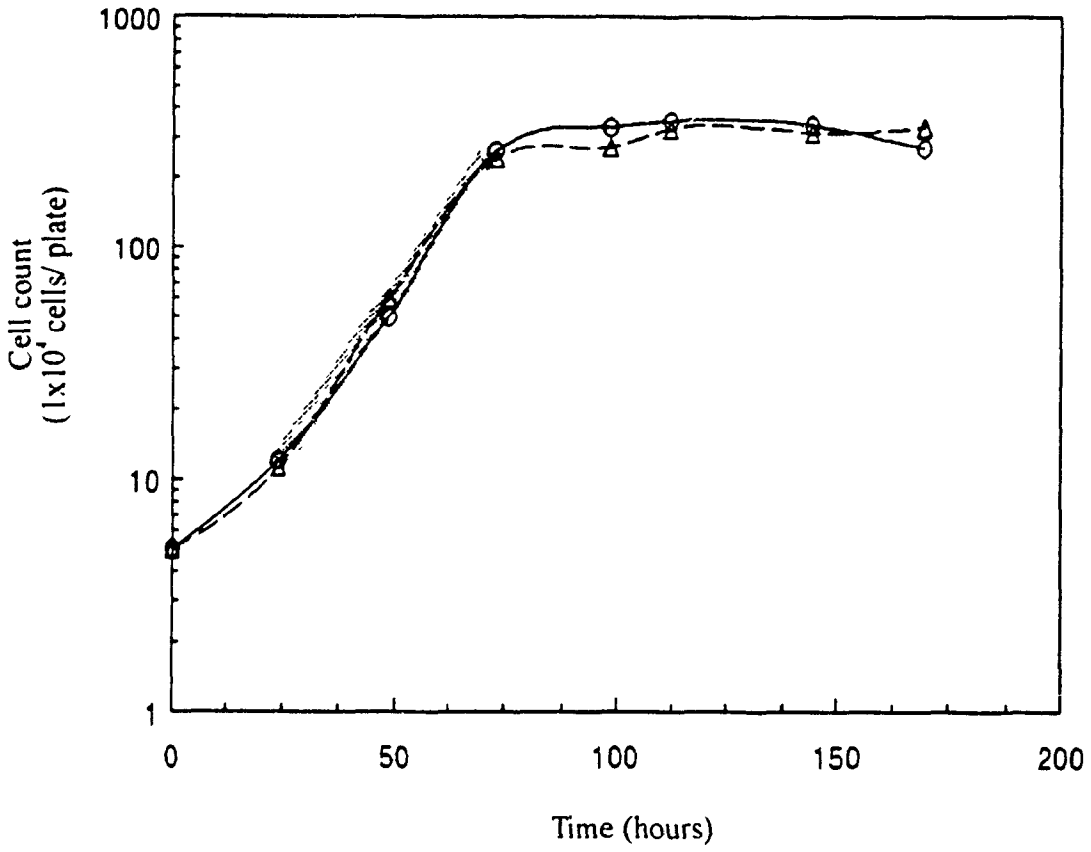

Fig 2.1: Growth curve: V-79 *vs* A1-j cells as monitored by daily cell counting. Cells were cultured in DMEM + 5% FBS over a period of 5-6 days and cell counts taken on each day. The figure above is representative of a typical experiment. Doubling times were estimated from the linear portions of each curve (shaded area), averaged from triplicate determinations of 3-4 experiments (±S.E.M.), and found to be 10.8 ± 0.3 and 10 6 ± 0 4 hours for V-79 (o) and A1-j (Δ) respectively (P>0.60).

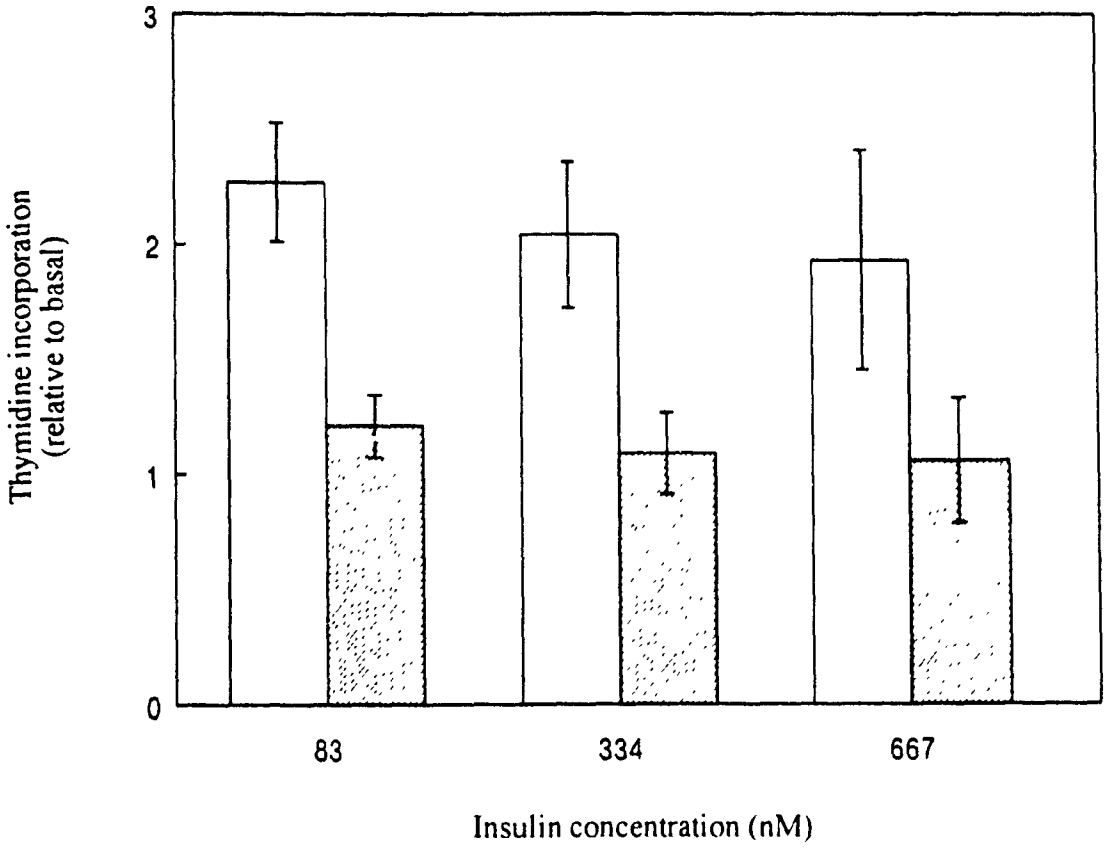

Fig 2.2: Insulin-stimulated growth in V-79 and A1-j cells as monitored by 3-day cell counting. Cells were plated and allowed to adhere overnight followed by treatment with varying concentrations of insulin. The results, representing the average ± S.E M from the triplicate determinations of 2-9 experiments, are expressed relative to basal cell numbers measured on the third day following treatment. V-79 cells ( ) exhibited approximately 2-fold growth stimulation at all of the insulin concentrations used ($P<0.01$), while A1-j cells ( ) showed no significant growth above basal ($P>0.10$)

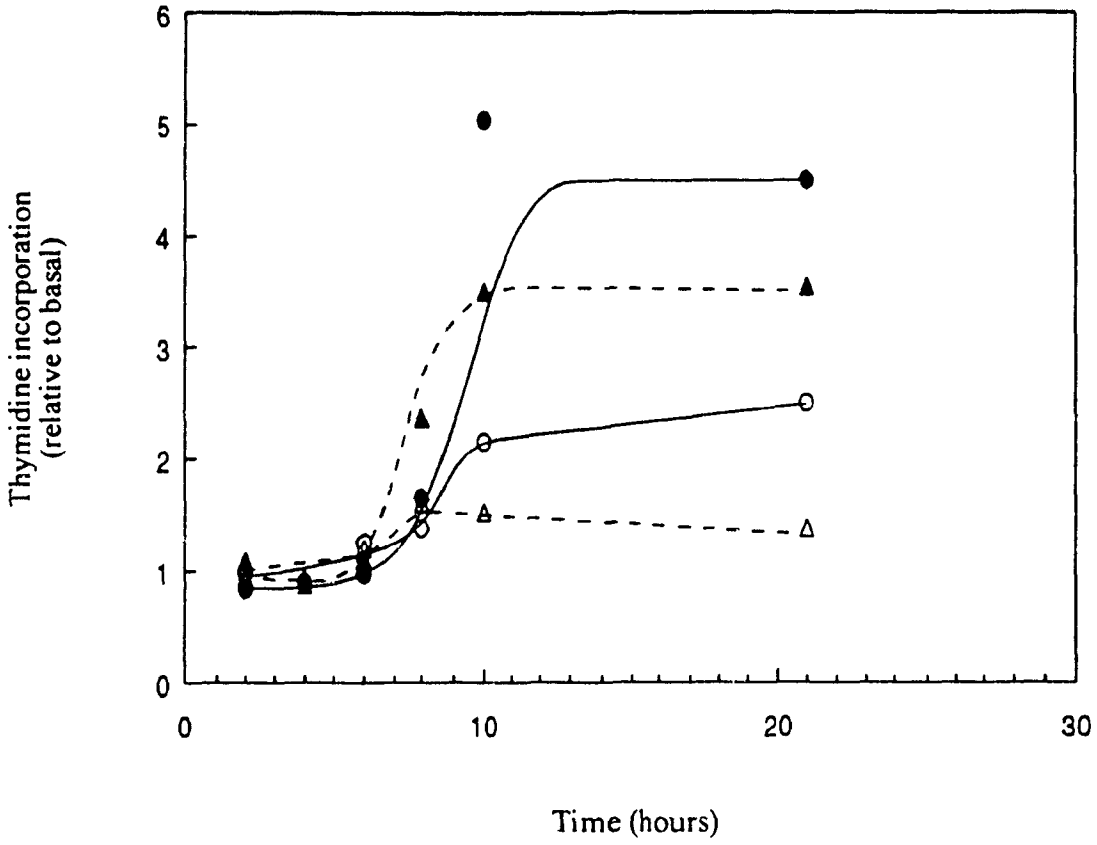

Fig 3.1A: Time course for thymidine incorporation into TCA-precipitable material. (○) V-79 cells stimulated with 667 nM insulin, (●) V-79 cells stimulated with 5% FBS, (△) A1-j cells stimulated with 667 nM insulin, (▲) A1-j cells stimulated with 5% FBS. The results are expressed relative to basal ^{3}H-thymidine incorporation levels.

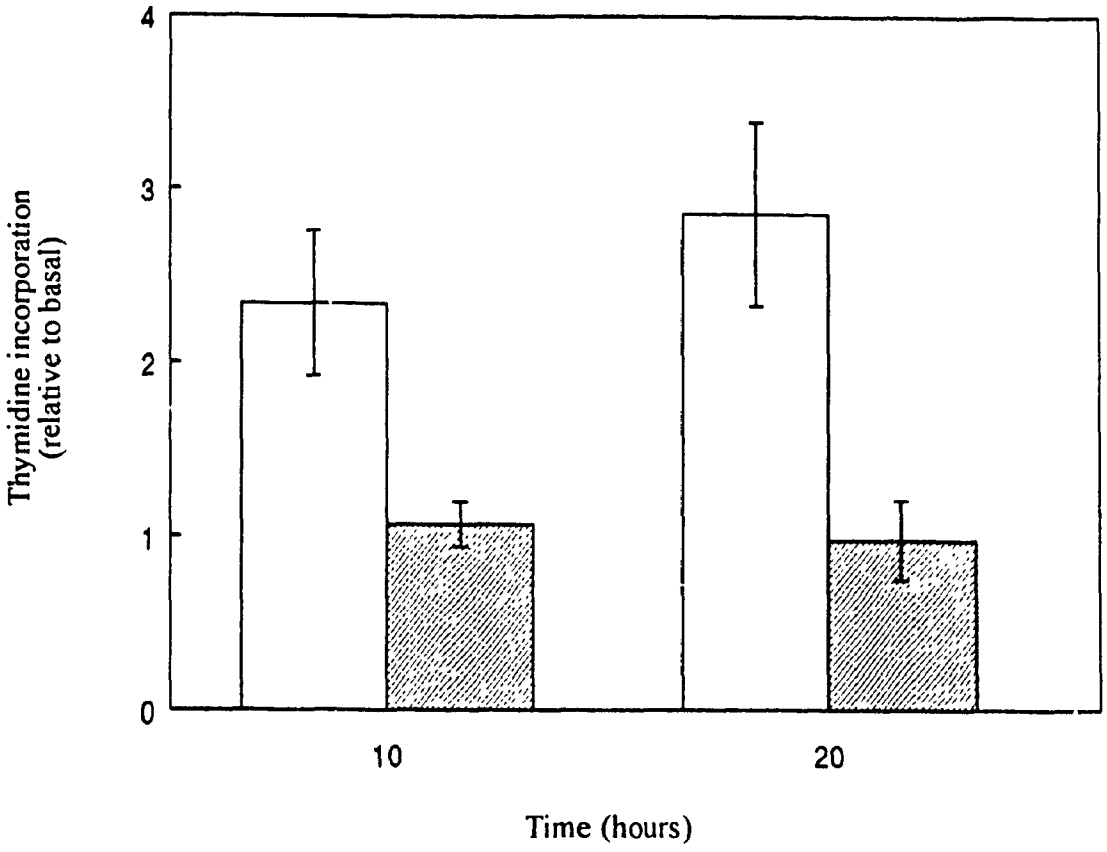

Fig 3.1B: Insulin-stimulated thymidine incorporation in V-79 and A1-j cells at 10 and 20 hours post stimulus. ^{3}H-Thymidine incorporation into TCA-precipitable material was measured following stimulation with 667 nM insulin. The results represent the average ± S.E.M. from the triplicate determinations of 3-4 separate experiments and are expressed relative to basal thymidine incorporation levels. V-79 cells ([ ]) showed greater than 2-fold stimulation with insulin at both time points (P<0 001), while A1-j cells ([▨]) showed no significant effect with the addition of insulin (P>0 10)

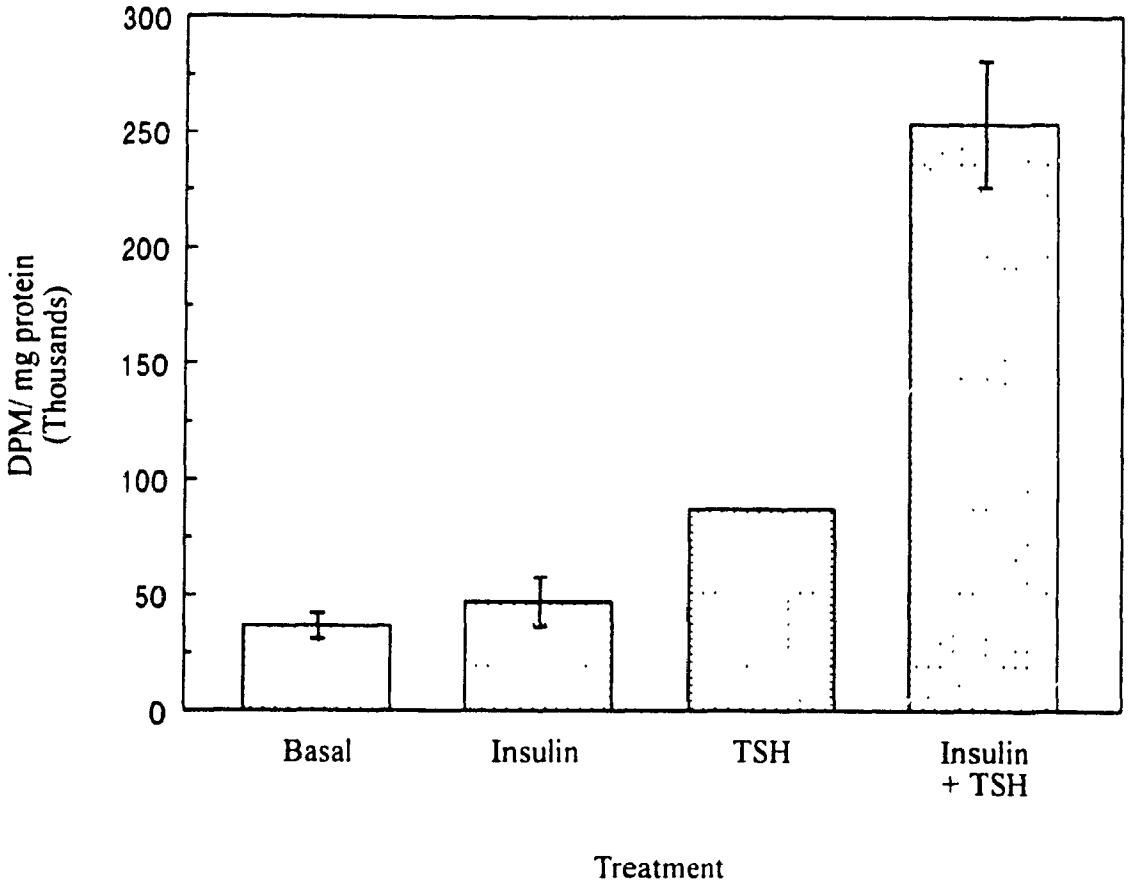

Fig 3.3A: Insulin and TSH synergism in stimulating thymidine incorporation in FRTL-5 cells. The addition of 6.7 nM insulin together with 1.0 nM TSH resulted in ^{3}H-thymidine incorporation greater than 2.9-fold above that resulting when either compound was added individually.

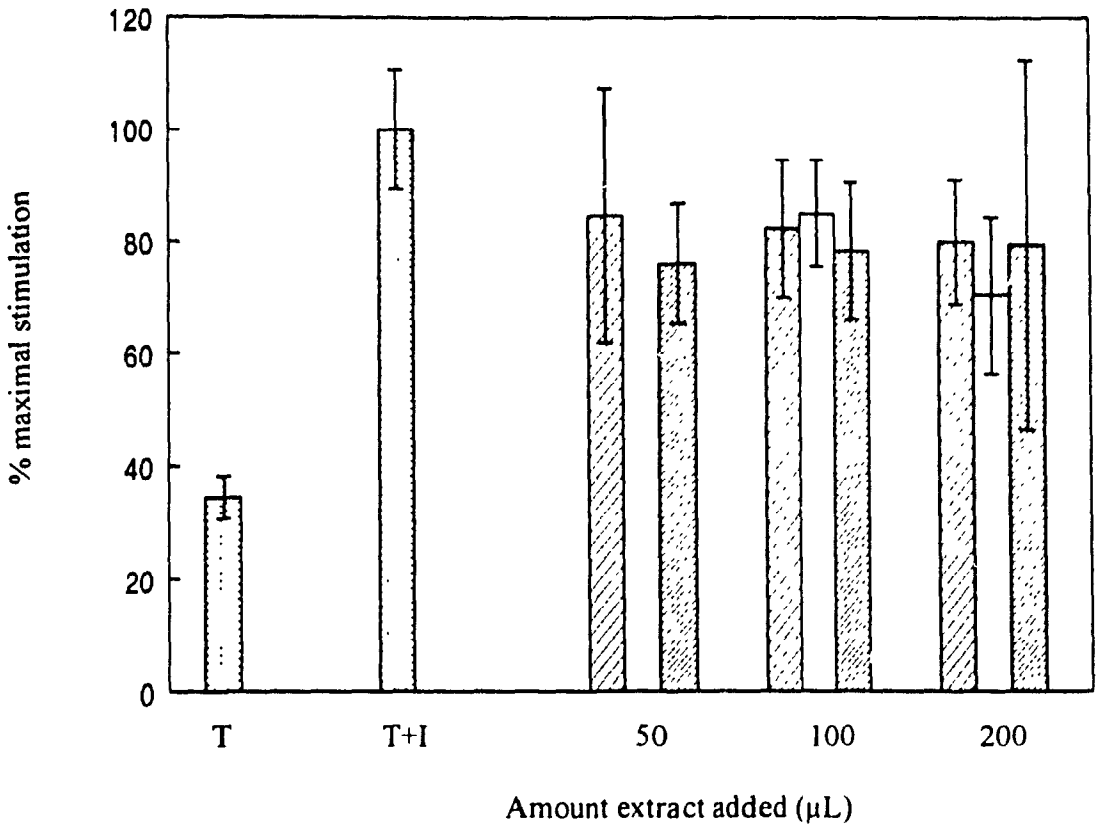

Fig 3.3B: The effect of adding cell-conditioned media on thymidine incorporation in FRTL-5 cells maximally stimulated with 6.7 nM insulin and 1.0 nM TSH. (▦) no media added, (▨) DMEM added, (□) V-79-conditioned DMEM added, (▨) A1-j-conditioned DMEM added The results represent the average ± S.D from triplicate determinations. Neither of the cell-conditioned samples was able to affect insulin and TSH synergism in a manner significantly different than DMEM alone (P>0.46) This demonstrates that neither cell line is secreting an inhibitory autocrine factor which neutralizes extracellular insulin

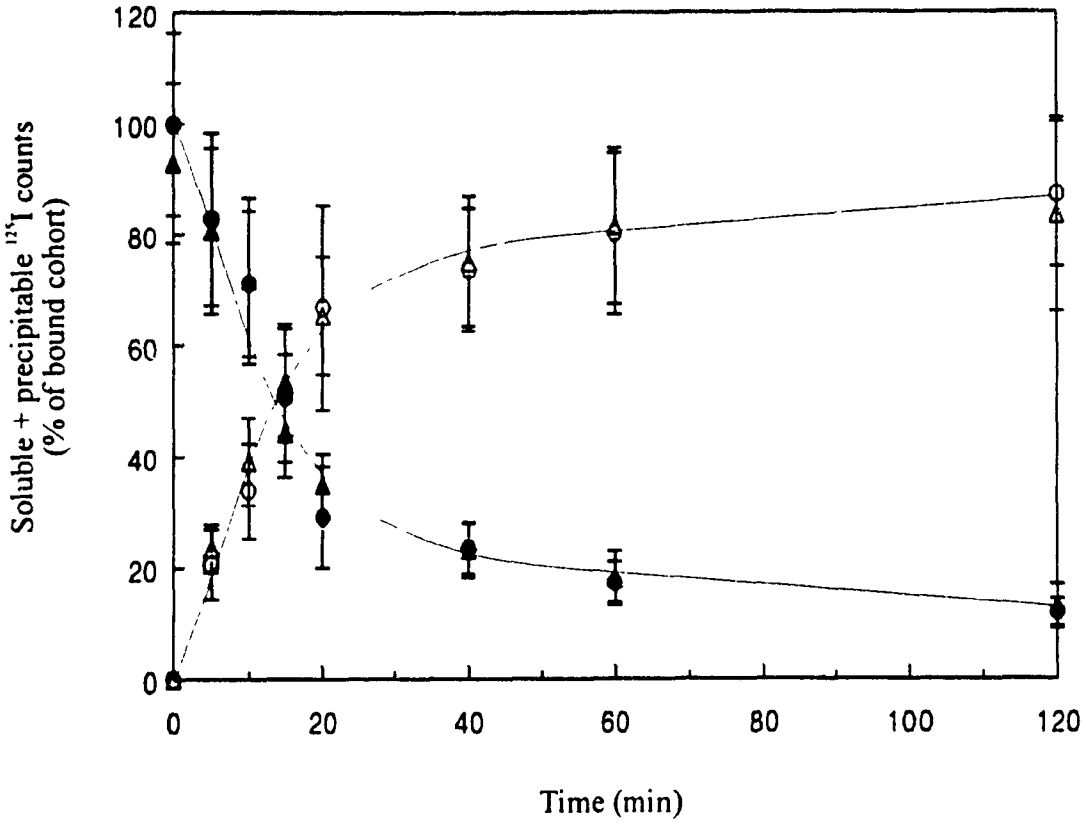

Fig 3.4A: The measurement of total insulin efflux from the cell monolayer to the conditioning buffer. Total ^{125}I-labelled insulin (soluble + precipitable counts) was measured in the cell monolayer and the conditioning buffer as a function of time following temperature-shift activation of insulin degradation. The results are expressed as a % of the bound insulin cohort measured in both fractions (monolayer + conditioning buffer). (○) V-79 conditioning buffer fraction, (●) V-79 cell monolayer fraction, (△) A1-j conditioning buffer fraction, (▲) A1-j cell monolayer fraction.

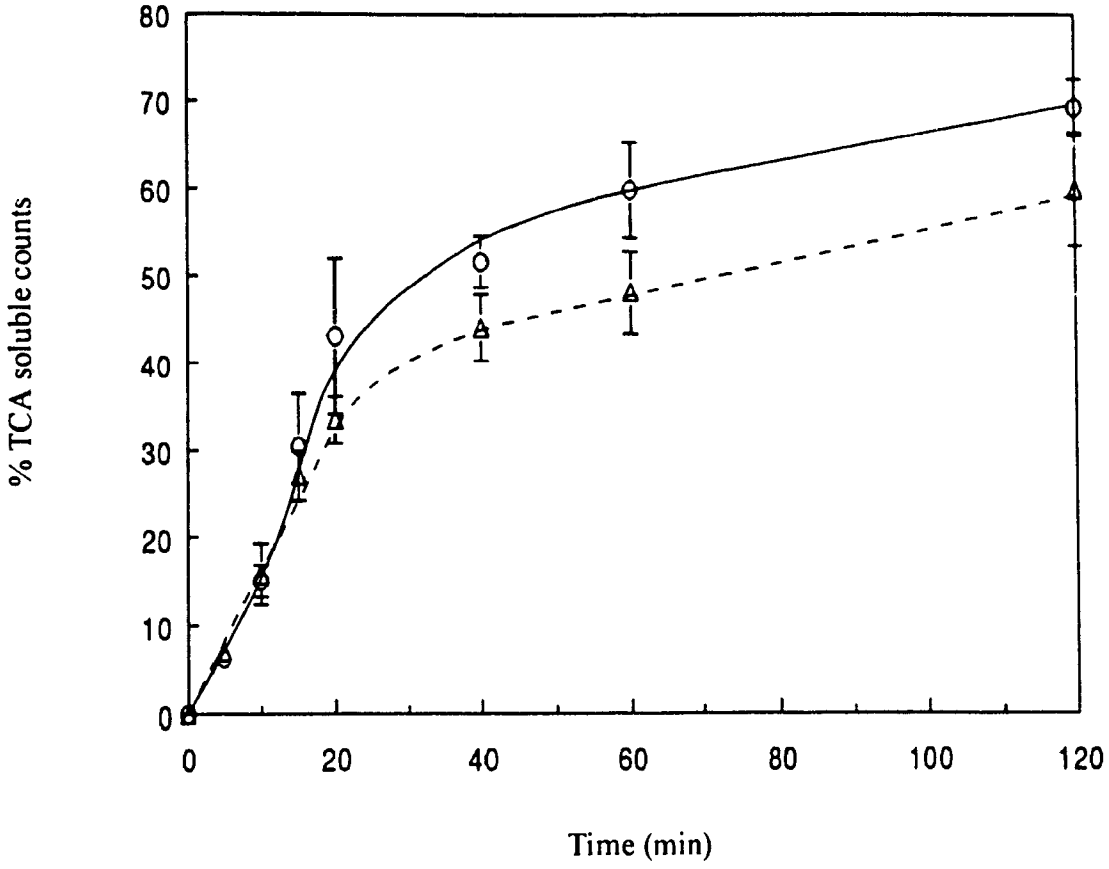

Fig 3.4B: Insulin degradation as monitored by % TCA-soluble ^{125}I counts in the conditioning buffer. The degradation of a pre-bound insulin cohort was initiated by a temperature shift from 4°C to 37°C and monitored over a 2-hour (120-min) time period. Although both cell lines exhibited similar degradation at 20 min or less ($P>0.12$), insulin degradation in A1-j cells (Δ) is significantly diminished relative to V-79 cells (O) after 20 min ($P<0.01$). The results represent the average ± S.E.M from the triplicate determinations of 3-8 separate experiments.

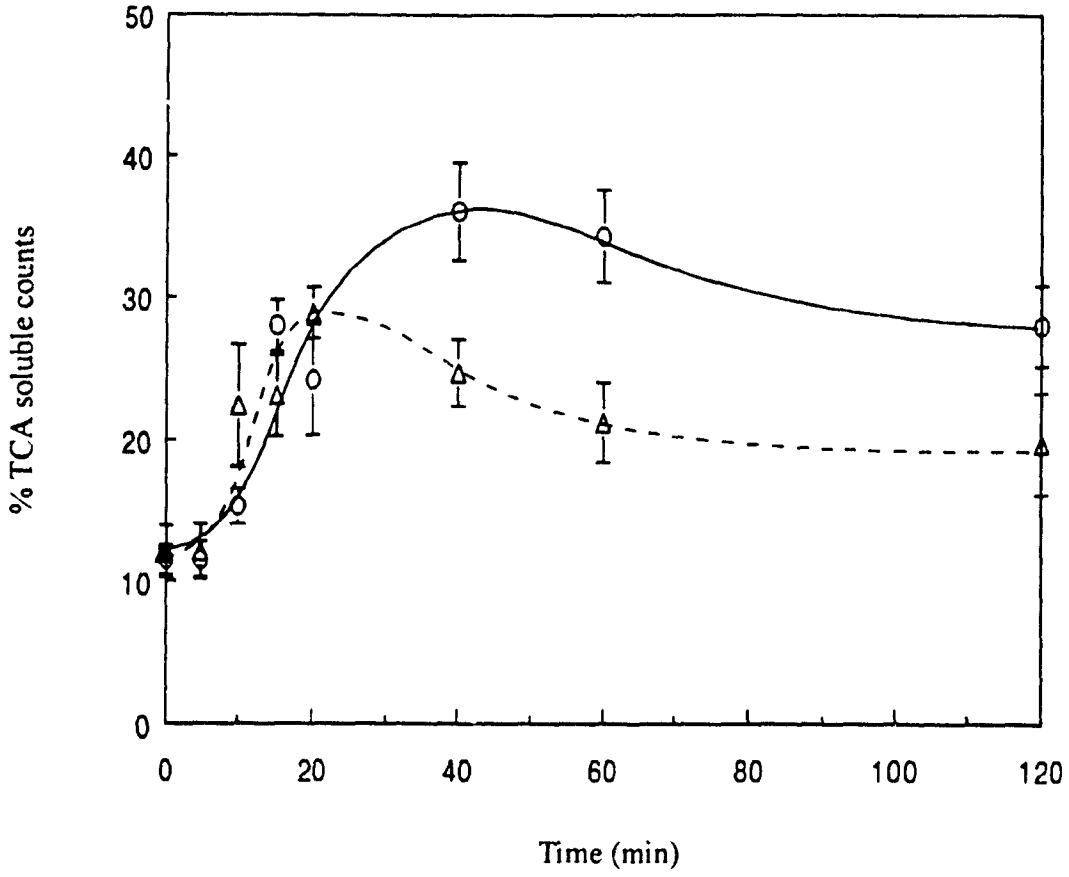

Fig 3.4C: Insulin degradation as monitored by % TCA-soluble ^{125}I counts in the cell monolayer. The degradation of a pre-bound insulin cohort was initiated by a temperature shift from 4°C to 37°C and monitored over a 2-hour (120-min) time period. Although both cell lines exhibited similar degradation at 20 min or less ($P>0.82$), insulin degradation in A1-j cells (Δ) is significantly reduced relative to V-79 cells (○) after 20 min ($P<0.001$). The results represent the average ± S E.M from the triplicate determinations of 3-8 separate experiments

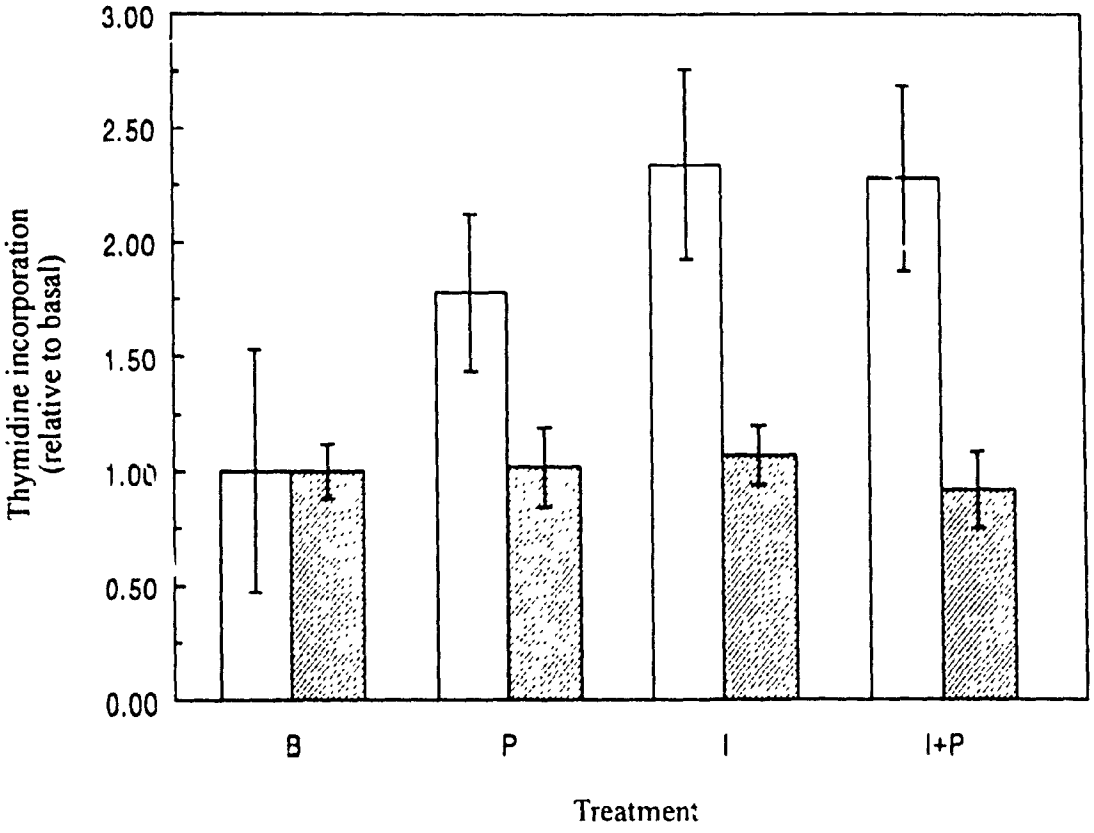

Fig 3.5A: The effect of bpV(phen) on 10 hour thymidine incorporation in V-79 and A1-j cells. B = basal conditions, P= 1.0 μM bpV(phen) added, I = 667 nM insulin added. The results represent the average ± S.E.M from the triplicate determinations of 3 separate experiments and are expressed relative to basal ^{3}H-thymidine incorporation into TCA precipitable material. Both insulin and bpV(phen), added alone or in combination, elicited approximately 2-fold stimulation above basal levels in (▯) V-79 cells ($P<0.025$); but had no significant effect in (▨) A1-j cells ($P>0.25$)

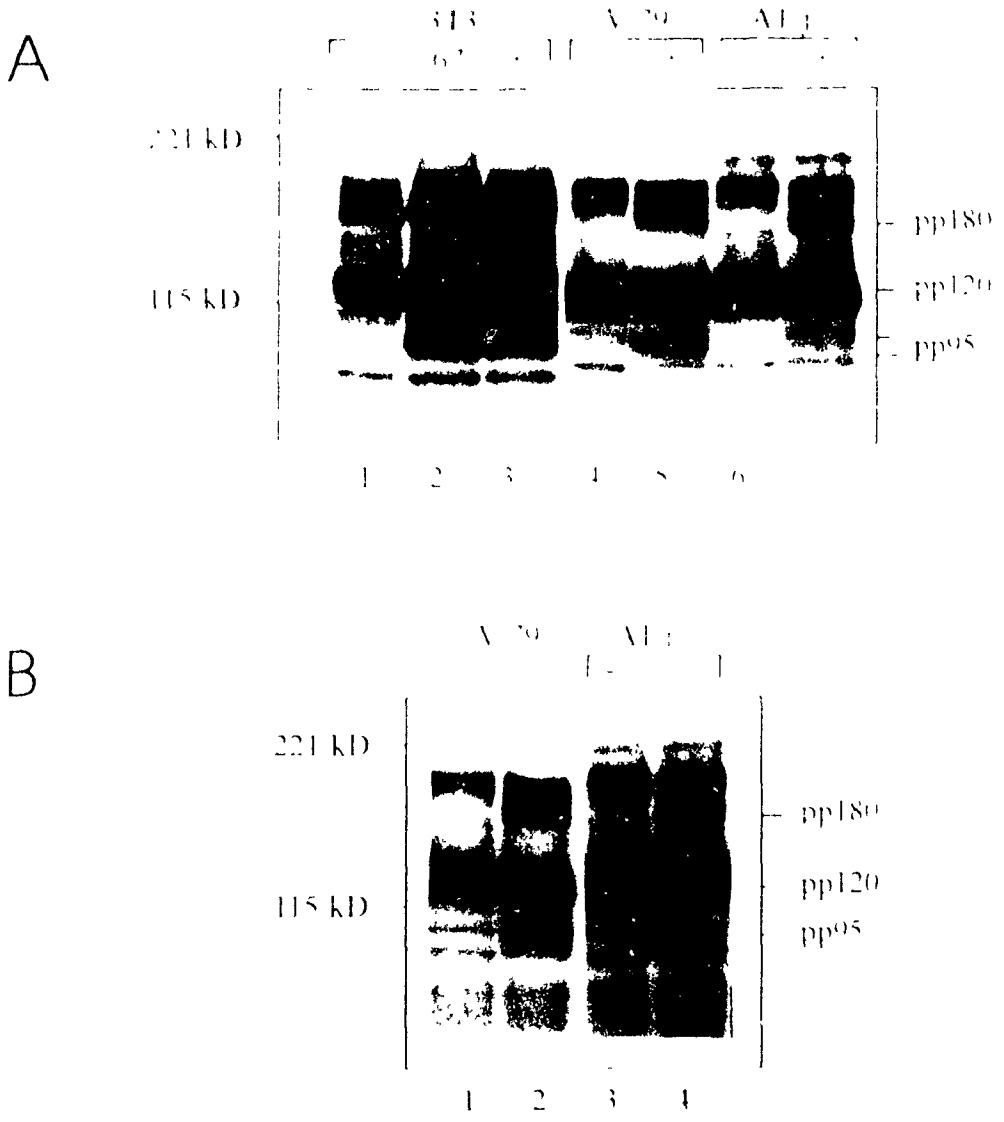

Fig 3.6: Insulin receptor autophosphorylation and endogenous kinase activity in V-79 and A1-j cells *in vivo*. A) Protein-matched extracts. 200 µg protein extracts from 3T3 cells (lanes 1-3), V-79 cells (lanes 4 and 5) and A1-j cells (lanes 6 and 7) were run on a 6% SDS-PAGE (see Materials and Methods for details). Following transfer to nitrocellulose paper, blots were probed for phosphotyrosine using ICN's PY-20 antibody followed by chemiluminescent detection. Positions of the high molecular weight markers is indicated to the left of the blot, while the 95, 120, and 180 kD bands are identified on the right hand side. (-) indicates basal stimulation, (+) 2 min stimulation with 667 nM insulin, and (67) indicates 2 min stimulation with 67 nM insulin. **B) Receptor-matched extracts.** V-79 and A1-j samples were loaded as above except that V-79 extracts (lanes 1,2) were underloaded (150 vs 200 µg) relative to A1-j extracts (lanes 3,4) to account for differences in surface insulin receptor expression. Underloading of V-79 extracts is reflected in a reduced pp120 band (lanes 1,2 vs 3,4), yet 95 and 180 kD bands are similar in both cell lines both in the - and + insulin states (compare lanes 1 with 3 and 2 with 4). The above figures are representative of the results obtained in 3-4 separate experiments.

Fig 4.1 Serum-stimulated expression of *c-fos* mRNA vs time

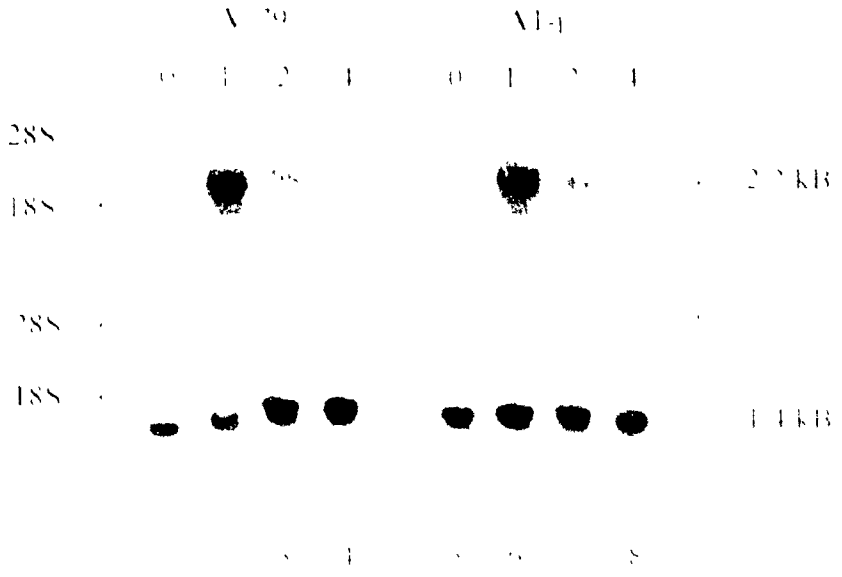

Fig 4.1A Northern blot Total RNA was extracted from V-79 cells (lanes 1-4) and A1-1 cells (lanes 5-8) cells at 0, 1, 2, and 4 hours following stimulation with 5% FBS. 10-µg samples were run on denaturing formaldehyde agarose electrophoresis, transferred to nitrocellulose paper and probed with *c-fos* (upper panel) and *GAPDH* (lower panel) DNA labelled with ^{32}P. 28S and 18S rRNA markers are indicated to the left of each panel. The *c-fos* and *GAPDH* bands were estimated at 2.2 and 1.4 kB respectively. This figure is representative of the results obtained in two separate experiments.

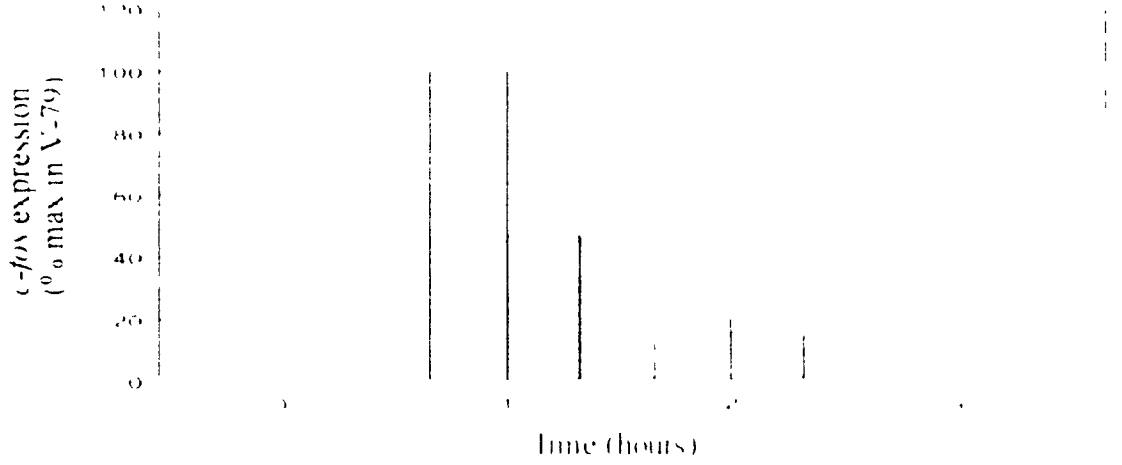

Fig 4.1B *c-fos* expression normalized to *GAPDH* mRNA content. The northern blots shown above were quantified on an optical densitometer and the *c-fos* readings divided by those of *GAPDH* for each lane. The results are expressed as % maximal expression of *c-fos* in V-79 cells. At most time points, and especially during maximal stimulation at 1 hour, A1-1 readings (▲) were diminished relative to those seen in V-79 cells (●).

Fig 4.2 Serum-stimulated expression of *c-jun* mRNA vs time.

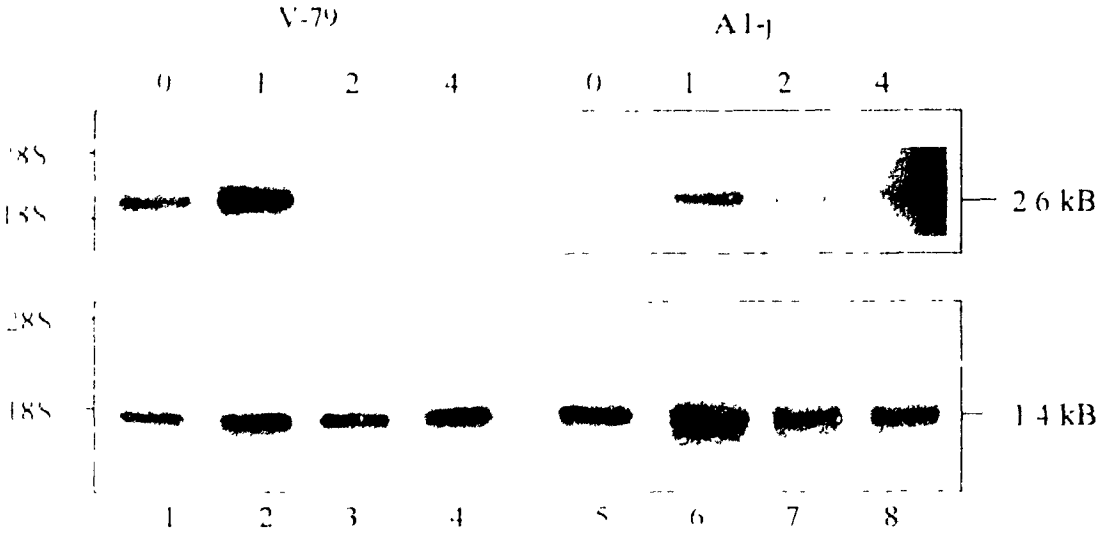

Fig 4.2A Northern blot. Total RNA was extracted from V-79 cells (lanes 1-4) and A1-1 cells (lanes 5-8) cells at 0, 1, 2 and 4 hours following stimulation with 5% FBS. 10 µg samples were run on denaturing formaldehyde agarose electrophoresis, transferred to nitrocellulose paper and probed with *c-jun* (upper panel) and *GAPDH* (lower panel) DNA labelled with ^{32}P. 28S and 18S rRNA markers are indicated to the left of each panel. The *c-jun* and *GAPDH* bands were estimated at 2.6 and 1.4 kB respectively. This figure is representative of the results obtained in two separate experiments.

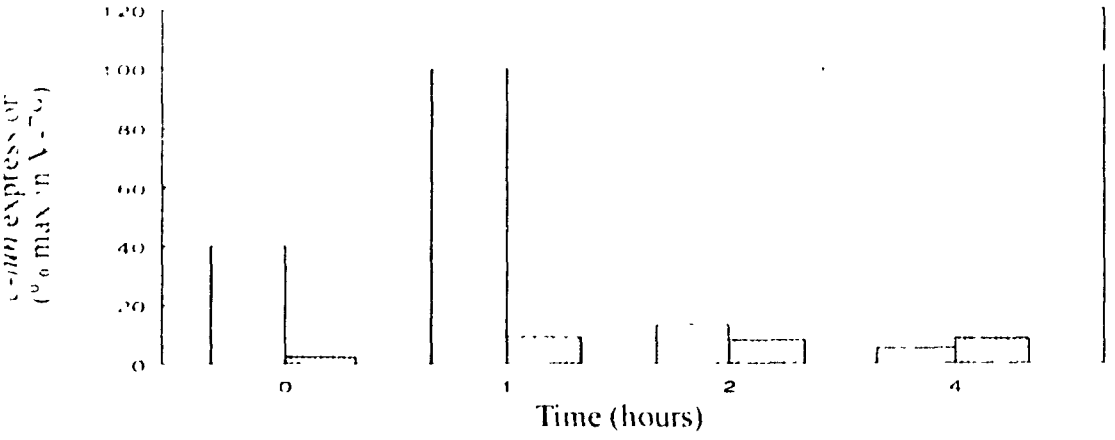

Fig 4.2B *c-jun* expression normalized to *GAPDH* mRNA content. The northern blots shown above were quantified on an optical densitometer and the *c-jun* readings divided by those of *GAPDH* for each lane. The results are expressed as % maximal expression of *c-jun* in V-79 cells. At most time points, and especially during maximal stimulation at 1 hour, A1-1 readings ( ) were diminished relative to those seen in V-79 cells ( )

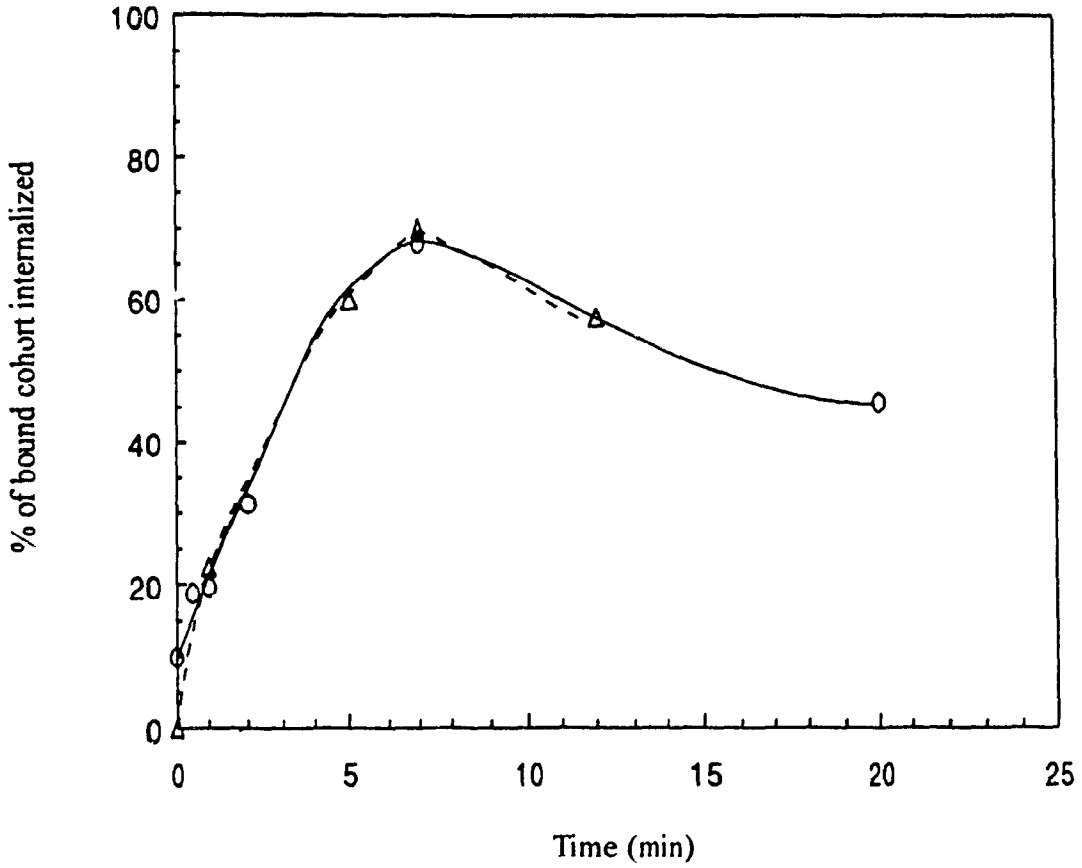

Fig X **Internalization of ^{125}I-insulin into V-79 and A1-j cells.** Cells were preincubated in the presence of trace amounts of insulin (0.16 nM) for 4 hours at 4°C. Unbound ^{125}I-insulin was then removed by washing in HHBSA and bound insulin was monitored at various times following a temperature shift to 37°C. The amount of insulin internalized was determined as the fraction of ^{125}I label resistant to acid dissociation. The results are expressed as the % of prebound ^{125}I-insulin internalized and represent the average ± S.E.M. from three separate experiments. (O) = V-79 cells, (Δ) = A1-j cells. Reproduced from Leckett and Germinario, 1992[1].

Fig XI **Model for the A1-j mutation.** Under normal circumstances (as one would expect to find in V-79 cells), internalized complexes of insulin and its receptor are directed through the endosomal network (EN) in an acidification-dependent process (A). It is here where insulin is released from the receptor and is segregated into vesicles which deliver it to the lysosomal compartment for destruction. Meanwhile, the insulin receptors are routed to a different set of vesicles (C) which are recycled back to the plasma membrane surface. In the A1-j cell line, however, the receptor complexes may have been re-routed to the prosome (D) where insulin proteolysis is mediated by the insulin degrading enzyme (IDE) at neutral pH and is thus independent of vesicular acidification. IDE associates with a larger holloenzyme complex called multicatalytic proteinase (MCP) whose proteolytic activity may be involved in the degradation of the insulin receptors brought into the prosome and thus account for the lower insulin receptor number in A1-j relative to V-79 cells. Remnants of insulin receptors catabolized in the prosomes are likely chanelled to the lysosomes for terminal degradation. Protein kinase C (PKC) has also been shown to interfere with insulin receptor recycling (Seedorf *et al.*, 1995[146]). One possible mechanism invloves direct competition with PTPase for an association with the receptor β-subunits (E). Depending upon the presence of other as of yet undefined cell context factors, PKC-associated receptors will either be targetted for lysosomal degradation or recycling back to the plasma membrane. Compiled from data reported in: Torrosian *et al.*, 1993[145]; Seedorf *et al.*, 1995[146]; Bennett *et al.*, 1994[185]; Duckworth *et al.*, 1994[186].

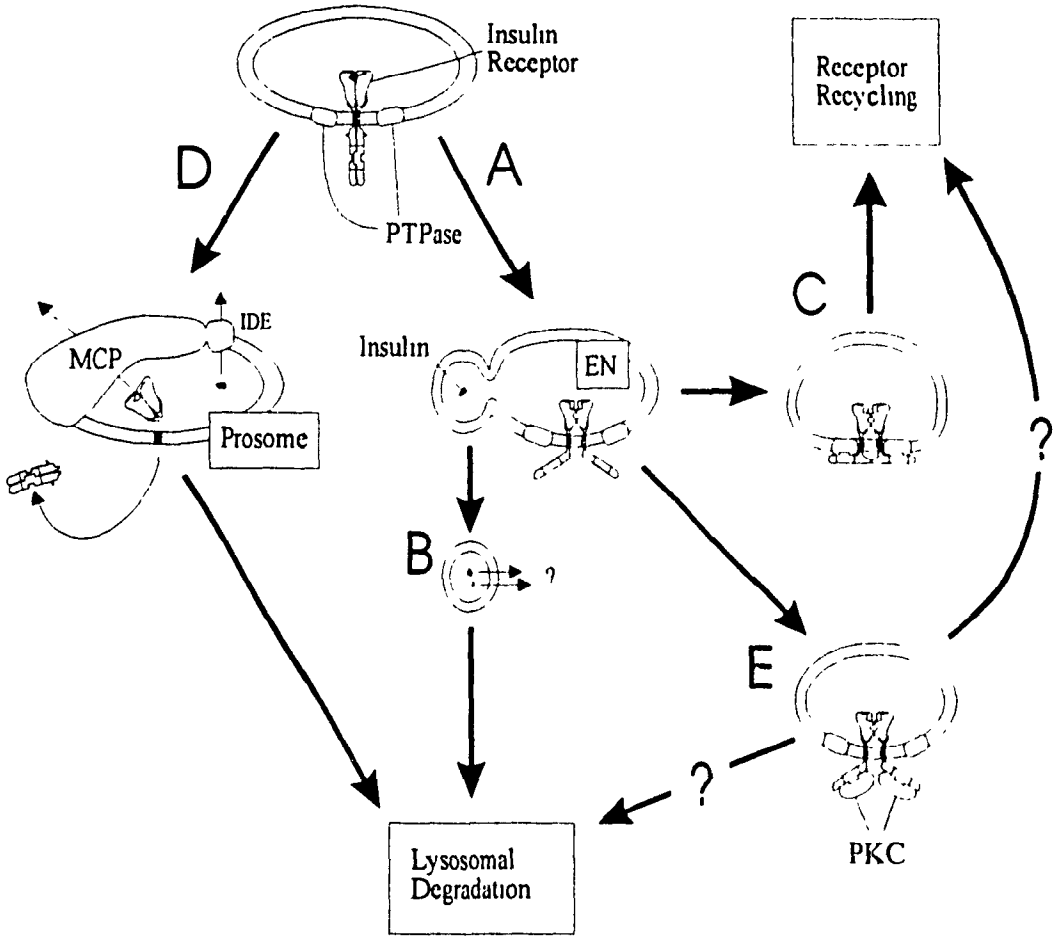
Insulin
Receptor
PTPase
D
A
Receptor
Recycling
C
IDE
MCP
Prosome
Insulin
EN
B
?
?
E
?
Lysosomal
Degradation
PKC

TABLES:

TABLE I
The effect of insulin in combination with other mitogens on V-79 and A1-j cell growth

% serum-stimulated growth

Cell line	Insulin	-EGF	+EGF	+THR	+EGF+THR
V-79	-	0	48±3	37±3	48±5
	+	53±3 *	82±4 *	90±4 *	101±3*
A1-j	-	0	40±5	32±3	45±9
	+	<2	39±5	34±2	42±7

170 nM insulin was added alone or in combination with 2 nM epidermal growth factor (EGF) or 30 nM α-thrombin (THR) in serum-free medium to V-79 and A1-j cells for 3 days followed by cell counting. The data represent hormonally induced increases in cell numbers over those observed under basal conditions and are presented as a % of serum-stimulated mitogenesis. The results represent the average ± S.E.M. from 3 separate experiments. * indicates a significant difference between -/+ insulin-stimulated values (student's t: $P<0.05$). These data have been reproduced from Leckett and Germinario, 1992[1].

TABLE 1.1
The effect of insulin concentration on hexose transport in V-79 and A1-j cells.

2DG uptake (relative to basal)

Insulin (nM)	V-79	A1-j
6.7	1.31 ± 0.08	1.23 ± 0.15
67	1.58 ± 0.12	1.67 ± 0.15
667	1.57 ± 0.20	1.58 ± 0.13
5% FBS	1.56 ± 0.18	1.66 ± 0.32

The average basal uptake values were 1954 ± 168 and 1992 ± 453 pmol 2DG/mg protein/5 min for V-79 and A1-j cells respectively (average ± S.E.M. from the triplicate determinations of 4 separate experiments). 2-way ANOVA revealed a significant increase in hexose transport above basal resulting from the addition of insulin or 5% FBS ($P < 0.01$), with no significant difference observed in the responses of the two cell lines ($P > 0.25$).

TABLE 1.2A
The time dependence of insulin-stimulated glycogen synthesis in V-79 and A1-j cells.

Glycogen synthesis (rel. to basal synth.)

Time (h)	V-79	A1-j
1	1.20 ± 0.18	1.22 ± 0.12
2	1.41 ± 0.34	1.02 ± 0.23
4	1.47 ±0.23	1.41 ± 0.14
6	1.45 ± 0.26	1.50 ± 0.23

Insulin was used at a concentration of 667 nM. 2-way ANOVA shows a significant increase in glycogen synthesis over time ($P<0.05$), but no significant difference between mutant and parental responses ($P>0.05$). The results represent the average ± S.E.M. from the triplicate determinations of 3 separate experiments.

TABLE 1.2B
The effect of insulin concentration on glycogen synthesis in V-79 and A1-j cells.

Glycogen synthesis (rel. to basal synth.)

[Insulin] (nM)	V-79	A1-j
6.7	1.13 ± 0.03	1.05 ± 0.03
13	1.22 ± 0.05	1.33 ± 0.03
34	1.30 ± 0.04	1.35 ± 0.07
67	1.35 ± 0.02	1.58 ± 0.04
335	1.45 ± 0.04	1.55 ± 0.03
667	1.56 ± 0.05	1.58 ± 0.10
5% FBS	1.44 ± 0.06	1.33 ±0.03

The average basal synthesis values were $1.89 \pm 0.40 \times 10^4$ and $1.68 \pm 0.55 \times 10^4$ DPM/ mg protein for V-79s and A1-js respectively. 2-way ANOVA revealed significant concentration dependence in both cell lines ($P < 0.001$), and that the A1-j response was significantly different from that of the V-79s ($P < 0.001$). The results represent the average ± S.E.M. from the triplicate determinations of 3 separate experiments.

TABLE 2.2
Insulin-stimulated growth in V-79 and A1-j cells as monitored by 3-day cell counts

Growth relative to basal

[Insulin] (nM)	V-79	A1-j
83	2.27 ± 0.26	1.21 ± 0.14
334	2.04 ± 0.33	1.09 ± 0.18
667	1.93 ± 0.48	1.06 ± 0.27
5% FBS	9.23 ± 2.20	8.41 ± 2.16

The average basal 3-day cell counts were $3.6 \pm 1.2 \times 10^5$ and $3.9 \pm 1.5 \times 10^5$ cells/ plate for V-79 and A1-j cells respectively. T-tests showed that V-79 responses to insulin were significantly elevated above basal ($P < 0.01$), while A1-j responses were not ($P > 0.10$). Both cell lines responded equally to stimulation with 5% FBS (students t: $P > 0.10$). The results represent the average ± S.E.M. from the triplicate determinations of 2-9 separate experiments.

TABLE 3.1
DNA synthesis in V-79 and A1-j cells as monitored by thymidine incorporation into TCA precipitable material.

A: 10 h post-stimulation

Relative to basal thymidine inc.

Stimulus	V-79	A1-j
667 nM Insulin	2.34 ± 0.42	1.07 ± 0.13
5% FBS	2.65 ± 0.52	2.23 ± 0.55

B: 20 h post-stimulation

Relative to basal thymidine inc.

Stimulus	V-79	A1-j
667 nM Insulin	2.86 ± 0.53	0.98 ± 0.23
5% FBS	6.81 ± 1.38	2.89 ± 0.63

At both time points V-79 cells showed a greater than 2-fold response to insulin (student's t: $P<0.001$, $n=4$), while A1-j cells showed no significant response (student's t: $P>0.10$, $n=3$). Although at 10 hours post-stimulus both cell lines exhibited comparable responses to treatment with 5% FBS, at the 20 h time point the A1-j response appears to be significantly diminished (student's t: $P<0.05$). The results represent the average ± S.E.M. from the triplicate determinations of 3 or 4 experiments.

TABLE 3.4A
The efflux of insulin from cell monolayers to the conditioning buffer expressed as % of bound cohort

Time (min)	V-79		A1-j	
	condit. buffer	cell associated	condit. buffer	cell associated
0	0.0±1.2	99.9±16.5	0.0 ± 1.1	92.9±14.5
5	20.6±6.3	82.8±15.6	23.4±4.4	80.7±14.9
10	33.8±8.5	71.2±13.1	39.1±7.9	71.7±15.0
15	51.5±12.6	50.7±7.8	53.4±9.7	44.2±8.1
20	66.9±18.4	29.0±9.1	65.4±10.6	34.8±5.6
40	73.7±11.1	23.4±4.6	75.1±11.8	23.1±4.9
60	80.1±14.6	17.3±3.7	81.5±14.1	18.0±4.9
120	87.2±13.0	11.9±2.3	83.5±17.5	13.0±4.0

The total amount of insulin in each cohort bound was 16.8 ± 2.1 fmol/ mg protein for V-79cells and 13.2 ± 1.5 fmol/ mg protein for A1-j cells. When insulin efflux is normalized with respect to these values, the efflux profiles are virtually identical in both cell lines (2-way ANOVA: $P>0.77$). The ANOVA also reveals a significant efflux of insulin into the extracellular fluid compartment or conditioning buffer (condit. buffer) over time ($P<0.0001$). Since insulin was not acid-dissociated from cell monolayers prior to solubilization and subsequent analysis, cell associated counts include both internalized insulin and surface bound insulin. The results represent the average ± S.E.M. from the triplicate determinations of 7-8 separate experiments.

TABLE 3.4B
Insulin degradation as monitored by %TCA-soluble ^{125}I-labelled insulin in the conditioning buffer.

Time (min)	V-79	A1-j
0	0.0 ± 0.4	0.0 ± 0.4
5	6.2 ± 0.9	7.0 ± 0.9
10	15.0 ± 1.8	15.8 ± 3.5
15	30.4 ± 6.1	27.1 ± 2.8
20	43.1 ± 8.9	33.5 ± 2.7
40	51.6 ± 2.9	44.1 ± 3.8
60	59.8 ± 5.5	48.1 ± 4.7
120	69.3 ± 3.2	59.9 ± 6.5

TABLE 3.4C
Insulin degradation as monitored by %TCA-soluble cell-associated ^{125}I-labelled insulin.

Time (min)	V-79	A1-j
0	11.5 ± 1.0	12.1 ± 1.8
5	11.5 ± 1.3	12.1 ± 1.9
10	15.3 ± 1.2	22.4 ± 4.3
15	28.0 ± 1.8	23.1 ± 2.8
20	24.2 ± 3.9	28.9 ± 1.8
40	36.1 ± 3.4	24.7 ± 2.4
60	34.3 ± 3.3	21.2 ± 2.8
120	28.0 ± 2.9	19.7 ± 3.6

Before 20 min there is no significant difference between the conditioning buffer and cell-associated degradation patterns in A1-j *vs* V-79 cell lines (2-way ANOVA: $P > 0.12$). After-20 min, however, A1-j cells appear to produce a significantly lower proportion of soluble ^{125}I counts than do V-79 cells (2-way ANOVA: $P < 0.01$). The results represent the average ± S.E.M from the triplicate determinations of 3-8 separate experiments.

TABLE 3.4D
The effect of adding inhibitors of the endosomal apparatus on 20 minute insulin degradation.

% cohort rescued

Inhibitor	V-79	A1-j
Bacitracin	7.9 ± 5.3	3.0 ± 5.3
Chloroquine	26.4 ± 1.4	18.4 ± 1.5
Monensin	9.0 ± 3.2	12.5 ± 1.6

The values are expressed as % cohort rescued totalled from both soluble counts decreased in the conditioning buffer and precipitable counts rescued in the cell-associated fraction. The only significant differential response was that observed with chloroquine where its effect on A1-j cells appears to be slightly reduced relative to their V-79 counterparts (student's t: $P < 0.05$). Bacitracin was added at a final concentration of 100 U/mL, Chloroquine at 100 μM, and Monensin at 25μM. The results represent the average ± S.E.M. from the triplicate determinations of 2 experiments.

TABLE 3.5
The effect of bpV(phen) on DNA synthesis as monitored by thymidine incorporation into TCA-precipitable material.

A: 10 h post stimulation

Relative to basal thymidine inc.

Stimulus	V-79	A1-j
Basal	1.00 ± 0.23	1.00 ± 0.11
bpV(phen)	1.78 ± 0.34	1.02 ± 0.17
Insulin	2.34 ± 0.42	1.07 ± 0.13
Insulin + bpV(phen)	2.28 ± 0.41	0.92 ± 0.17
5% FBS	2.65 ± 0.52	2.23 ± 0.55
5%FBS + bpV(phen)	2.66 ± 0.58	1.95 ± 0.24

B: 20 h post stimulation

Relative to basal thymidine inc.

Stimulus	V-79	A1-j
Basal	1.00 ± 0.24	1.00 ± 0.2?
bpV(phen)	1.76 ± 0.40	1.12 ± 0.30
Insulin	2.86 ± 0.53	0.98 ± 0.23
Insulin + bpV(phen)	2.53 ± 0.70	1.05 ± 0.29
5% FBS	6.81 ± 1.38	2.89 ± 0.63
5%FBS + bpV(phen)	5.38 ± 1.46	2.14 ± 0.78

Insulin was added at a final concentration of 667 nM and bpV(phen) at 1μM. The results represent the average ± S.E.M. from the triplicate determinations of 3 separate experiments. At both time points, insulin and bpV(phen) produced approximately 2-fold increases over basal thymidine incorporation in V-79 cells (student's t: $P<0.025$). Neither compound, added alone or together, was able to stimulate a significant response in A1-j cells ($P>0.25$).

REFERENCES:

1. **Leckett, B., Germinario, R.** (1992) Construction of a toxic insulin molecule: Selection and partial characterization of cells resistant to its killing effects. *Cytotechnology* **10:** 125-136.

2. **Wool, I., Wettenhall, R., Klein-Bremhaar, H., Abayang, N.** (1972) Insulin Action, Fritz, I Ed., Acad Press, NY, p 415

3. **Moses, AC**: Is insulin a growth factor? In LeRoith D (Ed): Insulin-Like Growth Factors: Molecular and Cellular Aspects. Boca Raton, CRC Press, 1991, pp 245-270.

4. **Koontz, J.W., Iwahashi, M.** (1981) Insulin as a potent, specific growth factor in a rat hepatoma ceil line. *Science* **211:** 947-949.

5. **Petersen, B., Blecher, M.** (1979) Insulin receptors and functions in normal and spontaneously 'ransformed cloned rat hepatocytes. *Exp Cell Res* **120:** 119-125.

6. **Hofmann, C., Marsh, J., Miller, B., Steiner D.** (1980) Cultured hepatoma cells as a model system for studying insulin processing and biological responsiveness. *Diabetes* **29:** 865-874.

7. **Nagaragian, L., Andersen, W.** (1982) Insulin promotes the growth of F9 embryonal cells apparently by acting through its own receptor. *Biochem Biophys Res Comm* **106:** 974-980.

8. **Mammounas, M., Gervin, D., Englesberg, E.** (1989) The insulin receptor as a transmitter of a mitogenic signal in Chinese hamster ovary CHO-K1 cells. *Proc Nat Acad Sci USA* **86:** 9294-9298.

9. **Pillemer, G., Lugasi-Evgi, H., Scharovski, G., Nao' D.** (1992) Insulin dependence of murine lymphoid T-cell leukemia. *Int J Cancer* **50:** 80-85.

10. **Moller, D., Flier, J.** (1991) Insulin Resistance - Mechanisms, Syndromes, and implication *New Engl J Med* **325 (No. 13):** 938-948.

11. **Clemmons, D.** Insulin-Like Growth Factor Binding Proteins: In LeRoith D (Ed): Insulin-Like Growth Factors: Molecular and Cellular Aspects. Boca Raton, CRC Press, 1991, pp 151-179.

12. **White, M., Khan, C.** (1994) The Insulin Signalling System. *J Biol Chem* **269:** 1-4.

13. **Fehlig, P., Bergman, M.** (1990) Integrated physiology of carbohydrate metabolism. In: Rifkin, H., Porte, D., Eds. Ellenburg and Rifkin's diabetes mellitus. 4th Ed., NY, Elsevier.

14. **Christoffersen, C., Bornfeldt, K., Rotella, C., Gonzales, N., Vissing, H., Shymko, R., Hoeve, J., Groffen, J., Heistercamp, M., De Meyts, P.** (1994) Negative Cooperativity in the insulin-like growth factor-I (IGF-I) receptor and a chimeric IGF-I/insulin receptor. *Endocrinology* **135:** 472-475.

15. **Soos, M., Field, C., Siddle, K.** (1993) Purified hybrid insulin/insulin-like growth factor-1 receptors bind insulin-like growth factor-1, but not insulin, with high affinity. *Biochem J* **290:** 419-426.

16. **Seino, S., Seino, M., Nishi, S., Bell, G.** (1989) Structure of the human insulin receptor gene and characterization of its promoter. *Proc Nat Acad Sci USA* **86:** 114-118.

17. **Finn, F., Ridge, K., Hofmann, K.** (1989) Labile disulphide bonds in human placental insulin receptor. *Proc Nat Acad Sci USA* **87:** 419-423.

18. **Shoelson, S., White, M., Khan, C.** (1988) Tryptic activation of the insulin receptor. Proteolytic cleavage of the α-subunit releases the β-subunit from inhibitory control. *J Biol Chem* **263:** 4852-4860.

19. **Waugh, S., DiBella, E., Pilch, P.** (1989) Isolation of a proteolytically derived domain of the insulin receptor containing the major site of cross-linking/binding. *Biochemistry* **28:** 3448-3455

20. **Schäffer, L., Ljungvist, L.** (1992) Identification of a disulphide bridge connecting the α-subunits of the extracellular domain of the insulin receptor. *Biochem Biophys REs Comm* **189:** 650-653.

21. **Cheatham, B., Khan, C.** (1992) Cysteine 647 in the insulin receptor is required for normal covalent interaction between α- and β-subunits and signal transduction. *J Biol Chem* **267:** 7108-7115.

22. **Xu, Q., Paxton, R., Fujita,-Yamaguchi, Y.** (1990) Substructural analysis of the insulin receptor by microsequence analysis of limited tryptic fragments isolated by sodium dodecyl sulphate-polyacrylamide gel electrophoresis in the absence or presence of dithiothreitol. *J Biol Chem* **265:** 18673-18681.

23. **Hedo, J., Khan, C., Hayashi, M., Yamada, K., Kasuga, M.** (1983) Biosynthesis and glycosylation of the insulin receptor. Evidence for a single polypeptide precursor of the two major subunits. *J Biol Chem* **258:** 10020-10026.

24. **Hedo, J., Kasuga, M., Van Obberghen, E., Roth, J., Khan, C.** (1981) Direct demonstration of glycosylation of insulin receptor subunits by biosynthetic and external labelling: evidence for heterogeneity. *Proc Nat Acad Sci USA* **78:** 4791-4795.

25. **Herzberg, V., Grigorescu, F., Edge, A., Spiro, Khan, C.** (1985) Characterization of insulin receptor carbohydrate by comparison of chemical and enzymatic deglycosylation. *Biochem Biophys Res Comm* **129:** 789-796.

26. **Collier, E., Gorden, P.** (1989) The insulin receptor contains O-linked oligosaccharide. *Diabetes* **38 (Suppl 2):** 178A(Abstr. No. 686).

27. **Wedekind, F., Baer-Pontzen, K., Bala-Mohan, S., Choli, D., Zahn, H., Brandenburg, D.** (1989) Hormone binding site of the insulin receptor: an analysis using photoaffinity-mediated avidin complexing. *Biol Chem Hoppe Seyler* **370:** 251-258.

28. **De Meyts, P., Wallach, B., Christoffersen, C., Ursø, B., Grønskov, K., Latus, L., Fumiatsu, Y., Ilondo, M., Shymko, R.** (1994a) The insulin-like growth factor-1 receptor: structure, ligand-binding mechanism and signal transmissic... *Horm Res* **42:** 152-169.

29. **Kjeldsen, T., Wiberg, F., Andersen, A.** (1994) Chimeric receptors indicate that phenylalanine 39 is a major contributor to insulin specificity of the insulin receptor. *J Biol Chem* **269:** 32942-32946.

30. **Lee, J., Pilch, P.** (1994) The insulin receptor: structure, function, and signalling. *Am J Physiol* **266 (Cell Physiol 35):** C319-C334.

31. **Shäffer, L.** (1994) A model for insulin binding to the insulin receptor. *Eur J Biochem.* **211:** 1127-1132.

32. **De Meyts, P.** (1994b) The structural basis of insulin and insulin-like growth factor-1 receptor binding and negative cooperativity, and its relevance to mitogenic versus metabolic signalling. *Diabetologia* **37 (Suppl 2):** S135-S148.

33. **Leconte, I., Auzan, C., Debant, A., Rossi, B., Clauser, B.** (1992) N-linked oligosaccharide chains of the insulin receptor β-subunit are essential for transmembrane signalling. *J Biol Chem* **267:** 17415-17423.

34. **Yamada, K., Goncalves, E., Carpentier, J., Khan, C., Shoelson, S.** (1995) Transmembrane domain inversion blocks ER release and insulin receptor signalling. *Biochemistry* **34:** 946-954.

35. **Cheatham, B., Khan, C.** (1995) Insulin action and the insulin signalling network. *Endocrine Rev* **16:** 117-142.

36. **Tavaré, J., Siddle, K.** (1993) Mutational analysis of insulin receptor function: consensus and controversy. *Biochim Biophys Acta* **1178:** 21-39.

37. **Frattali, A., Treadway, J., Pessin, J.** (1992) Transmembrane signalling by the human insulin receptor kinase: relationship between intramolecular β-subunit trans- and cis- autophosphorylation and substrate kinase activation. *J Biol Chem* **267:** 19521-19528.

38. **Frattali, A., Pessin, J.** (1993) Relationship between α-subunit ligand occupancy and β-subunit autophosphorylation in insulin/insulin-like growth factor-I hybrid receptors. *J Biol Chem* **268:** 7393-7400.

39. **Lee, J., O'Hare, T., Pilch, P., Shoelson, S.** (1993a) Insulin receptor autophosphorylation occurs asymmetrically. *J Biol Chem* **268:** 4092-4098.

40. **Wei, L., Hubbard, S., Hendrickson, W., Ellis, L.** (1995) Expression, characterization, and crystallization of the catalytic core of the human insulin receptor protein-tyrosine kinase domain. *J biol Chem* **270:** 8122-8130.

41. **White, M., Livingston, J., Backer, J., Lauris, V., Dull, T., Ullrich, A., Khan, C.** (1988) Mutation of the insulin receptor at tyrosine 960 inhibits signal transmission but does not affect its tyrosine kinase activity. *Cell* **54:** 641-649.

42. **Backer, J., Schroeder, G., Cahill, D., Ullrich, A., Siddle, K., White, M.** (1991) Cytoplasmic juxtamembrane region of the insulin receptor: a critical role in ATP binding. endogenous substrate phosphorylation, and insulin-stimulated bio-effects in CHO cells. *Biochemistry* **30:** 6366-6372.

43. **Feener, E., Backer, J., King, G., Wilden, P., Sun, X., Khan, C., White, M.** (1993) Insulin stimulates serine and tyrosine phosphorylation in the juxtamembrane region of the insulin receptor. *J Biol Chem* **268:** 11256-11264.

44. **Backer, J., Khan, C., Cahill, D., Ullrich, A., White, M.** (1990a) Receptor-mediated internalization of insulin requires a 12-amino acid sequence in the juxtamembrane region of the insulin receptor β-subunit. *J Biol Chem* **265:** 16450-16454.

45. **Backer, J., Shoelson, S., Weiss, M., Hua, Q., Cheatham, B., Haring, E., Cahill, D., White, M.** (1992) The insulin receptor juxtamembrane region contains two independent tyrosine/β-turn internalization signals. *J Cell Biol* **118:** 831-839.

46. **Mothe, I., Tartare, S., Kowalski-Chauvel, A., Kaliman, P., Van Obberghen, E., Ballotti, R.** (1995) Tyrosine kinase activity of a chimeric insulin-like growth factor-1 receptor containing the insulin receptor C-terminal domain. Comparison with the tyrosine kinase activities of the insulin and insulin-like growth factor-1 receptors using a cell-free system. *Eur J Biochem* **228:** 842-848.

47. **Myers, M., Sun, X., Cheatham, B., Jachna, B., Glasheen, E., Backer, J., White, M.** (1993) IRS-1 is a common element in the insulin and insulin-like growth factor-1 signalling to the phosphatidyl inositol 3'-kinase. *Endocrinology* **132:** 1421-1430.

48. **Baron, V., Kaliman, P., Alengrin, F., Van Obberghen, E.** (1995) Interaction of the C-terminal acidic domain of the insulin receptor with histone modulates the receptor kinase activity. *Eur J Biochem* **229:** 27-34.

49. **Lewis, R., Wu, G., MacDonald, R., Czech, M.** (1990a) Insulin-sensitive phosphorylation of serine 1293/1294 on the human insulin receptor by a tightly associated serine kinase. *J Biol Chem* **265:** 947-954.

50. **Lewis, R., Cao, L., Perregaux, D., Czech, M.** (1990b) Threonine 1336 of the human insulin receptor is a major target for phosphorylation by protein kinase C. *Biochemistry* **29:** 1807-1813.

51. **Takayama, S., White, M., Khan, C.** (1988) Phorbol ester-induced serine phosphorylation of the insulin receptor decreases its tyrosine kinase activity. *J Biol Chem* **263:** 3440-3447.

52. **Stadmauer, L., Rosen, O.** (1986) Increasing the cAMP content of IM-9 cells alters the phosphorylation state and protein kinase activity of the insulin receptor. *J Biol Chem* **261:** 3402-3407.

53. **Chin, J., Dickens, M., Tavaré, J., Roth, R.** (1993) Overexpression of protein kinase isozymes α, βI, γ, and ϵ in cells overexpressing the insulin receptor. Effects on receptor phosphorylation and signalling. *J Biol Chem* **268:** 6338-6347.

54. **Rafaeloff, R., Maddux, B., Brunetti, A., Sbaccia, P., Sung, C., Patel, R., Hawley, D., Goldfine, I.** (1991) Transmembrane signalling by insulin via insulin receptor mutated at tyrosine 1158, 1162, 1163. *Biochem Biophys Res Comm* **179:** 912-918.

55. **Rolband, G., Williams, J., Webster, N., Hsu, D., Olefsky, J.** (1993) Deletion of exon 21 of the insulin receptor eliminates tyrosine kinase activity but preserves mitogenic signalling. *Biochemistry* **32:** 13545-13550.

56. **Gottschalk, W.** (1991) The pathway mediating insulin's effects on pyruvate dehydrogenase bypasses the insulin receptor tyrosine kinase. *J Biol Chem* **266:** 8814-8818.

57. **Moller, D., Benecke, H., Flier, J.** (1991) Biologic activities of naturally occurring human insulin receptor mutations. *J Biol Chem* **266:** 10995-11001.

58. **Wong, E., Tan, C., Khoo, H., Ng, F., Lim, K., Ciaraldi, T.** (1995) Rat fibroblast cells overexpressing kinase-inactive human insulin receptors are insulin responsive: influence of growth conditions. *Endocrinology* **136:** 1459-1467.

59. **Sasaoka, T., Langlois, W., Rose, D., Olefsky, J.** (1995) Mechanisms of enhanced transmembrane signalling by an insulin receptor lacking a cytoplasmic β-subunit domain. *J Biol Chem* **270:** 10885-10892.

60. **Schlessinger, J., Ullrich, A.** (1992) Growth factor signalling by receptor tyrosine kinases. *Neuron* **9:** 383-391.

61. **Fantl, W., Johnson, D., Williams, L.** (1993) Signalling by receptor tyrosine kinases. *Annu Rev Biochem* **62:** 453-481.

62. **Sun, X., Rothenberg, P., Khan, C., Backer, J., Araki, E., Wilden, P., Cahill, D., Goldstein, B., White, M.** (1991) Structure of the insulin receptor substrate IRS-1 defines a unique signal transduction protein. *Nature* **352:** 73-77.

63. **Kelly, K., Ruderman, N.** (1993) Insulin-stimulated phosphatidyl inositol 3-kinase. Association with a 185 kD tyrosine-phosphorylated protein (IRS-1) and localization in a low density membrane vesicle. *J Biol Chem* **268:** 4391-4398.

64. **Kublaoui, B., Lee, J., Pilch, P.** (1995) Dynamics of signalling during insulin-stimulated endocytosis of its receptor in adipocytes. *J Biol Chem* **270:** 59-65.

65. **Gustafson, T., He, W., Craparo, A., Schaub, C., O'Neill, T.** (1995) Phosphotyrosine-dependent interaction of SHC and insulin receptor substrate 1 with the NPEY motif of the insulin receptor via a novel non-SH2 domain. *Mol Cell Biol* **15:** 2500-2508.

66. **Craparo, A., O'Neill, T., Gustafson, T.** (1995) Non-SH2 domains within insulin receptor substrate-1 and SHC mediate their phosphotyrosine-dependent interaction with the NPEY motif on the insulin-like growth factor I receptor. *J Biol Chem* **270:** 12639-15643.

67. **Kuhne, M., Pawson, T., Leinhard, G., Feng, G.** (1993) The insulin receptor substrate 1 associates with the SH2-containing phosphotyrosine phosphatase Syp. *J Biol Chem* **268:** 11479-11481.

68. **Lee, C., Li, W., Nishimura, R., Zhou, M., Batzer, A., Myers, M., White, M., Schlessinger, J., Skolnik, E.** (1993b) Nck associates with the SH2 domain-docking protein IRS-1 in insulin-stimulated cells. *Proc Nat Acad Sci USA* **90:** 11713-11717.

69. **Pelicci, G., Lanfrancone, L., Grignani, F., McGlade, J., Cavallo, F., Forni, G., Nicoletti, I., Pawson, T., Pelicci, P.** (1992) A novel transforming protein (SHC) with an SH2 domain is implicated in mitogenic signal transduction. *Cell* **70:** 93-104.

70. **Yamauchi, K., Pessin, J.** (1994) Insulin receptor substrate-1 (IRS-1) and SHC compete for a limited pool of GRB2 in mediating insulin downstream signalling. *J Biol Chem* **269:** 31107-31114.

71. **Pronk, G., McGlade, J., Pelicci, G., Pawson, T., Bos, J.** (1993) Insulin-induced phosphorylation of the 46- and 52-kDa Shc proteins. *J Biol Chem* **268:** 5748-5753.

72. **Pronk, G., De Vries-Smits, A., Buday, L., Downward, J., Maassen, J., Medema, R., Bos, J.** (1994) Involvement of Shc in insulin- and epidermal growth factor-induced activation of $p21^{ras}$. *Mol Cell Biol* **14:** 1575-1581.

73. **Yokote, K., Mori, S., Hansen, K., McGlade, J., Pawson, T., Heldin, K., Claesson-Welsh, L.** (1994) Direct interaction between Shc and the platelet-derived growth factor β-receptor. *J Biol Chem* **269:** 15337-15343.

74. **Obermeier, A., Lammers, R., Weismuller, K., Jung, G., Schlessinger, J., Ullrich, A.** (1993) Identification of Trk binding sites for SHC and phosphatidyl inositol 3'- kinase and formation of a multimeric signalling complex. *J Biol Chem* **268:** 22963-22966.

75. **Ravichandran, K., Burakoff, S.** (1994) The adapter protein SHC interacts with the interleukin-2 (IL-2) receptor upon IL-2 stimulation. *J Biol Chem* **269:** 1599-1602.

76. **Skolnik, E., Lee, C., Batzer, A., Vincenti, L., Zhou, M., Daly, R., Myers, M., Backer, J., Ullrich, A., White, M., Schlessinger, J.** (1993) The SH2/SH3 domain-containing protein GRB2 interacts with IRS-1 and SHC: implications for insulin control of ras signalling. *EMBO J* **12:** 1929-1936.

77. **Rozakis-Adcock, M., McGlade, J., Mbamalu, G., Pelicci, G., Daly, R., Li, W., Batzer, A., Thomas, S., Brugge, J., Pelicci, P., Schlessinger, J., Pawson, T.** (1992) Association of the Shc and GRB2/Sem5 SH2-containing proteins is implicated in the ras signalling pathway by tyrosine kinases. *Nature* **360:** 689-692.

78. **Whitman, M., Downes, C., Keeler, M., Keller, T., Cantley, L.** (1988) Type I phophatidyl inositol kinase makes a novel inositol phospholipid, phosphatidyl-3-phosphate. *Nature* **332:** 644-646.

79. **Escobedo, J., Navankasattusas, S., Kavanaugh, W., Milfray, D., Fried, V., Williams, L.** (1991) cDNA cloning of a novel 85kD protein that has SH2 domains and regulates binding of PI 3-kinase to the PDGF β-receptor. *Cell* **65:** 75-82.

80. **Skolnik, E., Margolis, B., Mohammadi, M., Lowenstein, E., Fischer, R., Drepps, A., Ullrich, A., Schlessinger, J.** (1991) Cloning of PI3 kinase-associated p85 utilizing a novel method for expression/cloning of target proteins for receptor tyrosine kinases. *Cell* **65:** 83-90.

81. **Shoelson, S., Sivaraja, M., Williams, K., Hu, P., Schlessinger, J., Weiss, M.** (1993) Specific phosphopeptide binding regulates a conformational change in the PI 3-kinase SH2 domain associated with enzyme activation. *EMBO J* **12:** 795-802.

82. **Sun, X., Crimmins, D., Myers, M., Miralpeix, M., White, M.** (1993) Pleiotropic insulin signals are engaged by multisite phosphorylation of IRS-1. *Mol Cell Biol* **13:** 7418-7428.

83. **Otsu, M., Hiles, I., Gout, I., Fry, M., Ruis-Larrea, F., Panayotou, G., Thompson, A., Dhand, R., Hsuan, J., Totty, N., Smith, A., Morgan, S., Courtneige, S., Parker, P., Waterfield, M.** (1991) Characterization of two 85 kD proteins that associate with receptor tyrosine kinases, middle T/pp60$^{c\text{-}src}$ complexes and PI3-kinase. *Cell* **65:** 91-104.

84. **Serunian, L., Haber, M., Fukui, T., Kim, J., Rhee, S., Lowenstein, J., Cantley, L.** (1989) Polyphosphoinositides produced by phosphatidyl inositol 3-kinase are poor substrates for phospholipases C from rat liver and bovine brain. *J Biol Chem* **264:** 17809-17815.

85. **Nakanishi, H., Brewer, K., Exton, J.** (1993) Activation of the zeta isozyme of protein kinase C by phosphatidyl inositol 3,4,5-triphosphate. *J Biol Chem* **268:** 13-16.

86. **Lienhard, G., Slot, J., James, D., Mueckler, M.** (1992) How cells absorb glucose. *Sci Amer* **Jan:** 86-91.

87. **Cheatham, B., Vlahos, C., Cheatham, L., Wang, L., Blenis, J., Khan, C.** (1994) Phosphatidyl inositol 3-kinase activation is required for insulin stimulation of pp70 S6 kinase, DNA synthesis and glucose transporter translocation. *Mol Cell Biol* **14:** 4902-4911.

88. **Blenis, J., Chung, J., Erikson, E., Alcorta, D., Erikson, R.** (1991) Distinct mechanisms for the activation of the RSK kinases/MAP2 kinase/ pp90^{rsk} and pp70^{rsk} kinase signalling systems are indicated by inhibition of protein synthesis. *Cell Growth Differ* **2:** 279-285.

89. **Fingar, D., Hauddorff, S., Blenis, J., Birnbaum, M.** (1993) Dissociation of pp70 ribosomal protein S6 kinase from glucose transport in 3T3-L1 adipocytes. *J Biol Chem* **268:** 3005-3008.

90. **Palen, E., Traugh, J.** (1987) Phosphorylation of ribosomal protein S6 by cAMP-dependent protein kinase and mitogen-stimulated S6 kinase differentially alters translation of globin mRNA. *J Biol Chem* **262:** 2518-2523.

91. **Chung, J., Kuo, C., Crabtree, G., Blenis, J.** (1992) Rapamycin-FKBP specifically blocks growth-dependent activation of and signalling by the 70kD S6 protein kinase. *Cell* **69:** 1227-1236.

92. **Lartey, P., Nellans, H., Tanaka, S.** (1994) New developments in macrolides: Structures and antibacterial and prokinetic activities. *Adv Pharmacol* **28:** 307-343.

93. **Lowenstein, E., Daly, R., Batzer, A., Li, W., Margolis, B., Lammers, R., Ullrich, A., Skolnik, E., Bar-Sagi, D., Schlessinger, J.** (1992) The SH2 and SH3 domain-containing protein GRB2 links receptor tyrosine kinases to Ras signalling. *Cell* **70:** 431-442.

94. **Li, N., Batzer, A., Daly, R., Yajnik, V., Skolnik, E., Chardin, P., Bar-Sagi, D., Margolis, B., Schlessinger, J.** (1993) Guanine-nucleotide-releasing factor hSos1 binds to Grb2 and links receptor tyrosine kinases to ras signalling. *Nature* **363:** 85-87.

95. **Marshall, M.** (1993) The effector interactions of p21^{ras}. *Trends Biochem Sci* **18:** 250-254.

96. **MacDonald, S., Crews, C., Wu, L., Driller, J., Clark, R., McCormick, F.** (1993) Reconstitution of the Raf-1-MEK-ERK Signal Transduction Pathway In Vitro. *Mol Cell Biol* **13:** 6615-6620.

97. **Huang, W., Alessandrini, A., Crews, C., Erikson, R.** (1993) Raf-1 forms a stable complex with Mek1 and activates Mek1 by serine phosphorylation. *Proc Nat Acad Sci USA* **90:** 10947-10951.

98. **Nishida, E., Gotoh, Y.** (1993) The MAP kinase cascade is essential for diverse signal transduction pathways. *Trends Biochem Sci* **18:** 128-131.

99. **Pelech, S., Sanghera, J.** (1992) Mitogen-activated protein kinases: Versatile transducers for cell signalling. *Trends Biochem Sci* **17:** 233-238.

100. **Dent, P., Lavoinne, A., Nakielny, S., Caudwell, F., Watt, P., Cohen, P.** (1990) The molecular mechanisms by which insulin stimulates glycogen synthesis in mammalian skeletal muscle. *Nature* **348:** 302-307.

101. **Stryer, L.** (1995a) Glycogen metabolism in: Biochemistry, 4th Ed. W.H. Freeman & Co., NY, pp 581-602.

102. **Blenis, J.** (1993) Signal transduction via the MAP kinases: proceed at your own RSK. *Proc Nat Acad Sci USA* **90:** 5889-5892.

103. **Angel, P., Karin, M.** (1991) The role of Jun, Fos and the AP-1 complex in cell-proliferation and transformation. *Biochim Biophys Acta* **1072:** 129-157.

104. **Mohn, K., Laz, T., Melby, A., Taub, R.** (1990) Immediate-early gene expression differs between regenerating liver, insulin-stimulated H-35 cells, and mitogen-stimulated Balb/c 3T3 cells. *J Biol Chem* **265:** 21914-21921.

105. **Weiland, M., Bahr, F., Höhne, M., Schůrmann, A., Ziehm, D., Joost, H.** (1991) The signalling potential of the receptors for insulin and insulin-like growth factor-1 (IGF-I) in 3T3 adipocytes: Comparison of glucose transport activity, induction of oncogene c-fos, glucose transporter mRNA, and DNA synthesis. *J Cell Phys* **149:** 428-435.

106. **Kim, S., Khan, C.** (1994) Insulin stimulates phosphorylation of c-Jun , c-Fos and Fos-related proteins in cultured adipocytes. *J Biol Chem* **269:** 11887-11892.

107. **Curran, T., Franza, R.** (1988) The AP-1 connection. *Cell* **55:** 395-397

108. **Shaw, P., Schroter, H., Nordheim, A.** (1989) The ability of a ternary complex to form over the serum response element correlates with serum inducibility of the human *c-fos* promoter. *Cell* **56:** 563-572.

109. **Boyle, W., Smeal, T., Defize, L., Angel, P., Woodgett, J., Karin, M., Hunter, T.** (1991) Activation of protein kinase C decreased phosphorylation of c-Jun at sites that negatively regulate its DNA-binding activity. *Cell* **64:** 573-584.

110. **Carpentier, J., Paccaud, J.** (1994) Molecular and cellular biology of insulin-receptor internalization. *Ann NY Acad Sci* **733:** 266-278.

111. **Carpentier, J., Paccaud, J., Gorden, P., Rutter, W., Orci, L.** (1992) Insulin-induced surface redistribution regulates internalization of the insulin receptor and requires autophosphorylation. *Proc Nat Acad Sci USA* **89:** 162-166.

112. **Carpentier, J., McClain, D.** (1995) Insulin receptor kinase activation releases a constraint maintaining the receptor on microvilli. *J Biol Chem* **270:** 5001-5006.

113. **Berhanu, P., Anderson, C., Paynter, D., Wood, W.** (1995) The amino acid sequence GPLY is not necessary for normal endocytosis of the human insulin receptor B isoform. *Biochem Biophys Res Comm* **209:** 730-738.

114. **Nesterov, A., Kurten, R., Gill, G.** (1995) Association of epidermal growth factor receptors with coated pit adaptins via tyrosine phosphorylation-regulated mechanism. *J Biol Chem* **270:** 6320-6327.

115. **Smith, R., Seely, B., Shah, N., Olefsky, J., Jarrett, L.** (1991) Tyrosine kinase-defective insulin receptors undergo insulin-induced microaggregation but do not concentrate in coated pits. *J Biol Chem* **266:** 17522-17530.

116. **Backer, J., Khan, C., White, M.** (1989a) Tyrosine phosphorylation of the insulin receptor and insulin receptor internalization. Studies in 2,4-dinitrophenol-treated cells. *Proc Nat Acad Sci USA* **86:** 3209-3213.

117. **Smith, R., Jarrett, L.** (1990) Differences in adenosine triphosphate dependency of receptor-mediated endocytosis of α2-macroglobulin and insulin correlate with separate routes of ligand-receptor complex internalization. *Endocrinology* **126:** 1551-1560.

118. **Rothman, J., Schmid, S.** (1986) Enzymatic recycling of clathrin from coated vesicles. *Cell* **46:** 5-9.

119. **Pearse, B., Bretscher, M.** (1981) Membrane recycling by coated vesicles. *Annu Rev Biochem* **50:** 85-101.

120. **Berg, T., Gjøen, T., Bakke, O.** (1995) Physiological functions of endosomal proteolysis. *Biochem J* **307:** 313-326.

121. **Mellman, I., Fuchs, R., Helenius, A.** (1986) Acidification of the endocytic and exocytic pathways. *Ann Rev Biochem* **55:** 663-700.

122. **Authier, F., Rachubinski, R., Posner, B., Bergeron, J.** (1994) Endosomal proteolysis of insulin by an acid thiol metalloprotease unrelated to insulin degrading enzyme. *J Biol Chem* **269:** 3010-3016.

123. **Bevan, A., Burgess, J., Drake, P., Shaver, A., Bergeron, J., Posner, B.** (1995) Selective activation of the Rat hepatic endosomal insulin receptor kinase. Role for the endosome in insulin signalling. *J Biol Chem* **270:** 10784-10791.

124. **Khan, M., Bacquiran, G., Brule, C., Burgess, J., Foster, B., Bergeron, J., Posner, B.** (1989) Internalization and activation of the Rat liver insulin receptor

kinase *in vivo*. *J Biol Chem* **264:** 12931-12940.

125. **Backer, J., Khan, C., White, M.** (1989b) Tyrosine phosphorylation of the insulin receptor during insulin-stimulated internalization in Rat hepatoma cells. *J Biol Chem* **264:** 1694-1701.

126. **Burgess, J., Wada, I., Ling, N., Khan, M., Bergeron, J., Posner, B.** (1992) Decrease in β-subunit phosphotyrosine correlates with internalization and activation of the endosomal insulin receptor kinase. *J Biol Chem* **267:** 10077-10086.

127. **Faure, R., Bacquiran, G., Bergeron, J., Posner, B.** (1992) The dephosphorylation of insulin and epidermal growth factor receptors. *J Biol Chem* **267:** 11215-11221.

128. **Lavan, B., Lienhard, G.** (1993) The insulin-elicited 60-kDa phosphotyrosine protein in Rat adipocytes is associated with phosphatidyl inositol 3-kinase. *J Biol Chem* **268:** 5921-5928.

129. **Olson, T., Bamberger, M., Lane, D.** (1988) Post-translational changes in tertiary and quaternary structure of the insulin proreceptor. *J Biol Chem* **263:** 7342-7351.

130. **Olson, T., Lane, D.** (1989) A common mechanism for posttranslational activation of plasma membrane receptors? *FASEB J* **3:** 1618-1624.

131. **Hedo, J., Collier, E., Watkinson, A.** (1987) Myristyl and palmityl acylation of the insulin receptor. *J Biol Chem* **262:** 954-957.

132. **Magee, A., Siddle, K.** (1988) Insulin and IGF-I receptors contain covalently bound palmitic acid. *J Cell Biochem* **37:** 347-357.

133. **Stryer, L.** (1995b) Protein synthesis in: Biochemistry. 4th Ed. WH Freeman & Co., NY., pp 875-910.

134. **Rouiller, D., McKeon, C., Taylor, S., Gorden, P.** (1988) Hormonal regulation of insulin receptor gene expression. Hydrocortisone and insulin act by different mechanisms. *J Biol Chem* **263:** 13185-13190.

135. **Saad, M., Folli, F., Khan, C.** (1995) Insulin and dexamethasone regulate insulin receptors, insulin receptor substrate-1, and phosphatidyl inositol 3-kinase in Fao hepatoma cells. *Endocrinology* **136:** 1579-1588.

136. **Lee, J., Tam, J., Tsai, M., Tsai, S.** (1992) Identification of *cis*- and *trans*-acting factors regulating the expression of the human insulin receptor gene. *J Biol Chem* **267:** 4638-4645.

137 **Goldstein, B., Khan, C.** (1989) Analysis of mRNA heterogeneity by ribonuclease H mapping: application to the insulin receptor. *Biochem Biophys Res Comm* **159:** 664-669.

138. **Levy, J., Hug, V.** (1992) Regulation of insulin receptor gene expression. Cell cycle-mediated effects on insulin receptor mRNA stability. *J Biol Chem* **267:** 25289-25295.

139. **Blake, A., Hayes, N., Slater, E., Strader, C.** (1987) Insulin receptor desensitization correlates with attenuation of tyrosine kinase activity, but not of receptor endocytosis. *Biochem J* **245:** 357-364.

140. **Treadway, J., Whittaker, J., Pessin, J.** (1989) Regulation of the insulin receptor kinase by hyperinsulinemia. *J Biol Chem* **261:** 15136-15143.

141. **Arsenis, G., Livingston, J.** (1986) Alterations in the tyrosine kinase activity of the insulin receptor produced by *in vitro* hyperinsulinemia. *J Biol Chem* **261:** 147-153.

142. **Knutson, V.** (1991a) Proteolytic processing of the insulin receptor β subunit is associated with insulin-induced receptor down-regulation. *J Biol Chem* **266:** 15656-15662.

143. **Knutson, V.** (1991b) Cellular trafficking and processing of the insulin receptor. *FASEB J* **5:** 2130-2138.

144. **Knutson, V.** (1992) Ligand-independent internalization and recycling of the insulin receptor. Effects of chronic treatment of 3T3-C2 fibroblasts with insulin and dexamethasone. *J Biol Chem* **267:** 931-937.

145. **Torossian, K., Nower, P., Schwartz, T., Fantus, G.** (1993) Phorbol esters inhibit insulin-induced receptor down-regulation in cultured human lymphocytes: association with diminished insulin receptor phosphorylation. *Biochem J* **290:** 151-158.

146. **Seedorf, K., Shearman, M., Ullrich, A.** (1995) Rapid and long term effects of protein kinase C on tyrosine kinase phosphorylation and degradation. *J Biol Chem* **270:** 18953-18960.

147. **Leckett, B.** (1991) The selection, isolation, and characterization of a Chinese hamster lung fibroblast cell line resistant to an insulin-diphtheria A-chain toxic conjugate molecule. Thesis, Dept. of Medicine, McGill University.

148. **Lowry, O., Rosebough, N.** (1951) Protein measurement with the Folin phenol reagent. *J Biol Chem* **193**: 265-275.

149. **Germinario, R., Lakshmi, T, Thirion, J.** (1989) Characteristics and regulation of hexose transport in a galactokinase-negative Chinese hamster fibroblast line: A good model for studies on sugar transport in cultured mammalian cells. *J Cell Physiol* **138**: 300-304.

150. **Germinario, R., McQuillan, A., Olivera, M., Manuel, S.** (1983) Enhanced insulin stimulation of sugar transport and DNA synthesis by glucocorticoids in cultured human skin fibroblasts. *Arch Biochem Biophys* **226**: 498-505.

151. **Lawrence, J.C., Guinovart, J., Larner, J.** (1977) Activation of rat adipose glycogen synthase by insulin. *J Biol Chem* **252**: 444-450.

152. **Perez-Rodriguez, R., Chambard, J., Van Obberghen-Schilling, E., Franchi, A., Pouysségur, J.** (1981) Emergence of hamster fibroblast tumours in nude mice - Evidence for *in-vivo* selection leading to loss of growth factor requirement. *J Cell Physiol* **109**:387-396.

153. **Ambesi-Impiombato, F., Parks, L., Coon, H.** (1980) Culture of hormone-dependent functional epithelial cells from Rat thyroids. *Proc Nat Acad Sci USA* **77:** 3455-3459.

154. **Backer, J.M., Khan, C.R., White M.F.** (1990b) The Dissociation and Degradation of Internalized Insulin Occur in the Endosomes of Rat Hepatoma Cells. *J Biol Chem* **265**: 14828-14835.

155. **Kuo, W., Gehm, B.,Rich-Rosner, M.** (1991) Regulation of Insulin Degradation: Expression of an Evolutionarily Conserved Insulin-Degrading Enzyme Increases Degradation by an Intracellular Pathway. *Mol Endocr* **5**:1467-1476.

156. **Posner, B., Faure, R., Burgess, J., Bevan, A., Lachance, D., Zhang-Sun, G., Fantus,I., Ng, J., Hall, D., Soo Lum, B., Shaver, A.** (1994) Peroxovanadium Compounds: a New Class of Potent Phosphotyrosine Phosphatase Inhibitors Which Are Insulino-mimetics. *J Biol Chem* **269**: 4596-4604.

157. **Keller, S., Aebersold, R., Garner, C., Lienhard, G.** (1993) The insulin-elicited 160 kDa phosphotyrosine protein in mouse adipocytes is an insulin receptor substrate ?. Identification by cloning. *Biochim Biophys Acta* **1172:** 323-326.

158. **Reed, B.C., Ronnett, V., Lane, M.** (1981) Role of Glycosylation and Protein Synthesis in Insulin Receptor Metabolism by 3T3-L1 Mouse Adipocytes. *Proc Nat Acad Sci* **78**: 2908-2912.

159. **Okajima, T., Tanabe, T., Yasuda, T.** (1993) Nonurea Sodium Dodecyl Sulphate-Polyacrylamide Gel Electrophoresis with High-Molarity Buffers for the

Separation of Proteins and Peptides. *Anal Biochem* **211**:293-300.

160. **Harlow, E.** (1988) Antibodies: A Lab Manual. *Cold Spring Harbor Press*, Cold Spring Harbor, NY.

161. **Maniatis, T., Fritsch, E., Sandbrook, J**: Molecular Cloning: A Laboratory Manual. Cold Spring Harbor, NY, Cold Spring Harbor, 1982.

162. **Angel, P., Hattori, K., Smeal, T., Karin, M.** (1988) The *jun* proto-oncogene is positively regulated by its product Jun/AP-1. *Cell* **55:** 875-885.

163. **Chomczynski, P., Sacchi, N.** (1987) Single-step Method of RNA Isolation by Acid Guanidinium Thiocyanate-Phenol-Chloroform Extraction. *Anal Biochem* **162**: 156-159.

164. **Leckett, B., Spurmanis, A., Allen C., Germinario, R.** (1993) Mutant Cell Line Demonstrating a Block in Insulin and Insulin-Like Growth Factor Type 1 (IGF-1) Induced Mitogenesis. *J Cell Phys* **155**: 179-184.

165. **Gansler, T., Smith, R., Jarett, L.** (1986) Cell type-specific variability of bacitracin's effects on insulin binding and intracellular accumulation. *Diabetes* **35:** 392-397.

166. **Blackard, W., Smith, R., Jarett, L.** (1986) Insulin processing by cultured hepatocytes. *Am J Physiol* **250 (Endocrinol. Metab. 43):** E148-E155.

167. **Hamel, F., Peavy, D., Ryan, M., Duckworth, W.** (1987) HPLC analysis of Insulin Degradation Products from Isolated Hepatocytes. *Diabetes* **36:** 702-708.

168. **Rothenberg, P., Lane, W., Karasik, A., Backer, J., White, M., Khan,C.** (1991) Purification and Partial Sequence analysis of pp185, the Major Cellular Substrate of the Insulin Receptor Tyrosine Kinase. *J Biol Chem* **266:** 8302-8311.

169. **White, M., Khan, C.** (1985) Insulin rapidly stimulates tyrosine phosphorylation of a Mr - 185,000 protein in intact cells. *Nature* **318:** 183-186.

170. **Goren, H., Boland, D.** (1991) Reverse phase chromatography of trypsin digests of a plasma membrane and a cytoplasmic insulin receptor substrate. *Biochem Biophys Res Comm* **176:** 1402-1407.

171. **Rees-Jones, R., Taylor, S.** (1985) An endogenous substrate for the insulin receptor-associated tyrosine kinase. *J Biol Chem* **260:** 4461-4467.

172. **Perotti, N., Accili, D., Marcus-Samuels, B., Rees-Jones, R., Taylor, S.** (1987) Insulin stimulates the phosphorylation of a 120 kDa glycoprotein substrate (pp120) for the receptor-associated protein kinase in intact H-35 hepatoma cells.

Proc Nat Acad Sci USA **84:** 3137-3140.

173. **Margolis, R., Taylor, S., Seminara, D., Hubbard, A.** (1988) Identification of pp120, an endogenous substrate for the hepatocyte insulin receptor tyrosine kinase, as an integral membrane of the bile canalicular domain. *Proc Nat Acad Sci USA* **85:** 7256-7259.

174. **Bhatia, P., Taylor, W., Greenberg, A., Wright, J.** (1994) Comparison of glyceraldehyde-3-phosphate dehydrogenase and 28S-ribosomal RNA gene expression as RNA loading controls for northern blot analysis of cell lines of varying malignant potential. *Anal Biochem* **216:** 223-226.

175. **Ryder, K., Nathans, D.** (1988) Induction of protooncogene *c-jun* by serum growth factors. *Proc Nat Acad Sci USA* **85:** 8464-8467.

176. **Werner, H., Woloschak, M., Stannard, B., Shen-Orr, Z., Roberts, C., LeRoith, D.** (1991) The insulin-like growth factor I receptor: molecular biology, heterogeneity, and regulation. In LeRoith D (Ed): Insulin-like growth factors: Molecular and cellular aspects. Boca Raton, CRC Press, 1991, pp 17-48.

177. **Melmed, S.** (1993) Editorial: Insulin and insulin-like growth factor I receptors: are there functional distinctions? *Endocrinology* **132:** 1419-1420.

178. **Thies, S., Ullrich, A., McClain, D.** (1989) Augmented mitogenesis and impaired metabolic signalling mediated by a truncated insulin receptor. *J Biol Chem* **264:** 12820-12825.

179. **Tartare, S., Mothe, I., Kowalski-Chauvel, A., Breittmeyer, J., Ballotti, R., Van Obberghen, E.** (1994) Signal transduction by a chimeric insulin-like growth factor-1 (IGF-1) receptor having the carboxyl terminal domain of the insulin receptor. *J Biol Chem* **269:** 11449-11455.

180. **Merion, M., Schlessinger, P., Brooks, R., Moering, J., Moering, T., Sly, W.** (1983) Defective acidification of endosomes in Chinese hamster ovary cell mutants "cross-resistant" to toxins and viruses. *Proc Nat Acad Sci USA* **80:** 5315-5319.

181. **Madshus, I.** (1994) The N-terminal α-helix of fragment B of Diphtheria toxin promotes translocation of fragment A into the cytoplasm of eukaryotic cells. *J Biol Chem* **269:** 17723-17729.

182. **Falnes, P., Choe, S., Madshus, I., Wilson, B., Olsnes, S.** (1994) Inhibition of membrane translocation of Diphtheria toxin A-fragment by internal disulphide bridges. *J Biol Chem* **269:** 8402-8407.

183. **Hamel, F., Mahoney, M., Duckworth, W.** (1991) Degradation of intraendosomal insulin by insulin-degrading enzyme without acidification. *Diabetes* **40:** 436-443.

184. **Manabe, T., Yoshimori, T., Henomatsu, N., Tashiro, Y.** (1993) Inhibitors of vacuolar-type H^+-ATPase suppresses proliferation in cultured cells. *J Cell Phys* **157:** 445-452.

185. **Bennett, R., Hamel, F., Duckworth, W.** (1994) Identification and isolation of a cytosolic proteolytic complex containing insulin degrading enzyme and the multicatalytic proteinase. *Biochem Biophys Res Comm* **202:** 1047-1053.

186. **Duckworth, W., Bennett, R., Hamel, F.** (1994) A direct inhibitory effect of insulin on a cytosolic proteolytic complex containing insulin-degrading enzyme and multicatalytic proteinase. *J Biol Chem* **269:** 24575-24580.

187. **Amsterdam, A., Pitzer, F., Baumeister, W.** (1993) Title? *Proc Nat Acad Sci USA* **90:** 99-103.

188. **Schuldiner, A., Barbetti, F., Raben, N., Scavo, L., Serrano, J.:** Insulin. in Le Roith D. (Ed): Insulin-Like Growth Factors: Molecular and Cellular Aspects. Boca Raton, CRC Press, 1991, pp 181-219.

189. **Blundell, T., Bedarkar, S., Rinderknecht, E., Humbel, R.** (1978) Insulin-like growth factor: A model for tertiary structure accounting for immunoreactivity and receptor binding. *Proc Nat Acad Sci USA* **75:** 180-184.

190. **Taylor, S., Najjar, S., Cama, A., Accili, D.:** Structure and function of the insulin receptor. in Le Roith D. (Ed): Insulin-like Growth Factors: Molecular and Cellular Aspects. Boca Raton, CRC Press, 1991, pp 221-244.

191. **Stryer, L.** (1995c) Signal Transduction Cascades. in: Biochemistry 4th Ed. WH Freeman & Co., NY, pp 325-360.